

AD-A093 253

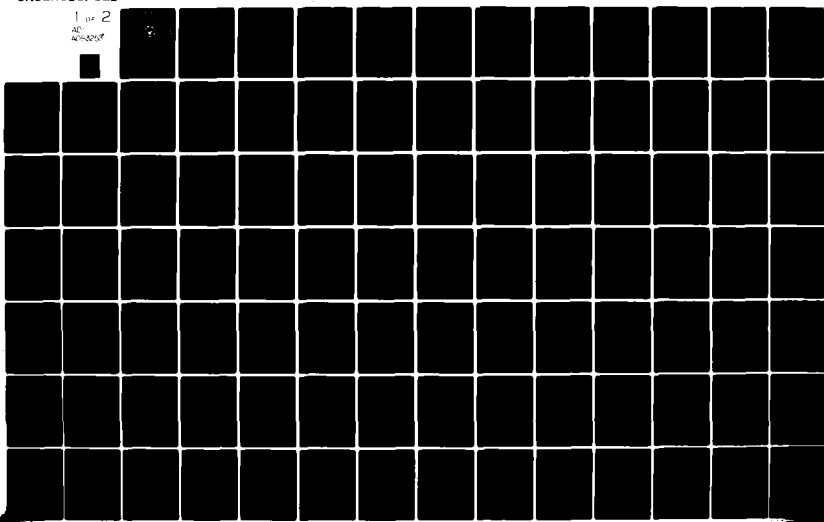
NAVAL POSTGRADUATE SCHOOL MONTEREY CA
A STUDY OF STATE FEEDBACK IMPLICIT MODEL FOLLOWING CONTROL FOR --ETC(U)
SEP 80 L E EPLEY

F/G 1/4

UNCLASSIFIED

NL

1 of 2
ALL INFORMATION CONTAINED
HEREIN IS UNCLASSIFIED



AD A 093253

LEVEL
NAVAL POSTGRADUATE SCHOOL
Monterey, California



THESIS

A STUDY OF STATE RATE FEEDBACK IMPLICIT
MODEL FOLLOWING CONTROL FOR
VSTOL AIRCRAFT

by

Lawrence Ernest Epley

September 1980

Thesis Advisor:

D. J. Collins

Approved for public release; distribution unlimited

DDC FILE COPY

80 12 29 160

REPORT DOCUMENTATION PAGE		READ INSTRUCTIONS BEFORE COMPLETING FORM
1. REPORT NUMBER	2. GOVT ACCESSION NO.	3. RECIPIENT'S CATALOG NUMBER
4. TITLE (and Subtitle) A STUDY OF STATE RATE FEEDBACK IMPLICIT MODEL FOLLOWING CONTROL FOR VSTOL AIRCRAFT		5. TYPE OF REPORT & PERIOD COVERED Engineer's Thesis September 1980
6. AUTHOR(S) Lawrence Ernest/Epley	7. PERFORMING ORG. REPORT NUMBER 9) Ma, + Th. 13,	
8. PERFORMING ORGANIZATION NAME AND ADDRESS Naval Postgraduate School Monterey, California 93940	10. PROGRAM ELEMENT, PROJECT, TASK AREA & WORK UNIT NUMBERS 13) 151	
11. CONTROLLING OFFICE NAME AND ADDRESS Naval Postgraduate School Monterey, California 93940	12. REPORT DATE 11) September 1980	
14. MONITORING AGENCY NAME & ADDRESS// different from Controlling Office Naval Postgraduate School Monterey, California 93940	15. SECURITY CLASS. (of this report) Unclassified	
16. DISTRIBUTION STATEMENT (of this Report) Approved for public release; distribution unlimited		
17. DISTRIBUTION STATEMENT (of the abstract entered in Block 20, if different from Report)		
18. SUPPLEMENTARY NOTES		
19. KEY WORDS (Continue on reverse side if necessary and identify by block number) VSTOL Aircraft Control, Aircraft Attitude Stabilization, Model Following, State Rate Feedback Implicit Model Following,		
20. ABSTRACT (Continue on reverse side if necessary and identify by block number) The State Rate Feedback Implicit Model Follower control concept is examined in detail from a classical and modern control theory viewpoint. State Rate Feedback Implicit Model Following (SRFIMF) is a concept whereby control of the dynamic response of a system is achieved by the measurement and feedback of a state rate, normally acceleration. In addition to a basic description of the concept, emphasis is placed on the effect of noise in the measurement of the		

Block 20 continued:

required feedback quantities. Control of the pitch attitude of the AV-8A Harrier VTOL aircraft is used as an example of the application of the control concept. The model of the Harrier used in this study includes the effect of both sensor measurement errors and gust load inputs.

R

Accession For	
NTIS	GR&AI <input checked="" type="checkbox"/>
DTIC TAB	<input type="checkbox"/>
Unpublished	<input type="checkbox"/>
Justification	
PV	
Distribution/	
Availability Codes	
Avail. for	
Distr	Special
P	

Approved for public release; distribution unlimited

A Study of
State Rate Feedback Implicit Model Following Control
for VSTOL Aircraft

by

Lawrence E. Epley
Lieutenant, United States Navy
B.S., Purdue University, 1973

Submitted in partial fulfillment of the
requirements for the degree of

AERONAUTICAL ENGINEER

from the

NAVAL POSTGRADUATE SCHOOL
September 1980

Author

Lawrence E. Epley

Approved by:

Daniel J. Collins

Thesis Advisor

Donald P. Taylor

Second Reader

G. S. Lindsay for M. F. D.
Chairman, Department of Aeronautical Engineering

William M. Tolles

Dean of Science and Engineering

ABSTRACT

The State Rate Feedback Implicit Model Follower control concept is examined in detail from a classical and modern control theory viewpoint. State Rate Feedback Implicit Model Following (SRFIMF) is a concept whereby control of the dynamic response of a system is achieved by the measurement and feedback of a state rate, normally acceleration. In addition to a basic description of the concept, emphasis is placed on the effect of noise in the measurement of the required feedback quantities. Control of the pitch attitude of the AV-8A Harrier VTOL aircraft is used as an example of the application of the control concept. The model of the Harrier used in this study includes the effect of both sensor measurement errors and gust load inputs.

TABLE OF CONTENTS

I.	INTRODUCTION -----	15
II.	DESCRIPTION OF THE SRFIMF CONTROLLER -----	19
	A. THE BASIC SCHEME -----	19
	B. THE GENERAL FORM OF THE SRFIMF CONTROLLER ---	29
	C. PRACTICAL EXAMPLES OF THE SRFIMF CONTROLLER -	32
III.	TIME AND FREQUENCY DOMAIN ANALYSIS OF THE SRFIMF -----	38
	A. REPRESENTATIVE AIRCRAFT PLANT DYNAMICS -----	38
	B. FREQUENCY RESPONSE AND BODE ANALYSIS -----	44
	C. ROOT LOCUS ANALYSIS -----	47
	D. SRFIMF SIMULATIONS -----	60
IV.	SENSOR NOISE ANALYSIS -----	73
	A. SRFIMF STOCHASTIC MODEL -----	73
	B. COVARIANCE ANALYSIS -----	85
	C. ALTERNATE MEASUREMENT SCHEMES -----	94
V.	APPLICATION OF THE SRFIMF CONCEPT TO THE HARRIER AIRCRAFT -----	107
	A. PITCH ATTITUDE CONTROL -----	107
	B. PITCH ATTITUDE GUST RESPONSE -----	122
VI.	CONCLUSIONS -----	130
	APPENDIX A - COMPUTER LISTINGS -----	132
	APPENDIX B - DATA -----	150
	LIST OF REFERENCES -----	155
	INITIAL DISTRIBUTION LIST -----	157

LIST OF TABLES

III-1	ASSUMED MODEL CONSTANTS -----	38
III-2	TYPICAL AIRCRAFT POLE LOCATIONS -----	41
III-3	AIRCRAFT MODES USED IN SIMULATIONS -----	43
III-4	PLANT PARAMETERS FOR ROOT LOCUS ANALYSIS ---	55
IV-1	SENSOR ERROR MODEL PARAMETERS -----	75
IV-2	STEADY STATE ERRORS AS A RESULT OF MEASUREMENT ERRORS -----	88
IV-3	STEADY STATE TRACKING ERRORS PRODUCED BY STRAPDOWN AND INERTIAL NAVIGATION SENSORS --	89
IV-4	STEADY STATE ERROR IN x_1 , x_2 AND x_3 FOR MEASUREMENTS MADE BY STRAPDOWN SENSORS -----	106
V-1	STEADY STATE VALUES OF σ_1 , σ_2 AND σ_5 AS A RESULT OF POSITION, VELOCITY AND ACCELERATION MEASUREMENT ERROR -----	118
V-2	STANDARD DEVIATION OF STEADY STATE TRACKING ERRORS IN x_1 , x_2 AND x_5 AS A RESULT OF SENSOR NOISE IN THE HARRIER AIRCRAFT -----	122
B-1	TABULATED DATA FOR FIGURES 4-4 THROUGH 4-6 -	150
B-2	TABULATED DATA FOR FIGURE 4-7 -----	151
B-3	TABULATED DATA FOR FIGURES 4-9 THROUGH 4-11 -----	152
B-4	TABULATED DATA FOR FIGURES 5-4 THROUGH 5-6 -	153
B-5	TABULATED DATA FOR FIGURE 5-7 -----	154

LIST OF FIGURES

2-1	IMPLICIT MODEL FOLLOWING SCHEME -----	21
2-2	SRFIMF POSITION CONTROLLER DEVELOPED BY INTUTIVE ARGUMENTS -----	24
2-3	THE GENERAL FORM OF THE SRFIMF CONTROLLER -----	30
2-4	PHYSICALLY REALIZABLE SRFIMF POSITION CONTROLLER -----	33
2-5	PHYSICALLY REALIZABLE SRFIMF RATE CONTROLLER --	33
2-6	SRFIMF CONTROLLER EMPLOYED ON THE RTA FOR SPEED CONTROL -----	37
2-7	SRFIMF CONTROLLER EMPLOYED ON RTA FOR PITCH ATTITUDE CONTROL -----	37
3-1	TYPICAL AIRCRAFT POLE LOCATIONS -----	42
3-2	FREQUENCY RESPONSE OF SRFIMF POSITION CONTROLLER, KRL = 1 -----	48
3-3	FREQUENCY RESPONSE OF SRFIMF POSITION CONTROLLER, KRL = 10 -----	49
3-4	FREQUENCY RESPONSE OF THE SRFIMF POSITION CONTROLLER, KRL = 25 -----	50
3-5	FREQUENCY RESPONSE OF SRFIMF POSITION CONTROLLER, KRL = 50 -----	51
3-6	FREQUENCY RESPONSE OF SRFIMF POSITION CONTROLLER, KRL = 100 -----	52
3-7	ROOT LOCUS PLOT OF OSCILLATORY POLE OF A SRFIMF POSITION CONTROLLER. THE OPEN LOOP PLANT HAS A NATURAL FREQUENCY OF 1.47 RAD/SEC AND A DAMPING RATIO OF -.441 -----	56
3-8	ROOT LOCUS OF THE OSCILLATORY POLE OF A SRFIMF POSITION CONTROLLER. THE OPEN LOOP PLANT HAS TWO POLES AT THE ORIGIN -----	57

3-9	ROOT LOCUS OF THE OSCILLATORY POLE OF A SRFIMF CONTROLLER. THE OPEN LOOP PLANT HAS A NATURAL FREQUENCY OF .95 RAD/SEC AND DAMPING RATIO OF 0.475 -----	58
3-10	ROOT LOCUS OF THE OSCILLATORY POLE OF A SRFIMF POSITION CONTROLLER. THE OPEN LOOP PLANT HAS REAL POLES AT -1.0 AND -.6 -----	59
3-11	PERFECT MODEL RESPONSE -----	62
3-12	SIMULATION OF SRFIMF POSITION CONTROL FOR AIRCRAFT MODE 1, TABLE III-3. THE OPEN LOOP PLANT HAS A NATURAL FREQUENCY OF 2.94 RAD/SEC AND DAMPING OF .2 -----	63
3-13	SIMULATION OF SRFIMF POSITION CONTROL FOR AIRCRAFT MODE 2, TABLE III-3. THE OPEN LOOP PLANT HAS A NATURAL FREQUENCY OF 2.5 RAD/SEC AND DAMPING RATIO OF 0.06 -----	64
3-14	SIMULATION OF SRFIMF POSITION CONTROL FOR AIRCRAFT MODE 3, TABLE III-3. THE OPEN LOOP PLANT HAS A NATURAL FREQUENCY OF 0.954 RAD/SEC AND A DAMPING RATIO OF 0.314 -----	65
3-15	SIMULATION OF SRFIMF POSITION CONTROL FOR AIRCRAFT MODE 4, TABLE III-3. THE OPEN LOOP PLANT HAS A NATURAL FREQUENCY OF 0.283 RAD/SEC AND DAMPING RATIO OF 0.353 -----	66
3-16	SIMULATION OF SRFIMF POSITION CONTROL FOR AIRCRAFT MODE 5, TABLE III-3. THE OPEN LOOP PLANT HAS REAL POLES AT -0.2 AND 0 -----	67
3-17	SIMULATION OF SRFIMF POSITION CONTROL FOR AIRCRAFT MODE 6, TABLE III-3. THE OPEN LOOP PLANT HAS A NATURAL FREQUENCY OF 1.47 RAD/SEC AND DAMPING RATIO OF -.204 -----	68
3-18	SIMULATION OF SRFIMF POSITION CONTROL FOR AIRCRAFT MODE 7, TABLE III-3. THE OPEN LOOP PLANT HAS REAL POLES AT 0.30 AND 0 -----	69
3-19	SIMULATION OF SRFIMF POSITION CONTROL FOR AIRCRAFT MODE 8, TABLE III-3. THE OPEN LOOP PLANT HAS A NATURAL FREQUENCY OF 0.17 RAD/SEC AND DAMPING RATIO OF 0.590 -----	70

3-20	SIMULATION OF SRFIMF POSITION CONTROL OF AIRCRAFT MODE 9, TABLE III-3. THE OPEN LOOP PLANT HAS TWO POLES AT THE ORIGIN -----	71
3-21	SIMULATION OF SRFIMF POSITION CONTROL OF AIRCRAFT MODE 10, TABLE III-3. THE OPEN LOOP PLANT HAS REAL POLES AT -1.0 AND -0.6 -----	72
4-1	EXPONENTIALLY CORRELATED NOISE SHAPING FILTER -----	74
4-2	HIGH FREQUENCY ERROR MODEL, POSITION CONTROLLER -----	76
4-3	TRACKING ERRORS IN X_1 AS A RESULT OF MEASUREMENT ERROR IN POSITION, VELOCITY AND ACCELERATION -----	91
4-4	TRACKING ERRORS IN X_2 AS A RESULT OF MEASUREMENT ERROR IN POSITION, VELOCITY AND ACCELERATION -----	92
4-5	TRACKING ERRORS IN X_3 AS A RESULT OF MEASUREMENT ERROR IN POSITION, VELOCITY AND ACCELERATION -----	93
4-6	FIRST ALTERNATE MEASUREMENT SCHEME. MEASURED ACCELERATION AND IMPLIED POSITION AND VELOCITY -----	94
4-7	ERROR IN X_1 , X_2 , AND X_3 AS A RESULT OF MEASUREMENT ERRORS IN ACCELERATION -----	97
4-8	SECOND ALTERNATE MEASUREMENT SCHEME, MEASURED POSITION AND VELOCITY. ESTIMATED ACCELERATION -----	98
4-9	TRACKING ERRORS OF X_1 AS A RESULT OF MEASUREMENT ERRORS IN POSITION AND VELOCITY -----	103
4-10	TRACKING ERRORS OF X_2 AS A RESULT OF MEASUREMENT ERRORS IN POSITION AND VELOCITY -----	104
4-11	TRACKING ERRORS OF X_3 AS A RESULT OF MEASUREMENT ERRORS IN POSITION AND VELOCITY -----	105
5-1	ROOT LOCUS OF THE OSCILLATORY POLES OF THE LONGITUDINAL AXIS OF THE HARRIER USING SRFIMF POSITION CONTROL -----	109

5-2	HARRIER LONGITUDINAL SIGNAL FLOW GRAPH TRANSFER FUNCTION SIMULATION -----	111
5-3	SIMULATION OF THE UNIT STEP RESPONSE OF THE PITCH ATTITUDE OF THE AV-8A HARRIER WITH SRFIMF CONTROL -----	112
5-4	SCHEMATIC REPRESENTATION OF THE AV-8A HARRIER PITCH AXIS WITH THE SRFIMF CONTROLLER. INCLUDING SENSOR NOISE -----	114
5-5	TRACKING ERROR IN X_1 AS A RESULT OF MEASURE- MENT ERROR IN POSITION, VELOCITY AND ACCELERATION FOR THE HARRIER LONGITUDINAL AXIS POSITION CONTROL -----	119
5-6	TRACKING ERROR IN X_2 AS A RESULT OF MEASURE- MENT ERROR IN POSITION, VELOCITY AND ACCELERATION FOR THE HARRIER LONGITUDINAL AXIS POSITION CONTROL -----	120
5-7	TRACKING ERROR IN X_5 AS A RESULT OF MEASURE- MENT ERROR IN POSITION, VELOCITY AND ACCELERATION FOR THE HARRIER LONGITUDINAL AXIS POSITION CONTROL -----	121
5-8	GUST SHAPING FILTER -----	124
5-9	SCHEMATIC REPRESENTATION OF THE AV-8A PITCH CONTROL USING A SRFIMF CONTROLLER WITH WIND GUST INPUT -----	126
5-10	STANDARD DEVIATION OF VEHICLE PITCH ACCELE- RATION AND PLANT INPUT, X_5 , AS A RESULT OF A GUST -----	129

LIST OF SYMBOLS

A	matrix of coefficients of the closed loop controller
A*	modal transformation of the matrix of coefficients of the closed loop controller
A(s)	SRFIMF controller compensator transfer function
B	matrix of control input coefficients
B*	modal transformation of the matrix of input coefficients
b	damping term in aircraft rigid-body second order modes
c	stiffness term in aircraft rigid-body second order modes
C*	modal transformation of the SRFIMF output matrix
C	SRFIMF output matrix
CPG	constant plant gain or control power gradient depending upon use
F	implicit model following feedback matrix
f	value of the highly damped root of a SRFIMF system
G	matrix of coefficients of the noise inputs to the SRFIMF system
G(s)	Laplace transform of airplane rigid-body modes
H(s)	transfer function representing the dynamic behavior of control force or moment application
h	height in feet of aircraft center of gravity
K	forward loop gain of SRFIMF controller
KRL	SRFIMF controller gain parameter
K _x	position feedback gain
K _x [.]	rate feedback gain

L matrix of coefficients of the model
L_w characteristic length of atmospheric turbulence
NASA National Aeronautics and Space Administration
P matrix of SRFIMF system covariances
Q matrix of SRFIMF exponentially corellated white noise strengths
RTA Research and Technology Aircraft
s Laplace transform variable
SRFIMF State Rate Feedback Implicit Model Following
T transformation matrix between state variable coordinates and modal coordinates
T_r correlation time of exponentially correlated sensor noises
T_g correlation time of exponentially correlated wind gust noise
U Vector of SRFIMF system inputs
V_{wind} nominal surface wind
W(s) SRFIMF control law
W_t(t) white noise
X(s) controlled variable
X vector of SRFIMF state variables
X* vector of SRFIMF modes
X_c commanded input
X_a* acceleration error mode
X_p* position error mode
X_v* velocity error mode
Y SRFIMF output vector

z vector of model states
 δ general transfer function control input
 δ_g gust input
 δ_e control stick input
 ζ second order response damping ratio
 θ pitch attitude angle
 μ white noise strength
 ξ exponentially correlated noise
 σ standard deviation
 σ_a standard deviation of acceleration error
 σ_g standard deviation of gust input
 σ_p standard deviation of position error
 σ_v standard deviation of velocity error
 τ control actuator time constant
 ω_n natural frequency of second order response

ACKNOWLEDGMENT

With sincere gratitude, the help and encouragement of numerous individuals is acknowledged. Most important, is the patient assistance of my teacher and advisor, Prof. Daniel Joseph Collins. The advise of Dr. J. Franklin and Mr. V. Merrick of the Guidance and Central Branch of the NASA Ames Aeronautical Research Center; Dr. Tsuyoshi Goka of Analytical Mechanics Associates, Inc., and the faculty of the Aeronautics Department of the U.S. Naval Postgraduate School has been invaluable in the production of this study. The work was made considerably easier with the help of Mrs. Adrian Schueneman who scrutinized and typed the early drafts.

Special thanks goes to my wife, Mary Anne, and my family for their support during the long and trying months required to produce this work.

I. INTRODUCTION

A State Rate Feedback Implicit Model Following (SRFIMF) flight controller has been proposed as a possible approach to improving the handling qualities of Vertical and Short Field Take Off and Landing (VSTOL) aircraft by Merrick at the NASA Ames Aeronautical Research Laboratory [1, 2]. The SRFIMF concept has potential applications in various types of control problems encountered in aircraft design, among which are attitude, guidance, and engine control. The concept has not been used in actual flight tests, however several detailed simulations [2, 3] have been conducted at NASA Ames in which SRFIMF control was applied. The most notable features of the control scheme are that:

1. The Input-output relationship of a system using SRFIMF control is insensitive to changes in airframe and propulsion dynamic characteristics.
2. The dynamic relationship of the output to the input is approximately that of a second order system whose frequency and damping is chosen by the designer.
3. The system is self trimming and the commanded output variable is independent of external disturbances.
4. The system has good gust alleviation.

This study presents a detailed analysis of the SRFIMF control concept as applied to the attitude control of VSTOL aircraft.

The following discussion is given to clarify the meaning of State Rate Feedback Implicit Model Following as used in this study. Model following refers to the ability of a control scheme to impart specified dynamic characteristics, given by a model, to the closed loop system. The model being considered here is a second order response in which the parameters of natural frequency and damping ratio are chosen by the designer. Typically a second order response is mathematically defined in terms of the states position and velocity. The state rate of the second order model is the acceleration. The State Rate Feedback Implicit Model Following controller, studied here, achieves model following by measurement and feedback of the system's state rate, acceleration. The result is that a priori knowledge of the plant is not required to produce model following.

To illustrate the use of state rate feedback, consider a plant of second order. With the states of the system x_1 and x_2 , defined as position and velocity, the representation of the plant in matrix notation is

$$\begin{aligned}\dot{x}_1 &= \begin{bmatrix} 0 & 1 \\ -c & -b \end{bmatrix} \begin{Bmatrix} x_1 \\ x_2 \end{Bmatrix} + \begin{Bmatrix} 0 \\ 1 \end{Bmatrix} U(t) \\ \dot{x}_2 &\end{aligned} \quad 1-1$$

The acceleration, \dot{x}_2 , equation is thus

$$\dot{x}_2 = -cx_1 -bx_2 + U(t) \quad 1-2$$

The values of b and c define the dynamic behavior of the plant. Design of a control system would in general require that b and c be known. The feedback scheme or control law of the SRFIMF controller is formulated so that the plant dependent quantities of b and c are only involved in the total quantity of $(-cX_1 - bX_2)$. With this arrangement the quantity, $(-cX_1 - bX_2)$, can be obtained by measurement of the state rate, acceleration, minus the input, U. Model following by measurement of the state rate, as in this illustration, is the basic concept of the SRFIMF controller.

The intent of this study is to provide a detailed analysis of the SRFIMF controller from a modern and classical control viewpoint. Particular emphasis will be placed on a basic description of the control scheme and the effects of measurement errors on the output of the closed loop system. The first two sections deal with a classical analysis of the controller as applied to the attitude position control of a general VSTOL aircraft. The third section considers the effect of measurement errors on the system from a modern control viewpoint. From that analysis, the steady state covariance of the state variables, as a result of measurement uncertainties, will be found. Finally, the previously developed analysis technique will be applied to an example where SRFIMF is used for pitch control of the Harrier aircraft. The effect of sensor errors will be examined and the response of the Harrier to gust inputs will be determined.

The following assumptions are made in this study:

1. The system is linear. Non-linear effects such as control saturation and actuator hysteresis are not considered.
2. The dynamic response of the plant will be represented at a single point by linearized, rigid-body, transfer functions.
3. Measurement uncertainties are represented as exponentially correlated noise and the effect of bias error is not considered. The basic description and development of the SRFIMF controller will be considered in section II.

II. DESCRIPTION OF THE SRFIMF CONTROLLER

A. THE BASIC SCHEME

It is desirable for a flight controller to impart specific dynamic characteristics to the closed loop response of an aircraft system. Often the desired response is given in terms of a natural frequency and damping ratio. Piloted simulations at NASA Ames [2] have indicated that a desirable response from the pilot's stick to the aircraft attitude is a second order response whose natural frequency, ω_n , is approximately 2 rad/sec and damping ratio, ζ , of 0.75. One possible approach to the design of an attitude controller is to apply model following techniques. Mathematically the model for attitude control dynamics can be represented by a transfer function in the frequency domain. If, as an example we let $\theta(s)$ represent the aircraft pitch angle and $\delta(s)$ the elevator control input, then the transfer function of a model for pitch attitude control can be written as

$$\frac{\theta(s)}{\delta(s)} = \frac{1}{s^2 + 2\zeta\omega_n s + \omega_n^2} \quad 2-1$$

In this example, if the desired response has a natural frequency of 2 rad/sec and damping ratio of 0.75, and equation 2-1 becomes

$$\frac{\theta(s)}{\delta(s)} = \frac{1}{s^2 + 3s + 4} \quad 2-2$$

This transfer function will be used to illustrate model following techniques in the development of the SRFIMF concept. The desired model response, given by 2-1, can also be expressed in state variable notation with states z_1 of position and z_2 velocity. The matrix of coefficients of the model is given the symbol L and equation 2-1 can be written as

$$\begin{aligned}\dot{z} &= [L]z + [B]U \\ &= \begin{bmatrix} 0 & 1 \\ -\omega_n^2 & -2\zeta\omega_n \end{bmatrix} z + \begin{Bmatrix} 0 \\ 1 \end{Bmatrix} U\end{aligned}\quad 2-3$$

Given somewhat arbitrary open loop plant dynamics, the object of model following is to produce a closed loop system whose dynamic characteristics are given by equation 2-1 or equation 2-3.

For a general system

$$\begin{aligned}\dot{x} &= Ax + Bu \\ y &= cx\end{aligned}\quad 2-4$$

the object of implicit model following is to force the output of the system to follow the model equation

$$\dot{z} = LZ + BU \quad 2-5$$

That is to say, the output, Y, should approximate Z ($Y \approx Z$) so that

$$\dot{y} = LY + BU \quad 2-6$$

By proper choice of the feedback gain F, as shown in figure 2-1, the output is forced to follow equation 2-6. The

implied model shown in the upper portion of the figure, is not actually generated but implied by the behavior of y .

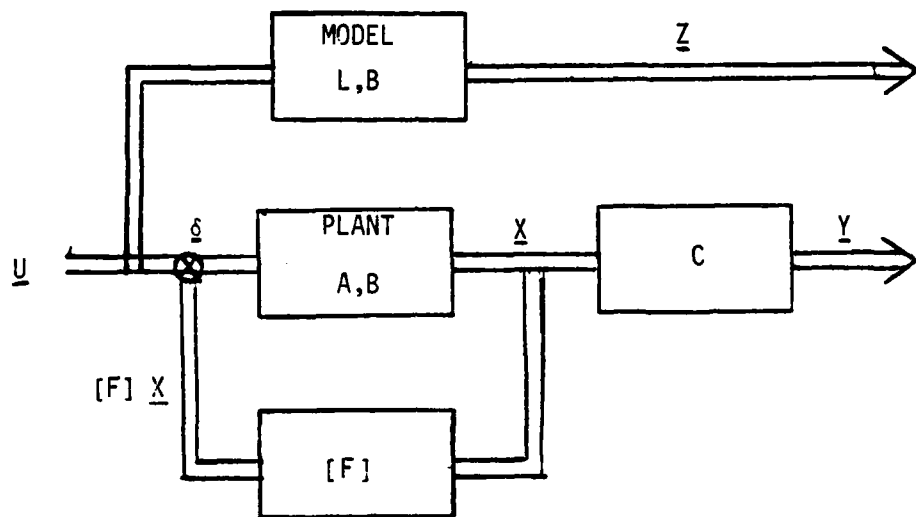


Figure 2-1 Implicit Model Following scheme

The formulation of the feedback law required in model following has been determined by Taylor [4] using optimal control techniques. In addition, Erzberger [5] has defined algebraic methods for determining if perfect model following can be achieved. This algorithm will be examined later in this section. In aircraft applications certain physical facts about the system allow a form of implicit model following to be obtained by simple intuitive reasoning.

Consider the problem of stabilizing the pitch attitude of a VSTOL aircraft. The following assumptions can be made and will lead to a simplified SRFIMF controller:

1. The desired model response is of second order with frequency, ω_n , of 2 rad/sec and damping ratio, ζ , of 0.75 from equation 2-1.

2. Measurements of angular position, angular rate and angular acceleration are available.

3. The control U is either a thrust or control deflection whose net result is to produce angular acceleration of the vehicle.

4. The open loop plant is arbitrary and the transfer function for θ , $\theta(s)/U(s) = G(s)$, may be unknown.

5. The control law which produces model following will be developed so that it represents the difference between the vehicle's angular acceleration, as measured, and the angular acceleration which would be implied by the model given in 1, above.

From assumption 1 we obtain the desired closed loop response as that of the model and express it as

$$\frac{\theta(s)}{U(s)} = \frac{1}{s^2 + K_x s + K_x} \quad 2-7$$

where $\theta(s)$ is the pitch attitude and the constants K_x and K_x' are defined for convenience and will be used throughout this study as

$$K_x = 2\zeta\omega_n = 3 \quad 2-8$$

$$K_x' = \omega_n^2 = 4 \quad 2-9$$

By requiring the model, equation 2-7, to hold we observe that the implied angular acceleration is

$$s^2\theta(s) = -K_x\theta(s) - K_{\dot{x}}s\theta(s) + U(s) \quad 2-10$$

$\theta(s)$ and $s\theta(s)$ are angular position and angular rates which, by assumption 2, are available from measurements. The quantity $U(s)$ is the input to the open loop plant. Given $\theta(s)$, $s\theta(s)$ and $U(s)$, the quantity $s^2\theta(s)$ can be calculated from equation 2-10.

We will define $W(s)$ as the control law for the system. $W(s)$ will be taken as the difference between the implied model acceleration $s^2\theta(s)$ and the actual measured acceleration

$$W(s) = s^2\theta(s) - (\text{measured acceleration}) \quad 2-11$$

Using equation 2-10 and substituting for $s^2\theta(s)$ one has

$$W(s) = -K_x\theta(s) - K_{\dot{x}}s\theta(s) + U(s) - (\text{measured acceleration}) \quad 2-12$$

Further the quantities $\theta(s)$ and $s\theta(s)$ will be determined by sensors so that

$$W(s) = -K_x \cdot (\text{measured position}) - K_{\dot{x}} \cdot (\text{measured rate}) + U(s) - (\text{measured angular acceleration}) \quad 2-13$$

The quantity $U(s)$ could be considered pilot or other control input to the plant. Since we also defined $W(s)$ as the control there is some ambiguity in the notation. The symbol $U(s)$ will be used consistently for the control feedback quantity as indicated in figure 2-2.

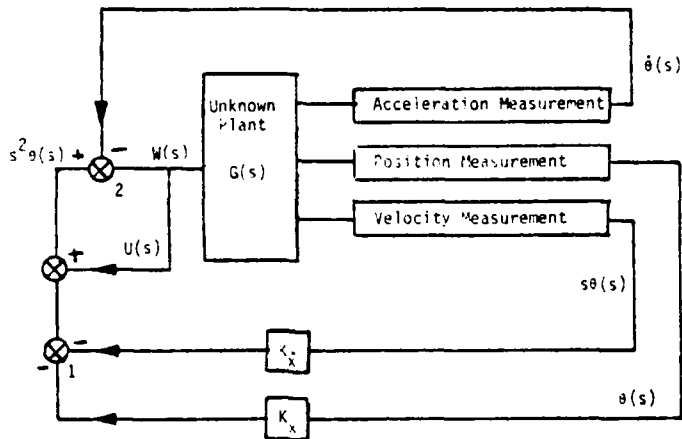


Figure 2-2 SRFIMF position controller developed by intuitive arguments.

Figure 2-2 shows schematically the control law and unknown plant $G(s)$. It can also be seen that the plant input, $U(s)$ is a feedback quantity and the implied acceleration, $s^2\theta(s)$ is compared to the measured acceleration at point 2 of the figure. The term state rate feedback is applied to this type of control because of acceleration feedback. It is this measurement which brings to the controller information about the plant making a priori knowledge of the transfer function for $\theta(s)$ unnecessary. This aspect of the SRFIMF controller is most clearly seen by application of the Erzberger criterion mentioned earlier.

The Erzberger criterion for exact implicit model following is obtained by analysis of the system in state space representation where the system is given by

$$\dot{X} = AX + BU \quad 2-14$$

$$Y = CX \quad 2-15$$

For implicit model following the output is approximated by

$$\dot{Y} = LY \quad 2-16$$

Taking the derivative of equation 2-15, one has

$$\dot{Y} = CX \quad 2-17$$

Substituting from equation 2-14

$$\dot{Y} = C(AX + BU) \quad 2-18$$

or

$$\dot{Y} = CAX + CBU$$

but from equations 2-15 and 2-16 one has

$$\dot{Y} = LY = LCX \quad 2-19$$

so that one has, on equating 2-18 and 2-19,

$$CAX + CBU = LCX$$

or

$$CBU = (LC - CA) \cdot X$$

Solving for the control, U , from 2-20 we have that

$$U = \left[(CB)^+ \cdot (LC - CA) \right] X \quad 2-21$$

where $(CB)^+$ is the pseudo, or generalized, inverse of (CB) . Eliminating U from 2-20 and 2-21, the condition for perfect model following becomes

$$[(CB)(CB)^+ - I][(LC) - (CA)] \cdot X = 0 \quad 2-22$$

The use of the pseudo inverse is based on the property of the pseudo inverse that $(CB)(CB)^+$ is an orthogonal projection operator on the range of (CB) . It then follows that if 2-22 holds for all X , the range of CB must contain the range of $(LC-CA)$. This implies that 2-16 is valid which has already been assumed to be the case.

We will now apply equation 2-22 to the pitch attitude controller given earlier. In this case $\theta(s)/U(s)$ is assumed to be the transfer function of an arbitrary second order system.

$$\frac{\theta(s)}{U(s)} = \frac{1}{s^2 + bs + c}$$

The desired closed loop performance is given by the model as in equation 2-7. For this example we initially take the feedback quantities to be angular position and angular rate. Defining the quantities in state variable representation we have the plant where

$$x_1 = \theta(t)$$

$$x_2 = \dot{\theta}(t)$$

$$\dot{X} = [A] X + BU$$

$$= \begin{bmatrix} 0 & 1 \\ -c & -b \end{bmatrix} \begin{Bmatrix} x_1 \\ x_2 \end{Bmatrix} - \begin{Bmatrix} 0 \\ 1 \end{Bmatrix} U$$

2-23

and

$$Y = CX$$

or

$$Y = \begin{bmatrix} 1 & 0 \\ 0 & 1 \end{bmatrix} \begin{Bmatrix} x_1 \\ x_2 \end{Bmatrix}$$

2-24

Calculation of the pseudo inverse depends upon the relative rank of C and B in this case, following Noble [6], the pseudo inverse of (CB) is given as

$$(CB)^+ = [(CB)^+ \cdot (CB)]^{-1} \cdot (CB)^T$$

From 2-23 and 2-24

$$(CB) = \begin{Bmatrix} 0 \\ 1 \end{Bmatrix}$$

therefore

$$(CB)^+ = [0 \ 1]$$

To determine if perfect model following is possible, we substitute into 2-22 using 2-23, 2-24, 2-8, 2-9 and the above for (CB) and (CB)⁺

$$[(CB)(CB)^+ - I] = \begin{bmatrix} -1 & 0 \\ 0 & 0 \end{bmatrix} \quad 2-25$$

$$[(LC) - (CA)] = \begin{bmatrix} 0 & 0 \\ -(K_x + c) & -(K_{\dot{x}} + b) \end{bmatrix} \quad 2-26$$

The result is that

$$[(CB)(CB)^+ - I] [(LC) - (CA)] \equiv 0 \quad 2-27$$

Equation 2-27 shows that perfect model following is possible for all X using position and rate feedback only. The control can be determined by equation 2-21 with the result

$$U_c = [(-K_x + c)(-K_{\dot{x}} + b)] \begin{Bmatrix} X_1 \\ X_2 \end{Bmatrix} \quad 2-28$$

$$= -K_x X_1 - K_{\dot{x}} X_2 + cX_1 + bX_2 \quad 2-29$$

The control law given in equation 2-29 requires that the constants c and b be known in order to produce the desired model following. In the previous discussion we stated that the addition of acceleration feedback provided the needed information about the plant. To show this, note that the latter two terms of equation 2-29, $cX_1 + bX_2$, can be interpreted in terms of the acceleration of the system, X_2 , since

$$\dot{X}_2 = -cX_1 - bX_2 + U(s) \quad 2-30$$

one has

$$\dot{X}_2 - U(s) = -cX_1 - bX_2 \quad 2-31$$

or rewriting equation 2-29 one has

$$U_C = -K_X X_1 - K_{\dot{X}} \dot{X}_2 + U(s) - \dot{\dot{X}}_2 \quad 2-32$$

We can compare this to equation 2-13 rewritten in the same notation

$$W(s) = -K_X X_1 - K_{\dot{X}} \dot{X}_2 + U(s) - (\text{measured angular acceleration}) \quad 2-33$$

Note, X_1 and X_2 are the measured angular position and measured angular rate. This comparison shows that the measured acceleration supplies the terms needed for perfect model following without a need for a knowledge of the plant dynamics.

The significance of this result is that state rate feedback can be used to provide information about the plant in applications where the plant has unknown and changing dynamic characteristics. This conclusion was reached based upon the assumption that the plant was of second order. We shall now consider a more general form of the SRFIMF controller and we will show that model following can be achieved by measurement of state rate for a higher order plant.

B. THE GENERAL FORM OF THE SRFIMF CONTROLLER

The preceding discussion presented an intuitive description of the principal operation of the SRFIMF controller and the use of state rate feedback. It is the intent of this section to develop a general form of state rate feedback and

to show again that model following can be achieved without a priori knowledge of the plant by using measurement of the state rate. We begin by examining the basic SRFIMF controller as developed by Merrick at NASA Ames. The block diagram of this controller is shown in figure 2-3.

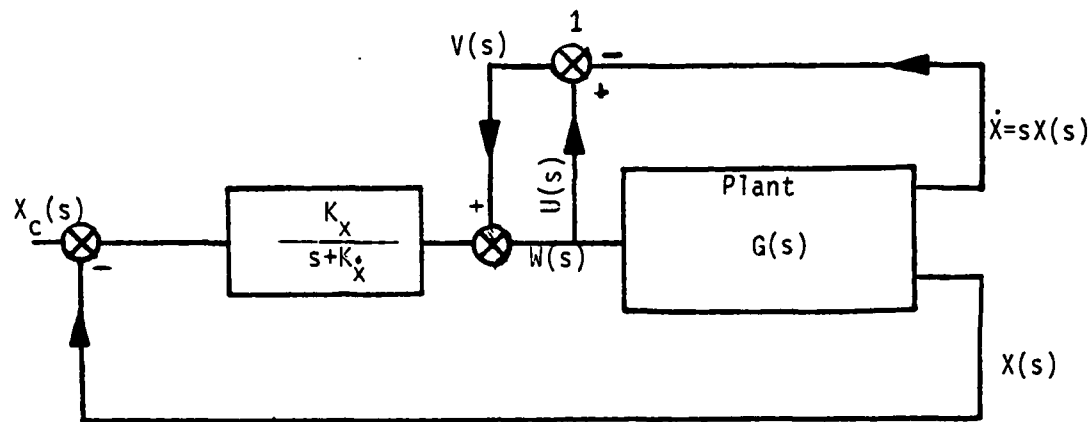


Figure 2-3 The general form of the SRFIMF controller.

Assume that figure 2-3 represents a velocity controller, then the feedback quantities $X(s)$ and $sX(s)$ are velocity and acceleration respectively. It can be seen that at position 1 we are summing (- acceleration + $U(s)$). It will be shown that the transfer function between the input $X_c(s)$ and the output $X(s)$ does not depend upon the plant transfer function $G(s)$ and that the closed loop response is that of a second order system whose damping and natural frequency are determined by the choice of feedback constants K_x and $K_{\dot{x}}$.

From figure 2-3 $W(s)$ is given by

$$W(s) = U(s) - sX(s) + [X_C(s) - X(s)] \cdot \left[\frac{K_X}{s + K_{\dot{X}}} \right] \quad 2-34$$

and for $V(s)$ we write

$$V(s) = U(s) - sX(s) \quad 2-35$$

from the definition of the transfer function $G(s)$ we have
that

$$X(s) = W(s) G(s) \quad 2-36$$

Combining 2-34 and 2-36 we have that

$$X(s) = \left\{ U(s) - sX(s) + \frac{(X_C(s) - X(s)) K_X}{s + K_{\dot{X}}} \right\} G(s) \quad 2-37$$

Since $U(s) = W(s)$ as seen from figure 2-3, we have

$$X(s) = U(s) \cdot G(s) \quad 2-38$$

and equation 2-37 can be rewritten as

$$X(s) = X(s) - sX(s)G(s) + \frac{(X_C(s) - X(s)) K_X}{s + K_{\dot{X}}} G(s) \quad 2-39$$

and

$$sX(s)G(s) = \frac{(X_C(s) - X(s)) K_X}{s + K_{\dot{X}}} \cdot G(s) \quad 2-40$$

$G(s)$ on both sides of equation 2-40 cancels and the result becomes

$$\frac{X(s)}{X_C(s)} = \frac{K_X}{s^2 + K_{\dot{X}}s + K_X} \quad 2-41$$

Equation 2-41 shows that the closed loop response of the SRFIMF is identically that of a second order system whose natural frequency and damping ratio is completely determined by the constant feedback gains which are given by

$$\omega_n = K_x \quad \zeta = \frac{K_x}{2\sqrt{K_x}}$$

The results of this analysis indicate that the SRFIMF controller is an excellent candidate for VSTOL aircraft applications. The form of the controller shown in figure 2-2 could be used to control a position such as attitude while the general form shown in figure 2-3 might be used to control rates or velocity. It will now be necessary to examine the requirements necessary to implement a SRFIMF controller in an aircraft. In particular, the exact relationship between $U(s)$ and $W(s)$ must be considered. The next section will examine practical examples of SRFIMF controllers in a realistic aircraft environment.

C. PRACTICAL EXAMPLES OF THE SRFIMF CONTROLLER

Two types of controllers are illustrated in this section, a position controller, figure 2-4, and a velocity controller, figure 2-5. A first order actuator is included in the plant of each controller. Also included is a compensator in the control feedback loop involving $U(s)$. The system is not realizable without the compensator. These controllers will be used in the analysis of this report.

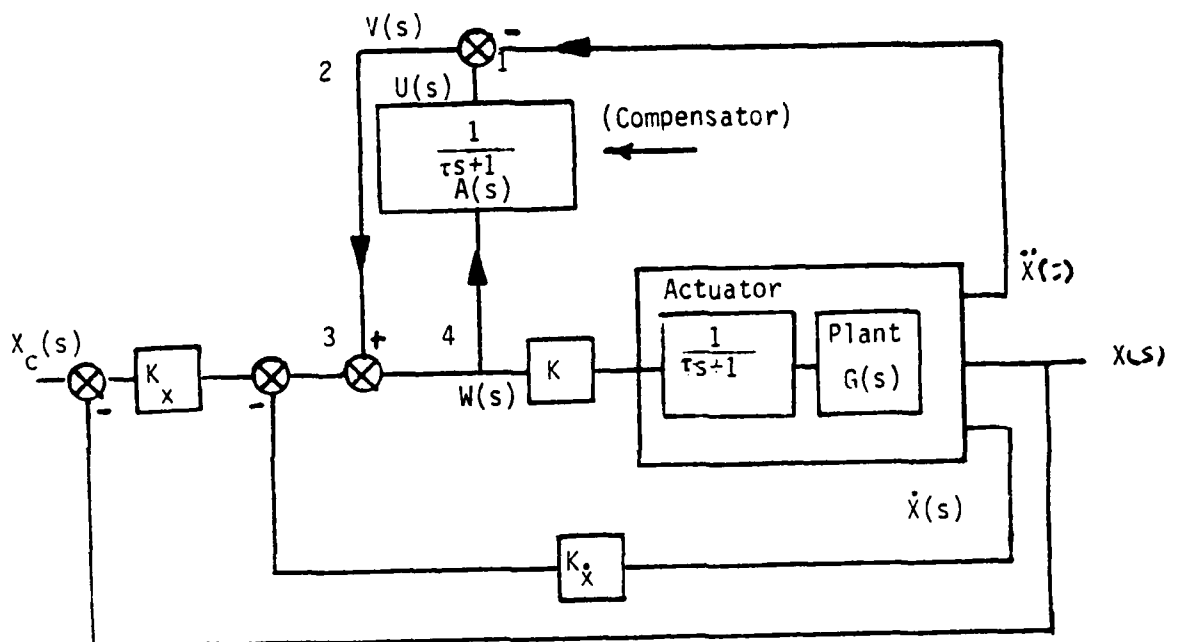


Figure 2-4 Physically realizable SRFIMF position controller.

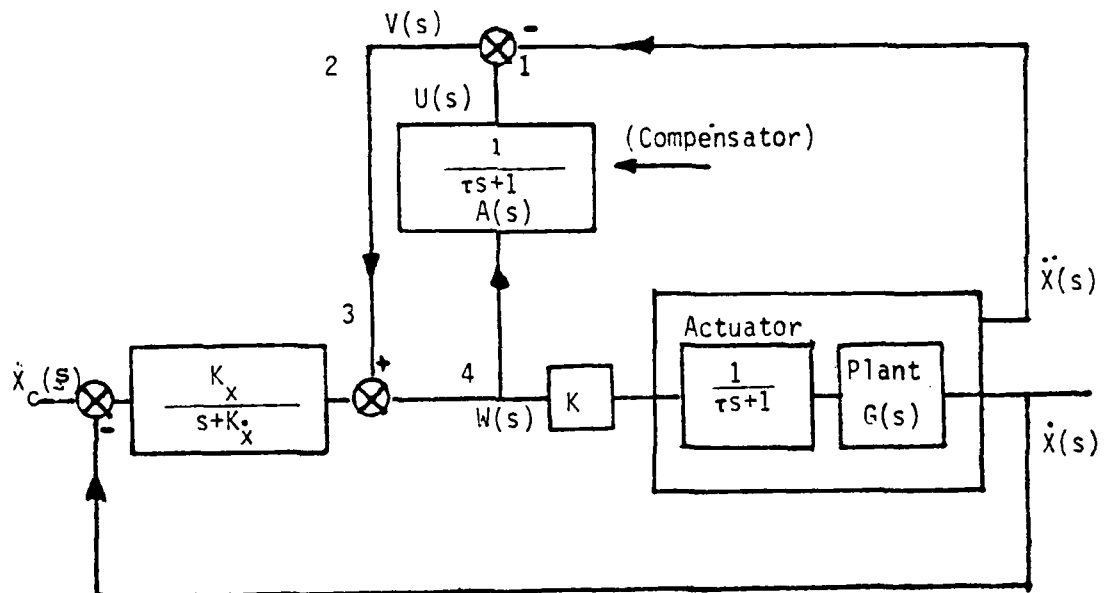


Figure 2-5 Physically realizable SRFIMF rate controller.

The plant is assumed to be driven by a control actuator and because of that a phase lag can be expected to exist between the commanded control signal, $W(t)$ and the input of the plant. The effect of the actuator will be modeled by using the first order transfer function

$$\frac{H(s)}{W(s)} = \frac{1}{(\tau s + 1)} \quad 2-42$$

where $H(s)$ is the output of the actuator, $W(s)$ is the input and τ is the actuator time constant assumed to be 0.1 sec for all of the examples considered in this work. Recall from a previous section that SRFIMF feedback contained a term $U(t)$ which represented the control input to the plant and that $W(t)$ was assumed to equal $U(t)$. Because of the fact that $U(t)$ was equal to $W(t)$ the output signal of the controller could be used to cancel the $U(t)$ term in the acceleration feedback.

It was shown that

$$\text{acceleration} = -cX_1 - bX_2 + U(t) \quad 2-43$$

and it was assumed that

$$U(t) = W(t) \quad 2-44$$

In order for equation 2-44 to be valid, the system would need to have instantaneous response to any input. Because of the action of the control actuator this is not possible and a compensator is placed in the feedback loop between $W(s)$ and the summing junction at 1, as shown in figures 2-4 and 2-5. The compensator transfer function is $A(s)$. $A(s)$ is chosen so that the output of the compensator is dynamically identical to the input of the plant, after the control actuator. When the control is represented by a first order lag, as in this case, $A(s)$ is the same as the transfer function of the actuator. In cases of higher order actuator dynamics the result is more complicated. An algorithm for determining the necessary transfer function, $A(s)$, which must be used in the feedback is given by Merrick [2]. We will assume a first order actuator and a compensator of the form $1/(ts + 1)$ as shown in figures 2-4 and 2-5, for the remainder of this work.

Actual controllers used at NASA Ames are illustrated in figures 2-6 and 2-7. Figure 2-6 is a speed controller. The quantities VD and VDD represent the measured speed and acceleration. VC is the commanded speed and $W(s)$ is the output of the controller. Figure 2-7 is a SRFIMF position controller used to control the pitch attitude, θ , of the RTA vehicle. The limiters seen in the figures are not included in the model studied here. The purpose of the limiter is to prevent the control feedback loop from acting as an integrator when the plan control is saturated. This condition could occur

when a large difference between the commanded variable, X , and the input variable, X_C , existed and the plant control was saturated. In this condition $W(s)$ would increase without bound and a reversal of the input would be delayed because of the very high value of $W(t)$ at the time the control reversal was applied. The limiter was not considered here because of the assumption of linearity.

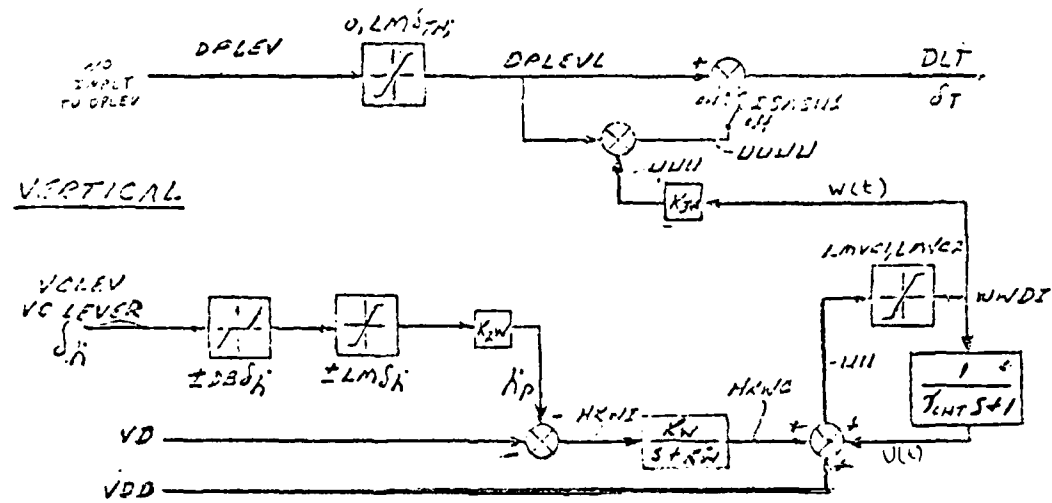


Figure 2-6 SRFIMF controller employed on the RTA for speed control.

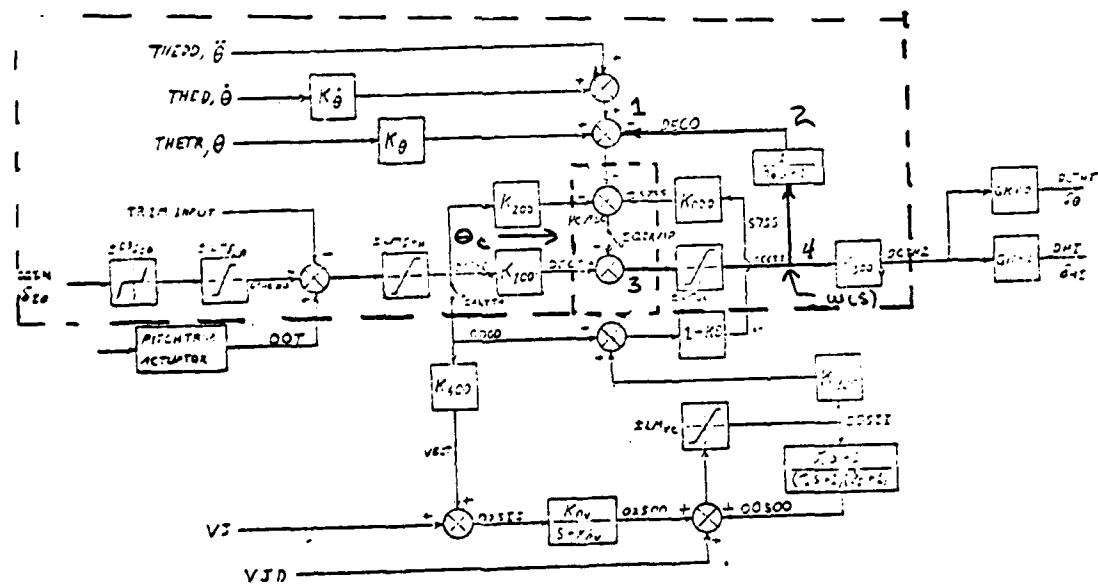


Figure 2-7 SRFIMF controller employed on RTA for pitch attitude control.

III. TIME AND FREQUENCY DOMAIN ANALYSIS OF THE SRFIMF

A. REPRESENTATIVE AIRCRAFT PLANT DYNAMICS

The State Rate Feedback Implicit Model Follower controller presented in section II, figure 2-4 will now be examined using Root Locus, Bode Analysis and Time Simulations. Root Locus analysis will show the asymptotic behavior of the closed loop poles and Bode analysis will show the filter characteristics of the controller. Simulated time response of the controller will be shown in order to demonstrate the ability of the SRFIMF to follow the given model and to show graphically the self trimming feature of the controller. The model and representative plant will next be defined.

The model for the system is taken as a second order system with a transfer function given by

$$\frac{M(s)}{U(s)} = \frac{K_x}{s^2 + K_x s + K_x} \quad 3-1$$

The gains K_x and $K_{\dot{x}}$ are selected to yield two different models, one a position controller and the other a rate controller as shown in the following table.

	ω_n	ζ	K_x	$K_{\dot{x}}$	Pole Location
Attitude Control	2 rad/sec	.75	4	3	-1.5 1.32i
Rate Control	1.23 rad/	.7023	1.57	1.76	-.88 .89i

TABLE 3-1 Assumed Model Constants.

The values listed in table 3-1 are based upon piloted simulations at NASA Ames [2] and reflect what has been judged to be representative of good handling qualities.

The plant transfer function is also taken as a second order system

$$G(s) = \frac{CPG}{s^2 + bs + c} \quad 3-2$$

While initially this assumption may seem unrepresentative of a real aircraft, proper choice of b and c can represent the dynamic behavior of the individual modes of any aircraft, provided that first order modes are taken two at a time. To illustrate, consider the general transfer function

$$C(s) = \frac{\prod_{i=1}^M (s + z_i)}{s \prod_{J=1}^q (s + p_J) \prod_{K=1}^r (s^2 + 2\zeta_K \omega_K s + \omega_K^2)} \quad 3-3$$

If the poles are distinct then equation 3-3 can be expanded into partial fractions as follows

$$C(s) = \frac{a}{s} + \sum_{J=1}^q \frac{a_J}{s + p_J} + \sum_{K=1}^r \frac{b_K(s + \zeta_K \omega_K) + C_K w_n \sqrt{1 - \zeta_K^2}}{s^2 + 2\zeta_K \omega_K s + \omega_K^2} \quad 3-4$$

It can be seen from the above that the response of a higher order system is composed of a summation of first and second order terms. When the first order terms are taken two at a

time, the total system response can be expressed as the sum of only second order terms with constant numerators. The assumption of linearity allows us to analyze the modes independently. It remains to choose values of b and c which represent typical aircraft modes. To do this, it will be necessary to survey several representative aircraft. From this survey a number of modes will be selected as typical of VSTOL applications. It will be assumed that acceptable control of each of the modes will lead to acceptable control of the system. This method of analysis leads to considerable simplification since it allows the plant to be taken as a second order system. While this simplified plant will serve the majority of the analysis, a more complex plant will be examined in section V.

Table 3-2 is a listing of pole locations for selected aircraft. Figure 3-1 is a sketch of these poles in the complex plane and an assumed envelope of VSTOL pole locations. Table 3-3 lists points which will be considered by time simulation. From this list, four representative modes will be examined by root locus.

AIRCRAFT	FLIGHT CONDITION	FREQUENCY/DAMPING		OSCILLATORY POLES		REAL POLES	
		ω_n	ζ	Re.	Im.	$1/T_1$	$1/T_2$
F106	S.L. M=.2	2.42	.62	-1.5	1.9	-.169	-.59
	Lateral/Directional 20,000', M=.9	3.01	.159	-.48	3.0	-1.84	+.006
A4 Longitudinal	S.L. M=.2 short period	1.56	.31	-.48	1.5		
	long period	1.52	.087	-.013	.15		
	15,000', M=.9 short period	.623	.344	+.20	.585		
	long period	.12	-.078	+.01	.12		
A4	S.L. M=.2	1.89	.05	-.09	1.89	-.065	-.56
Lateral/Directional	15,000', M=.9	6.61	.096	-.641	6.6	-2.48	-.006
VZ4	0 kts.	.731	-.439	+.32	.66	-.82	-.137
	Longitudinal 26.5 kts.	2.16	.4	-.086	.20		
	75.6 kts. short period	3.4	.374	-.127	3.4		
VZ4	long period	.316	.346	-.11	.30		
	0 kts.	.669	-.347	+.30	.63	-.65	-.90
	Lateral/Directional 75 kts.	1.59	.421	-.67	1.4		
H13 (helio)	0 kts.	.43	-.250	+.10	.42	-.69	-.87
	115 kts.	.38	-.043	+.016	.40	-.9	-1.05
Harrier	0 kts.	.31	-.48	+.148	.27	-.33	-.02
Longitudinal	60 kts.	.32	-.91	+.30	.13	-.073	-1.0
Harrier	0 kts.	.52	-.50	+.26	.45	-.015	-.58
Lateral/Directional	60 kts.	1.2	-.28	+.336	1.15	-.068	-1.26
	120 kts.	1.8	-.15	+.27	1.78	-.056	-1.73

Table 3-2 Typical aircraft pole locations where the characteristic equation has the form

$$(s + 1/T_1)(s + 1/T_2)(s^2 + 2\zeta\omega_n s + \omega_n^2) = 0$$

Source: References [4 & 6]

TYPICAL AIRCRAFT POLES

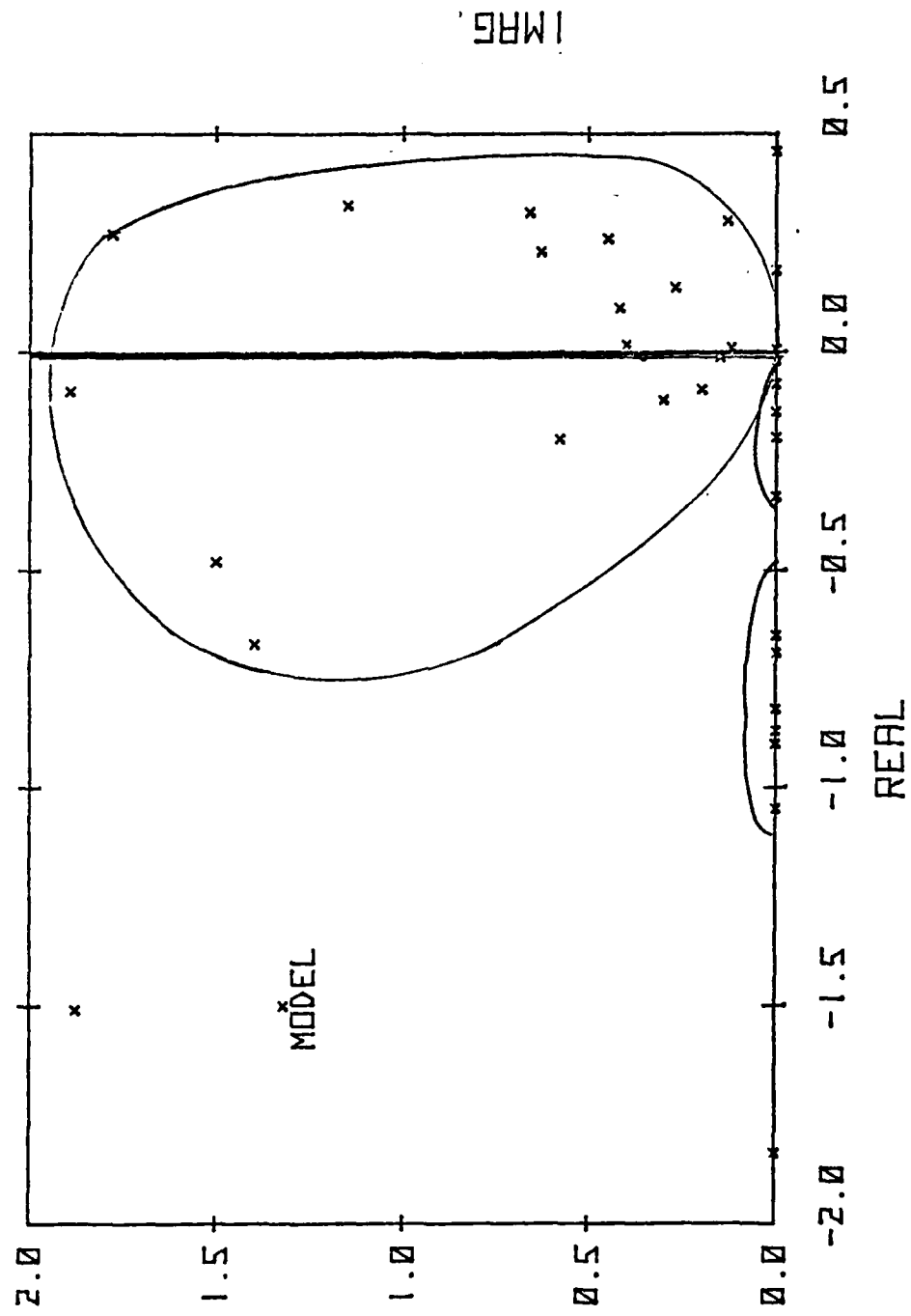


Figure 3-1 Typical aircraft pole locations.

<u>Mode #</u>	<u>Real</u>	<u>Im.</u>	<u>b</u>	<u>c</u>
1	-.6	3.	1.2	8.64
2	-.15	2.15	0.3	6.23
3	-.3	1.0	0.6	0.91
4	-0.1	0.3	0.2	0.08
5	-0.2/0.		0.2	0.0
6	0.3	1.5	-0.6	2.16
7	0.3	0.0	-0.6	0.0
8	0.1	0.14	-0.2	0.03
9	0.0	0.0	0.0	0.0
10	-1.0/ 0.6		1.6	0.6

Table 3-3 Aircraft modes used in simulations.

The modes were chosen to be typical of
VSTOL aircraft as seen in figure 3-1.

B. FREQUENCY RESPONSE AND BODE ANALYSIS

The object of Bode Analysis is to examine the frequency response characteristics of the SRFIMF controller. It will be necessary to develop the transfer function of the position controller shown in figure 2-4. The plant transfer function is given in general as

$$G(s) = \frac{X(s)}{W(s)} = \frac{CPG}{s^2 + bs + C}$$

As in earlier sections the control actuator transfer function, $H(s)$, is assumed to be of the form

$$H(s) = \frac{1}{(\tau s + 1)} \quad 3-5$$

The transfer function of the plant is given by $G(s)$, the output position, defined as $X(s)$ and the commanded input is $X_C(s)$. The compensator shown in figure 2-4, and described in section 2-3 is

$$A(s) = \frac{1}{(\tau s + 1)} \quad 3-6$$

From figure 2-4 we can write at point 1, the equation

$$V(s) = A(s)W(s) - s^2X(s)$$

where $s^2X(s)$ is now the acceleration feedback. We write the control quantity, $W(s)$, from figure 2-4 as

$$W(s) = U(s) - K_x s X(s) - K_x [-X(s) - X_C(s)] \quad 3-7$$

and also note

$$x(s) = K \cdot G(s) \cdot H(s) \cdot W(s)$$

3-8

Combining and rearranging the above expressions we have
that

$$X_C(s) K_X = \left(\frac{(1 - A(s))}{K} \cdot \frac{1}{G(s)H(s)} + s^2 + K_X s + K_X \right) \cdot X(s)$$

and further rearrangement leads to the transfer function for
the input-output relation

$$\frac{X(s)}{X_C(s)} = \frac{K_X}{\left(\left[\frac{1-A(s)}{K} \right] \cdot \frac{1}{G(s)H(s)} \right) + s^2 + K_X s + K_X} \quad 3-9$$

It will be convenient to separate the constant plant gain,
CPG, from the plant transfer function. The remaining transfer
function, defined as $G'(s)$, has a unity constant gain. Stated
another way

$$G(s) = CPG \cdot G'(s)$$

3-10

The parameter KRL is thus defined as

$$KRL = K \cdot CPG / \tau$$

Substituting for $A(s)$, $H(s)$, and KRL and, rearranging 3-9 we
are left with

$$\frac{X(s)}{X_C(s)} = \frac{KRL \cdot K_X}{s \left(\frac{1}{G'(s)} \right) + KRL (s^2 + K_X s + K_X)} \quad 3-12$$

Equation 3-12 shows the effect of the SRFIMF gain parameter,
 KRL . As KRL increases, the model term $(s^2 + K_X s + K_X)$,

becomes more dominant in the closed loop transfer function.

Using equation 3-12, we can examine the frequency response of the controller.

Assuming the plant transfer function to be a second order system given by $G(s)$, equation 3-2, equation 3-12 can be rewritten as

$$\frac{X(s)}{X_C(s)} = \frac{KRL \cdot K_X}{s^3 + (KRL + b)s^2 + (KRL K_X + c)s + K_X \cdot KRL} \quad 3-13$$

The dominant effect of KRL in equation 3-13 is again seen in the coefficients of the s and s^2 terms. From table 3-2 we see that a likely range in the values of b and c are $-0.6 \leq b \leq 1.6$ and $0.0 \leq c \leq 8.64$. If KRL is of the order of 25 and b and c are in the range of 2 and 8 respectively, then KRL will dominate the terms of equation 3-13 which contain b and c . Equation 3-13 can be simplified by neglecting b and c with resulting transfer function for the closed loop system written as

$$\frac{X(s)}{X_C(s)} = \frac{KRL \cdot K_X}{s^3 + KRL(s^2 + KRL K_X s + K_X)} \quad 3-14$$

From this later representation it is clear that the plant dynamics which were determined by the coefficients b and c no longer play a role in the frequency response analysis.

Equation 3-14 expressed in Bode form becomes

$$\frac{X(s)}{X_C(s)} = \frac{KRL \cdot K_X}{(i\omega)^3 + KRL(i\omega)^2 + KRL K_X(i\omega) + KRL K_X} \quad 3-15$$

Equation 3-15 was plotted for frequencies from .01 to 100 and for KRL values of 1, 10, 25, 50 and 100. Figures 3-2 to 3-6 are the plots of the frequency response of the closed loop system. It can be seen that the frequency response of the system is that of a low pass filter with a break frequency of around 3.0 and a 40 db/Dec roll off. It is also seen that the response is very nearly in phase with the input for frequencies lower than 3.0. The results of the frequency response analysis show that the controller possesses good frequency response characteristics from the input to the output in that it has a flat response for all input frequencies of interest and little, if any phase shift. It has also been shown by Merrick [2] that the controller attenuates plant disturbances in the form of applied accelerations. The question of control disturbances will be examined from a different point of view in section V. We shall now consider the requirements for the gain, KRL, by root locus analysis.

C. ROOT LOCUS ANALYSIS

The intent of the root locus analysis is to determine the magnitude of the SRFIMF controller gain parameter, KRL, necessary for acceptable model following. Plots of the root locus of the oscillatory pole will show that the desired closed loop pole location is approached asymptotically as KRL is increased. Acceptable performance is determined by the specific application for which the SRFIMF controller is used. We begin by examining the equations for the closed loop system developed in the preceeding section.

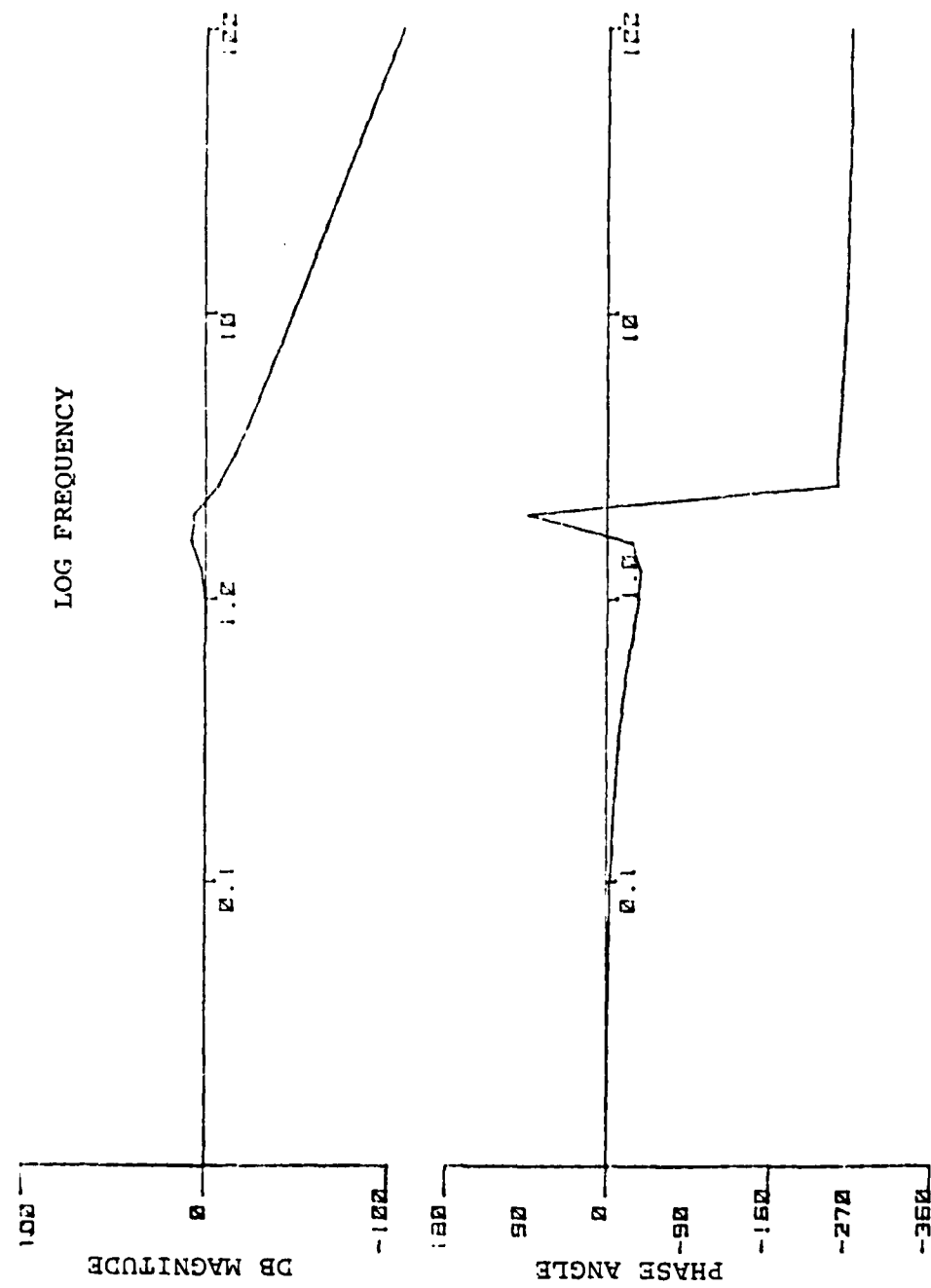


Figure 3-2 Frequency response of SRFIMF position controller, KRL = 1.

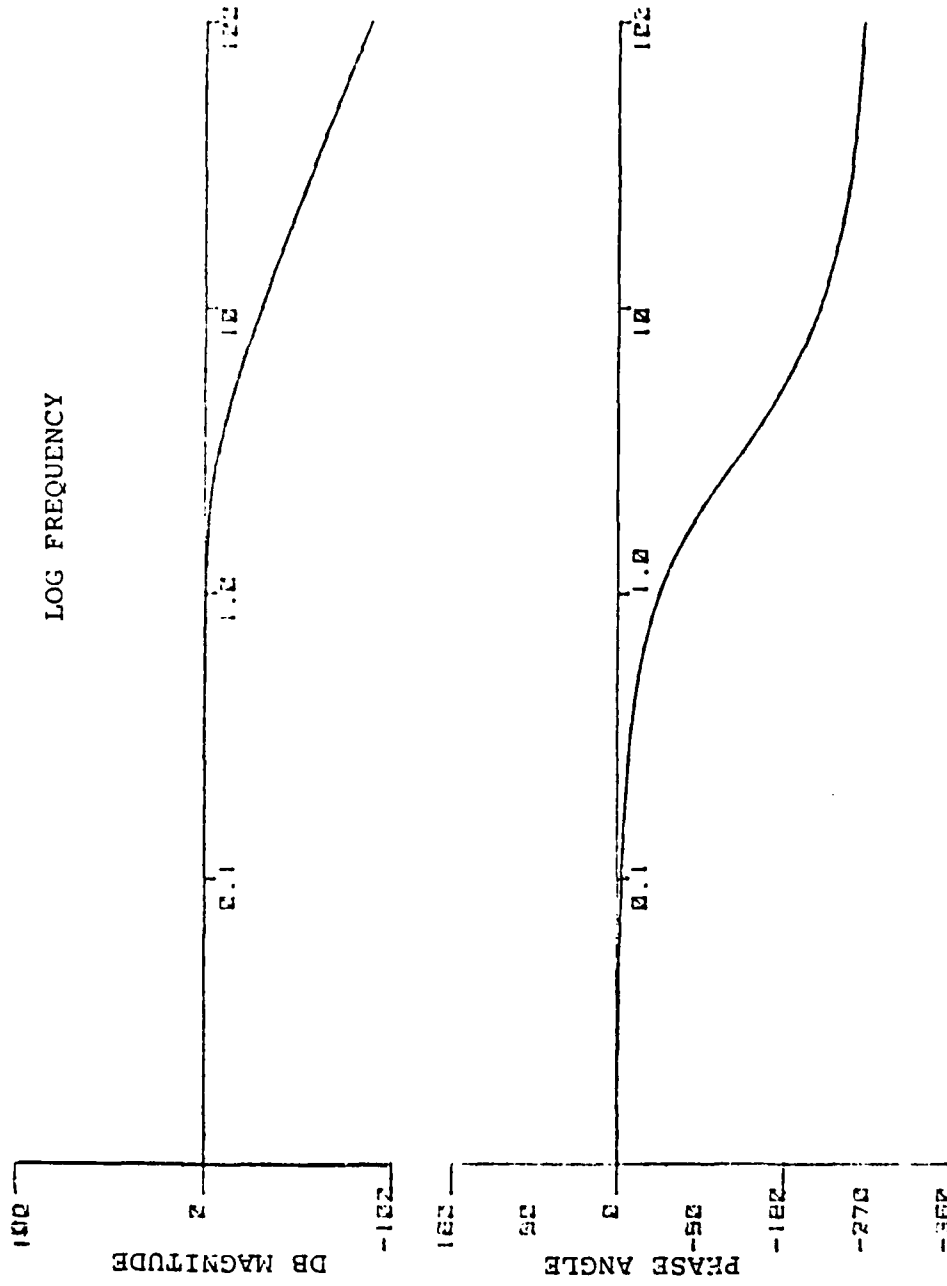


Figure 3-3 Frequency response of SRFIMF position controller, KRL = 10.

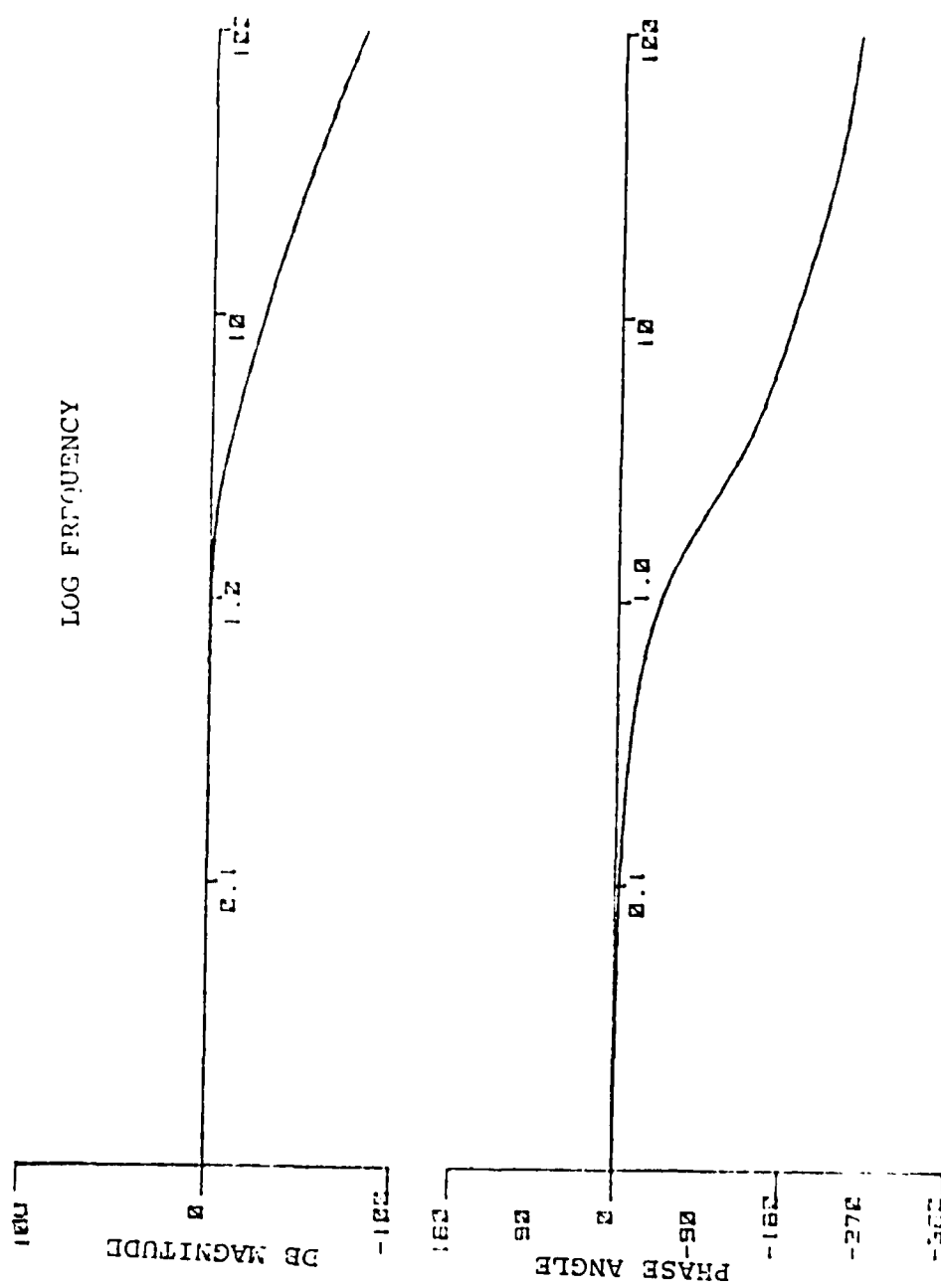


Figure 3-4 Frequency response of the SRFIMF position controller, K_{RL} = 25.

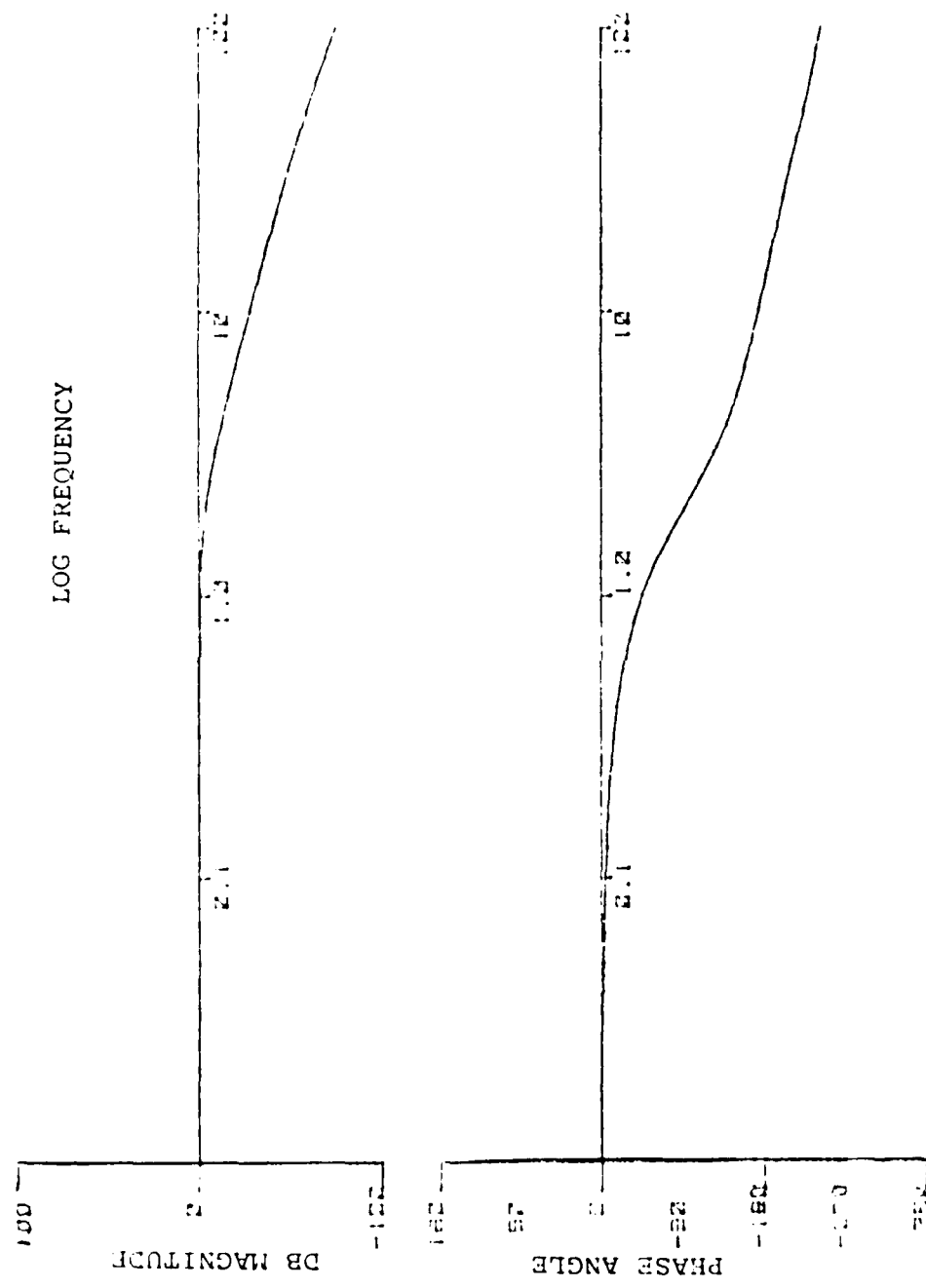


Figure 3-5 Frequency response of SRFIMF position controller, K_{RL} = 50.

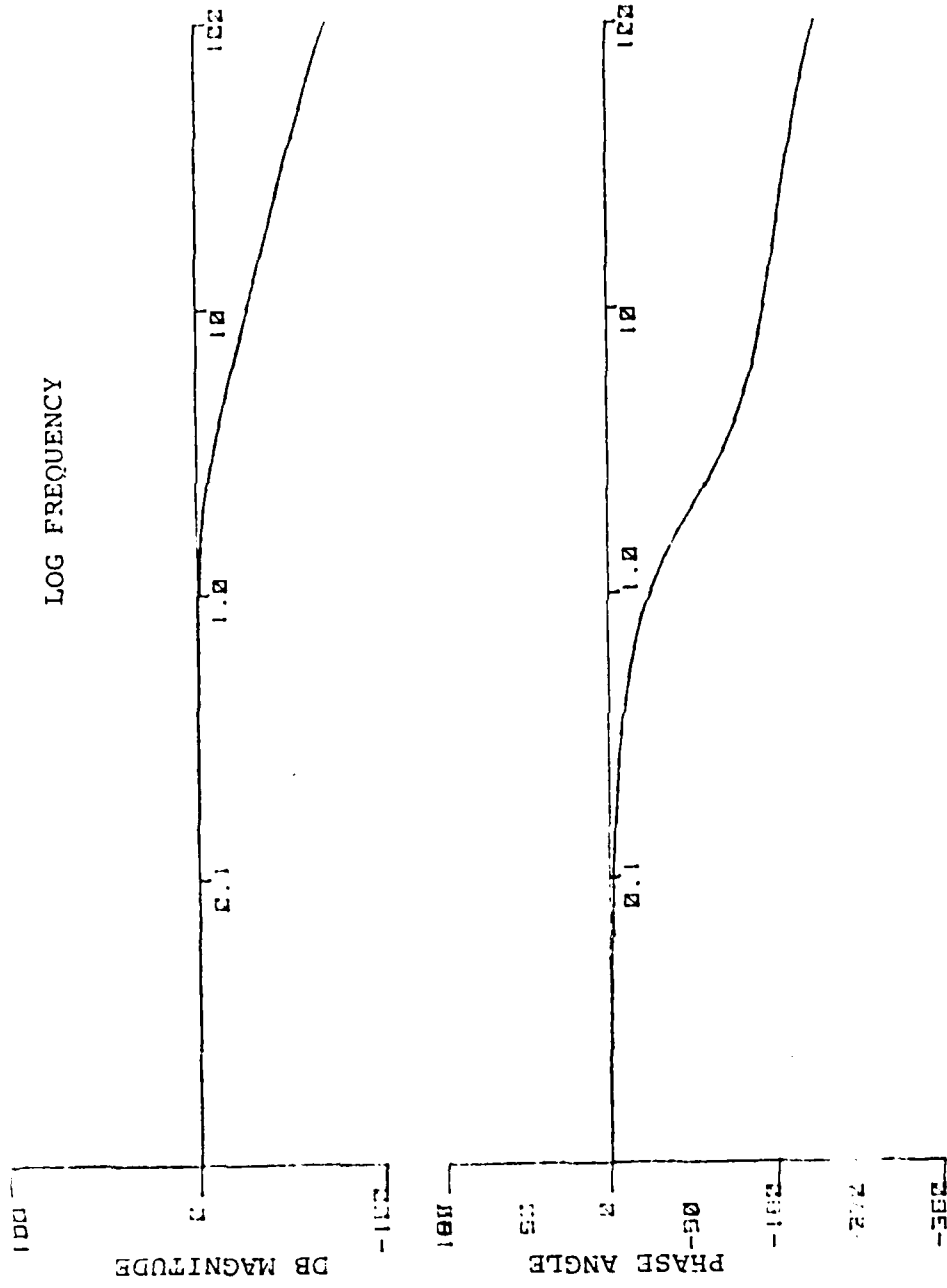


Figure 3-6 Frequency response of SRIMF position controller, $K_{RL} = 100$.

The characteristic equation for the system can be obtained by setting the denominator of equation 3-13 to zero. The resulting equation is

$$s^3 + (b + KRL)s^2 + (c + K_x \cdot KRL)s + KRL \cdot K_x = 0 \quad 3-16$$

At least one root of 3-16 must be real and the factor corresponding to the real root is defined as $(s + f)$. Assuming that the system described by the transfer function, equation 3-13, represents a model following system, then the second factor of 3-16 must be given by the model. In other words, assuming perfect model following, equation 3-16 must factor as

$$(s + f) (s^2 + K_x s + K_x) = 0 \quad 3-17$$

As KRL becomes large, the SRFIMF closed loop system response does approach perfect model following, and it can be stated that as KRL increases the condition is approached where

$$\begin{aligned} s^3 + (b + KRL)s^2 + (c + K_x \cdot KRL)s + KRL \cdot K_x &\longrightarrow \\ (s + f) \cdot (s^2 + K_x s + K_x) & \end{aligned} \quad 3-18$$

In other words, the dynamic behavior of the system's oscillatory mode is approximately given by the model parameters K_x and K_x . Expanding the right hand side of 3-18 we have for increasing KRL

$$\begin{aligned} s^3 + (b + KRL)s^2 + (c + K_x \cdot KRL)s + KRL \cdot K_x &\longrightarrow \\ s^3 + (K_x + f)s^2 + (K_x + K_x f)s + f \cdot K_x & \end{aligned} \quad 3-19$$

Comparing coefficients reveals that for increasing KRL

$$b + KRL \Rightarrow K_{\dot{x}} + f \quad 3-20a$$

$$c + K_x KRL \Rightarrow K_x f + K_x \quad 3-20b$$

$$KRL \Rightarrow f \quad 3-20c$$

The relationships of 3-20 are not equalities, but they indicate that while KRL is increasing, the difference between KRL and f remains finite.

Therefore, it can be said that one real pole is on the negative real axis and its location is approximated by the value of KRL since f is approaching KRL as KRL becomes large relative to b or c. To examine the behavior of the oscillatory pole as KRL is increased, it will be necessary to rearrange equation 3-9 into root locus form. Setting the denominator of 3-9 equal to zero yields

$$\left[\frac{1 - A(s)}{K} \right] \cdot \left[\frac{1}{H(s) G(s)} \right] + s^2 + K_{\dot{x}} s + K_x = 0 \quad 3-21$$

Substituting for A(s), H(s) and G(s) and rearranging, the general relation for the root locus is

$$0 = 1 + \frac{KRL (s^2 + K_{\dot{x}} s + K_x)}{s} G'(s) \quad 3-22$$

where $G'(s)$ is an arbitrary plant transfer function divided by its constant gain, CPG, as was shown by equation 3-10.

Equation 3-21 will now be used to determine the root locus for the position controller where $G'(s)$ is given by one of four of the modes assumed to be typical of VSTOL aircraft as listed in table 3-4. The cases considered are

	<u>Mode # from Table 3-2</u>	<u>b</u>	<u>c</u>
Case 1	6	-.6	2.16
Case 2	3	.6	.91
Case 3	9	0	0
Case 4	10	1.6	.6

Table 3-4 Plant Parameters for Root Locus Analysis

The root locus computer program developed by Melsa and Jones [7] was used to evaluate and plot the root locus given by equation 3-21. The gain constant, KRL, was varied from 0 to 100. The resulting root locus trajectory of the oscillatory poles for the four mode cases are shown in figures 3-7 to 3-10. From the figures it can be seen that in all cases the oscillatory pole approaches the desired value given by the model, in this case $-1.5, 1.32i$. Because of scaling, the real pole described earlier is not shown in the figures. It can also be seen that the pole location of the closed loop system is within 5 percent of the desired value for KRL of between 25 and 50. Although a value of KRL equal to 25 is normally sufficient, a KRL value of 50 will be used for the remainder of this work.

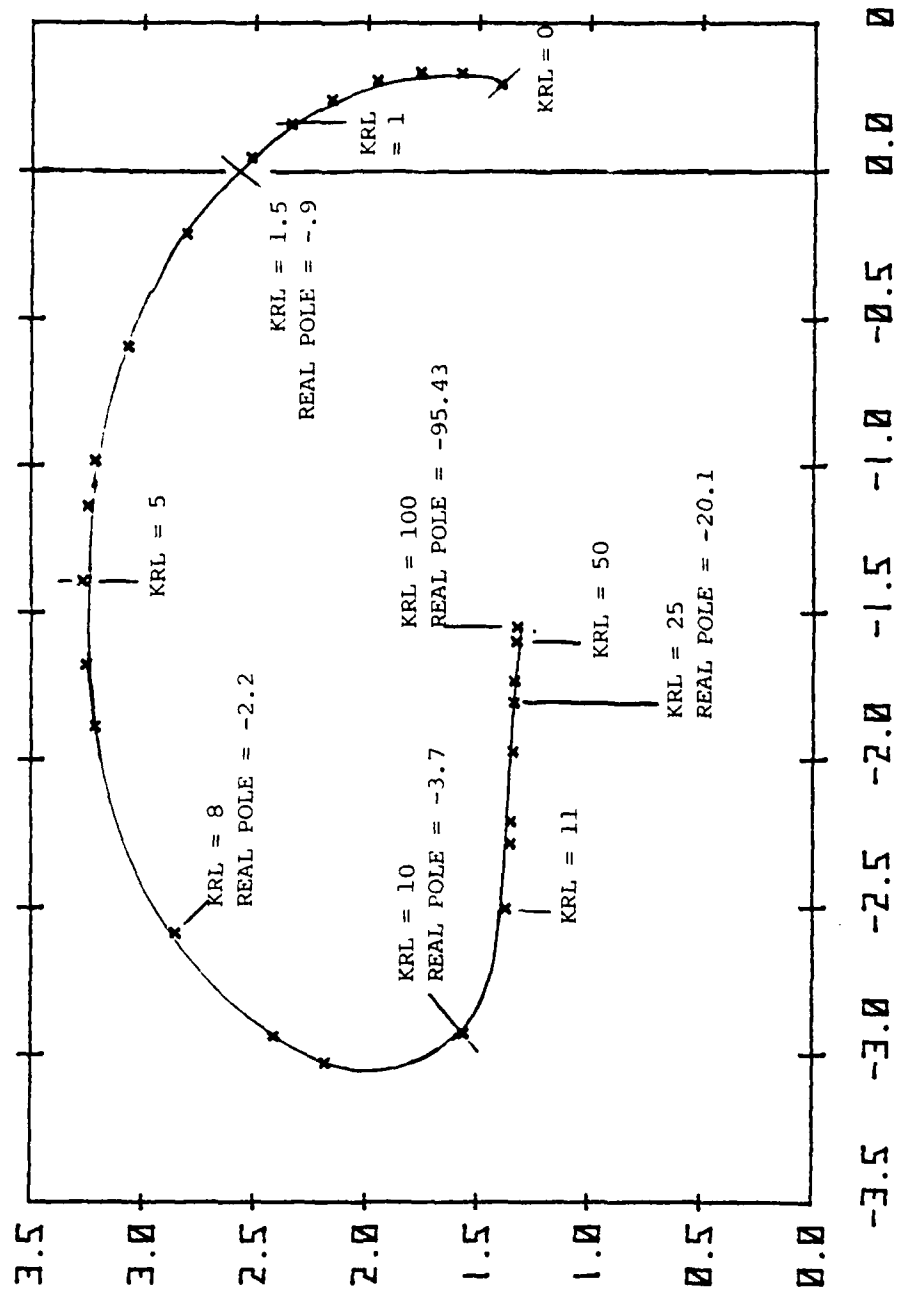


Figure 3-7 Root locus plot of oscillatory pole of a SRFIMF position controller. The open loop plant has a natural frequency of 1.47 rad/sec and a damping ratio of .441.

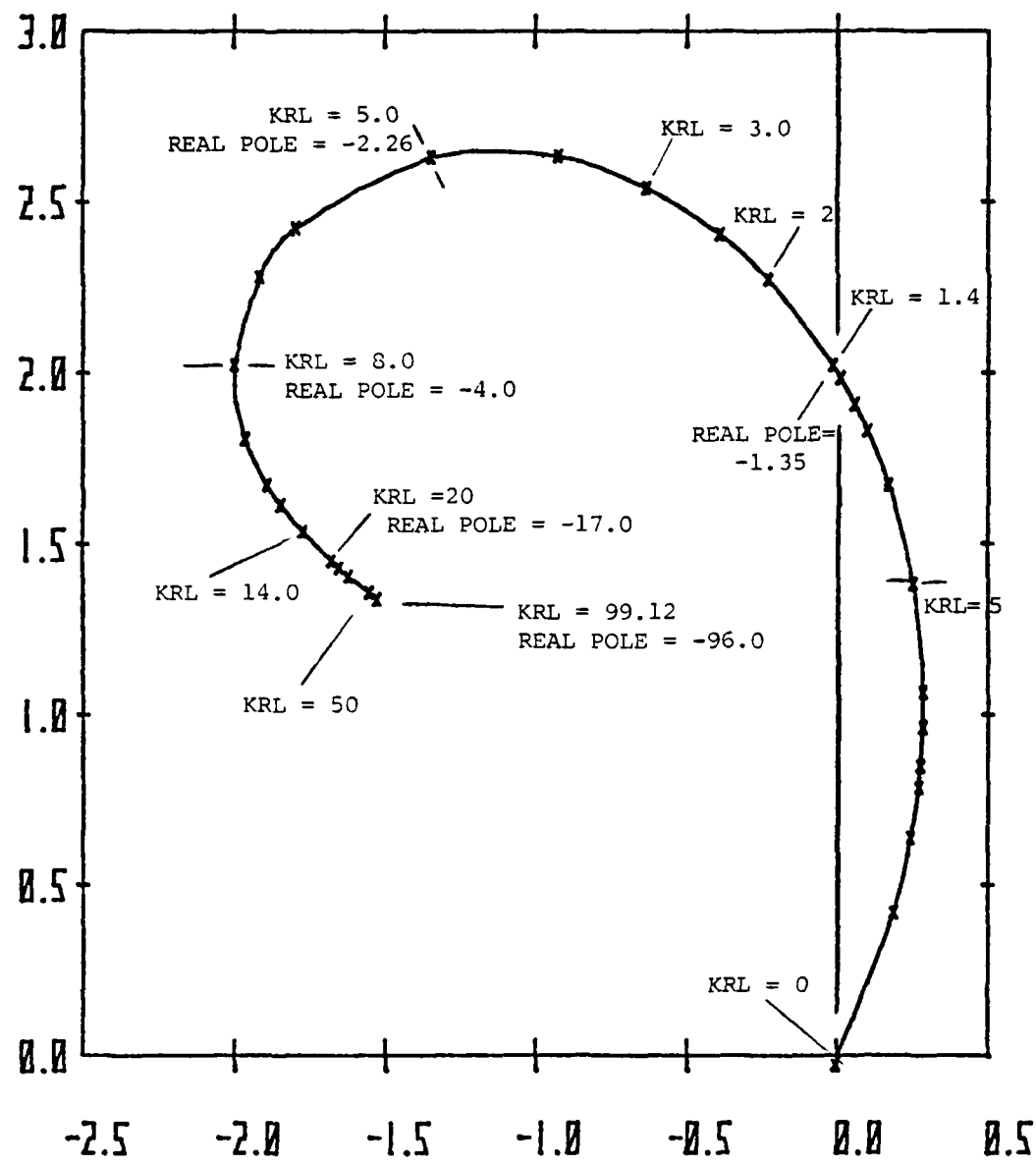


Figure 3-8 Root locus of the oscillatory pole of a SRFIMF position controller. The open loop plant has two poles at the origin.

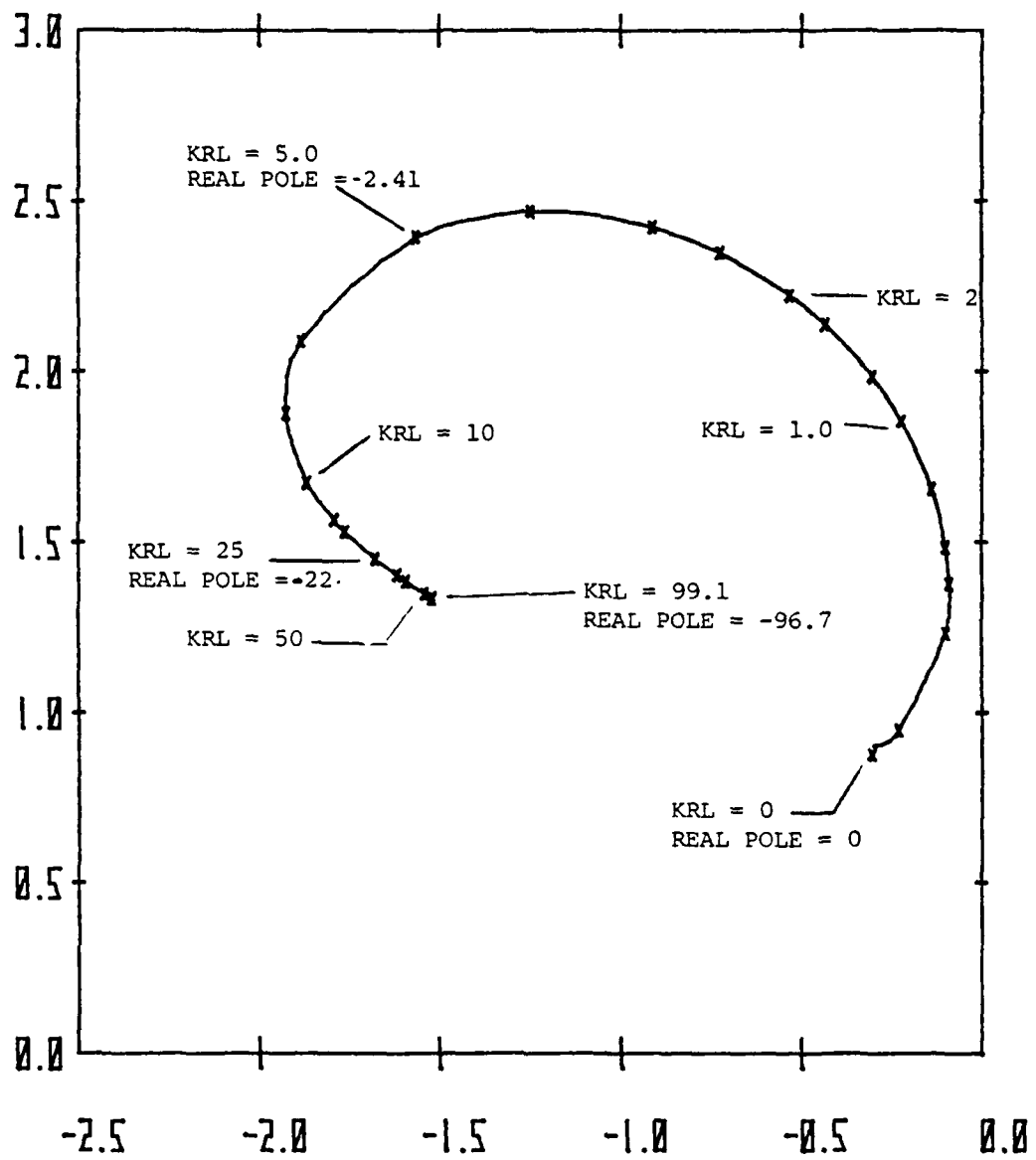


Figure 3-9 Root locus of the oscillatory pole of a SRFIMF controller. The open loop plant has a natural frequency of .95 rad/sec and damping ratio of 0.475.

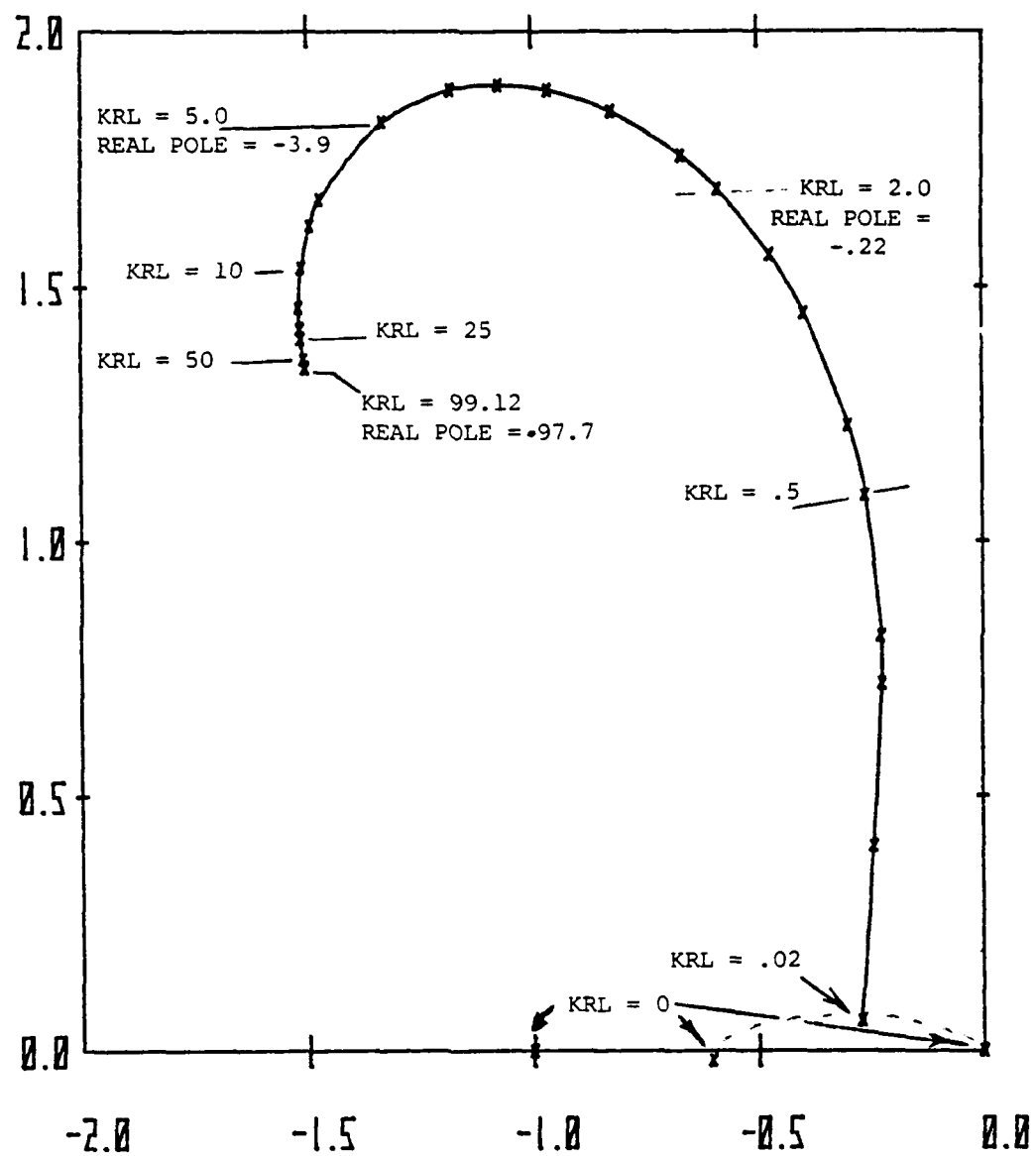


Figure 3-10 Root locus of the oscillatory pole of a SRFIMF position controller. The open loop plant has real poles at -1.0 and -0.6 .

The root locus behavior of a more complex plant will be shown in section V where the SRFIMF controller will be applied to a transfer function of the Harrier aircraft. The system will next be simulated for each of the sample VSTOL aircraft modes listed in table 3-2.

D. SRFIMF SIMULATIONS

The simulated response of a plant under the control of SRFIMF position controller was done for all ten of the typical VSTOL aircraft modes listed in table 3-2. The time histories were generated using the CSMP program, reference [6]. The open loop plant for each of the ten systems was assumed to be of the form

$$G(s) = \frac{X(s)}{\delta(s)} = \frac{CPG}{s^2 + bs + c}$$

with CPG = 1 and b and c given in table 3-2.

The model was as assumed in section II, a second order with a natural frequency of 2 rad/sec and damping ratio, of 0.75. The constants K_x and $K_{\dot{x}}$ were 3 and 4 respectively as determined by equations 2-8 and 2-9. The simulation of the model response is shown in figure 3-9. The rise time of the modeled response is approximately 1.2 seconds. The model response has a slight overshoot (2.9 percent) with a peak time at 2.4 seconds. Settling to within 1 percent occurs immediately after the peak response. For the simulations, KRL was taken to be 50 and the actuator time constant, τ , was 0.10 seconds. The

input to the system and to the open loop plant was a unit step function, representing X_C , at $t = 0$. A sample listing of the CSMP source code is given in Appendix A.

Figures 3-11 to 3-21 show the time histories of the open and closed loop response of each of the ten simulated systems. It can be seen from the figures that the closed loop response of each system is indistinguishable from the model response. Figures 3-11 to 3-21 graphically show that the response of the closed loop system is approximated by the model response regardless of the plant being controlled. In addition, the self trimming feature of the controller is seen. In all cases the steady state value of the output of the closed loop system is the same as the input, X_C , namely 1.

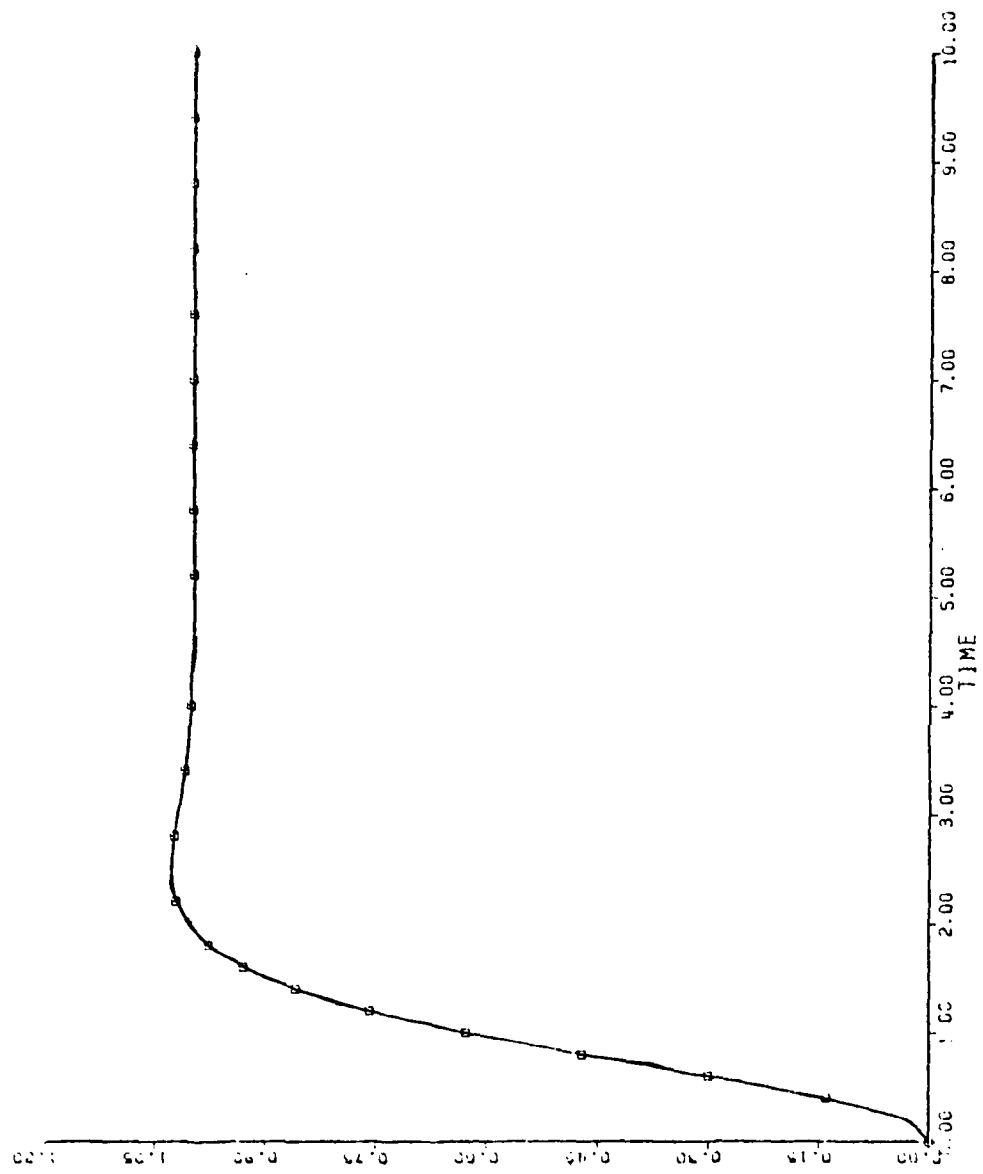


Figure 3-11 Perfect model response. $K_x = 4$, $K_{\dot{x}} = 3$, $\omega_n = 2$, $\zeta = 0.75$.

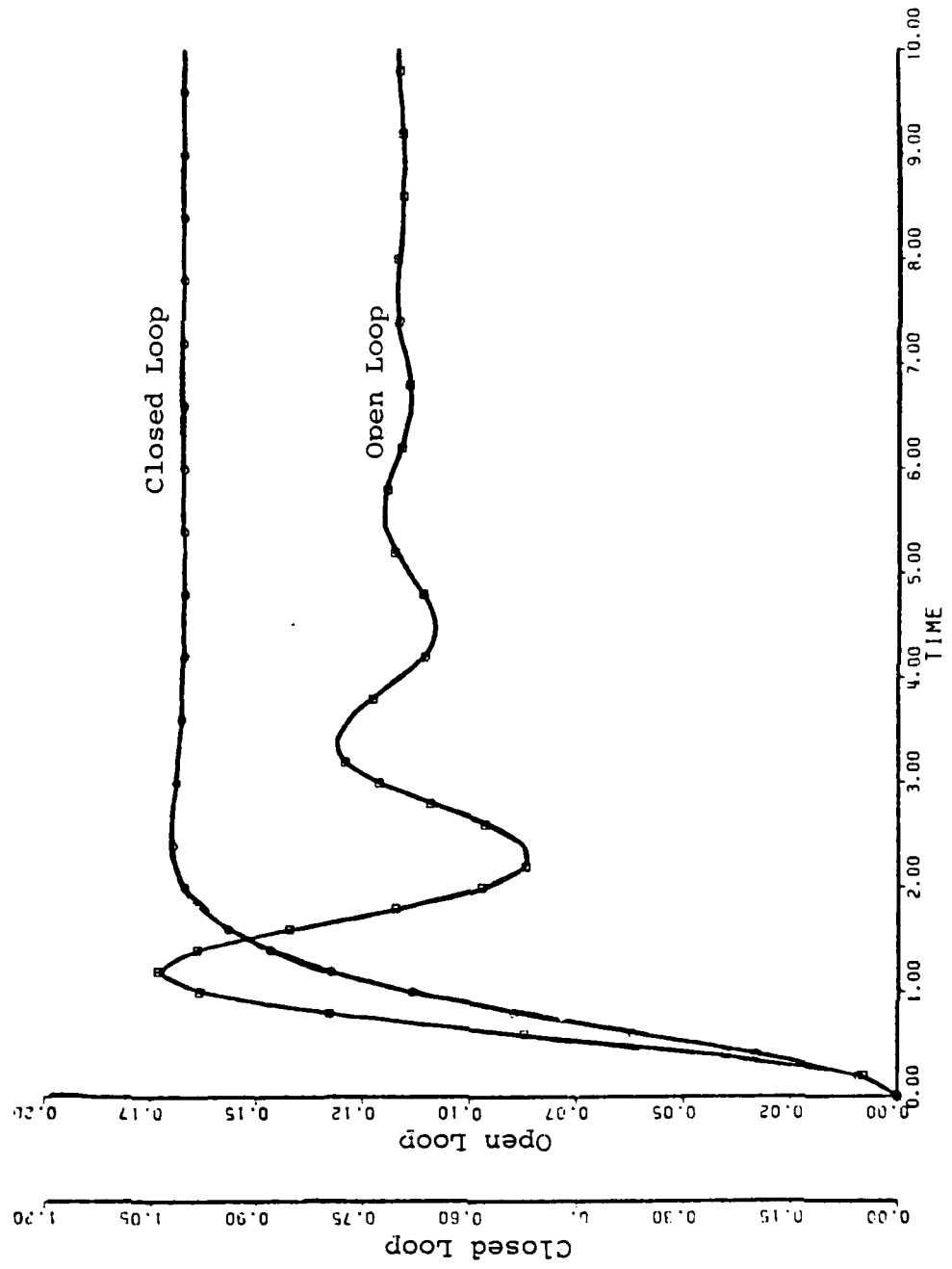


Figure 3-12 Simulation of SRFIMF position control for aircraft mode 1, table 3-3. The open loop plant has a natural frequency of 2.94 rad/sec and damping of .2.

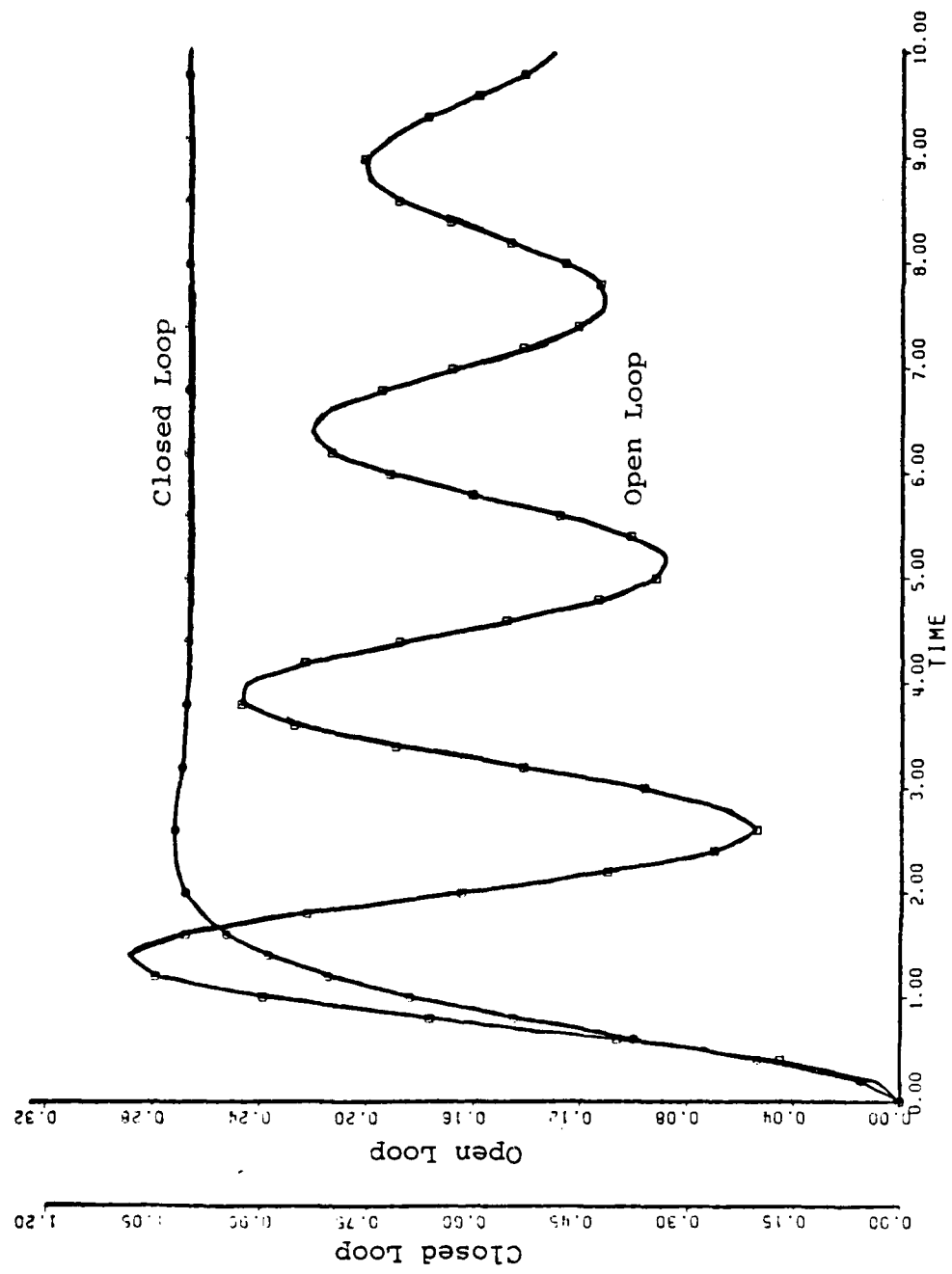


Figure 3-13 Simulation of SRFIMF position control for aircraft mode 2, table 3-3. The open loop plant has a natural frequency of 2.5 rad/sec and damping ratio of 0.06.

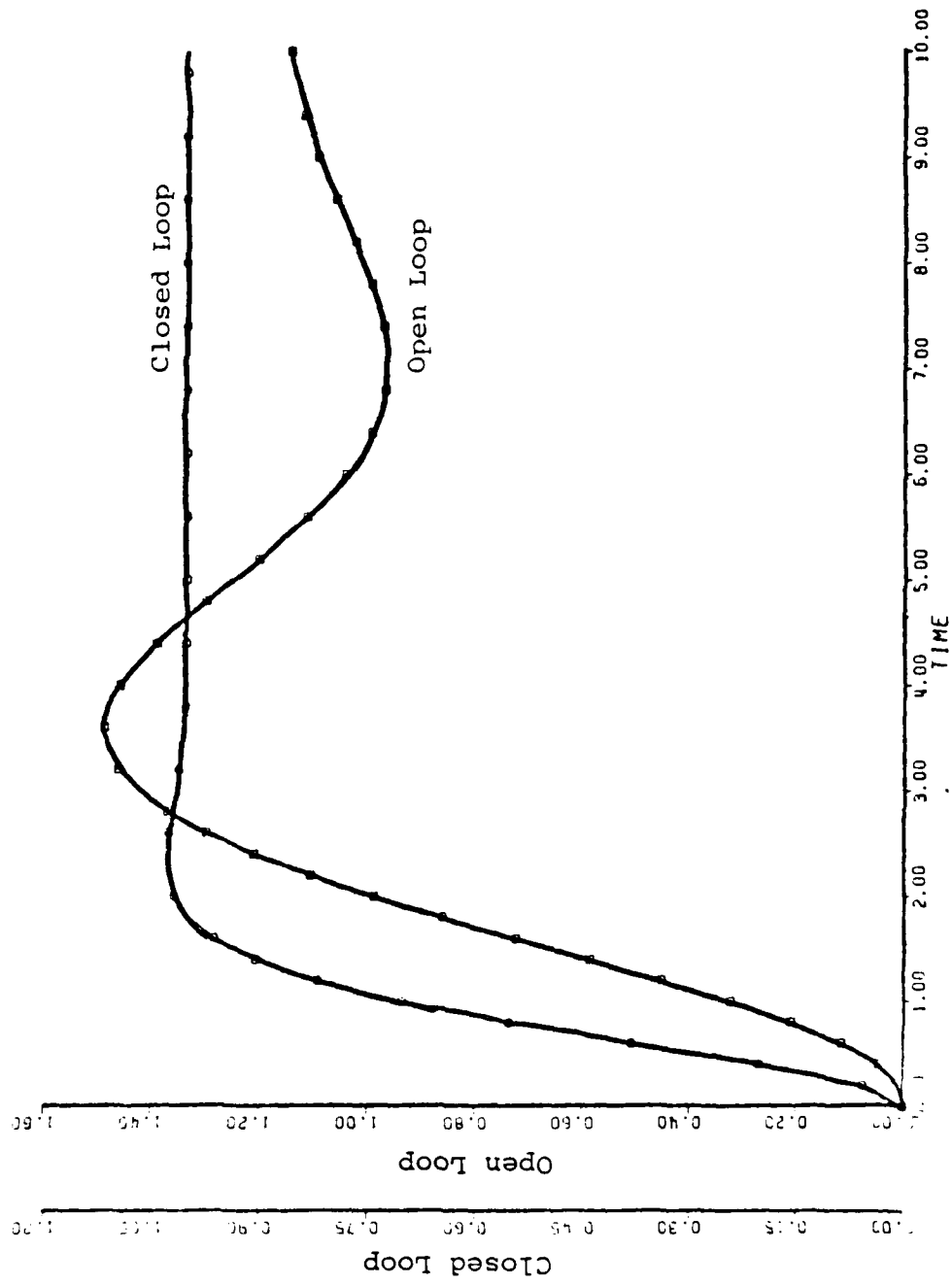


Figure 3-14 Simulation of SRFIMF position control for aircraft mode 3, table 3-3. The Open loop plant has a natural frequency of 0.954 rad/sec and a damping ratio of 0.314.

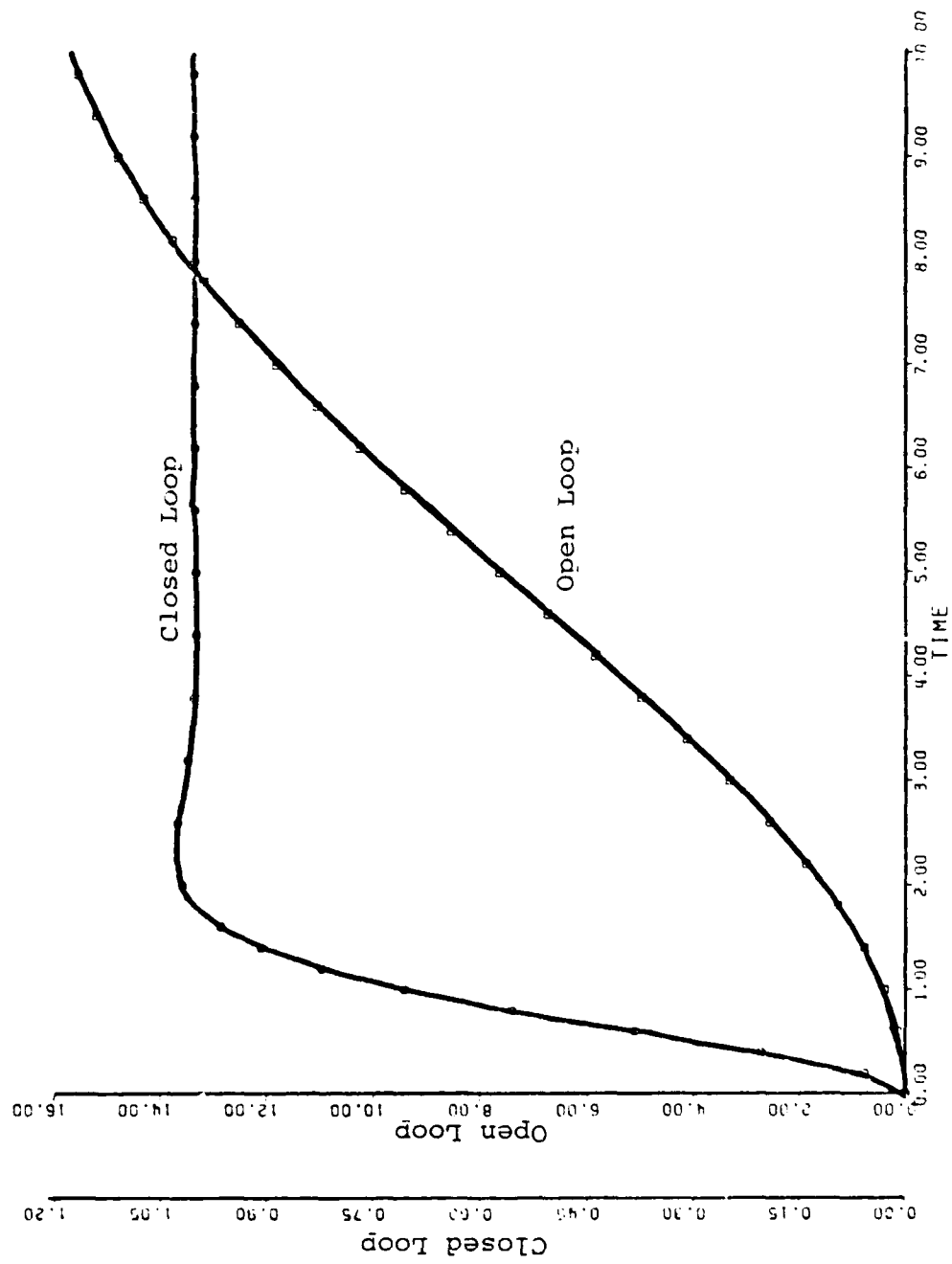


Figure 3-15 Simulation of SRFIMF position control for aircraft mode 4, table 3-3. The open loop plant has a natural frequency of 0.283 rad/sec and damping ratio of 0.353.

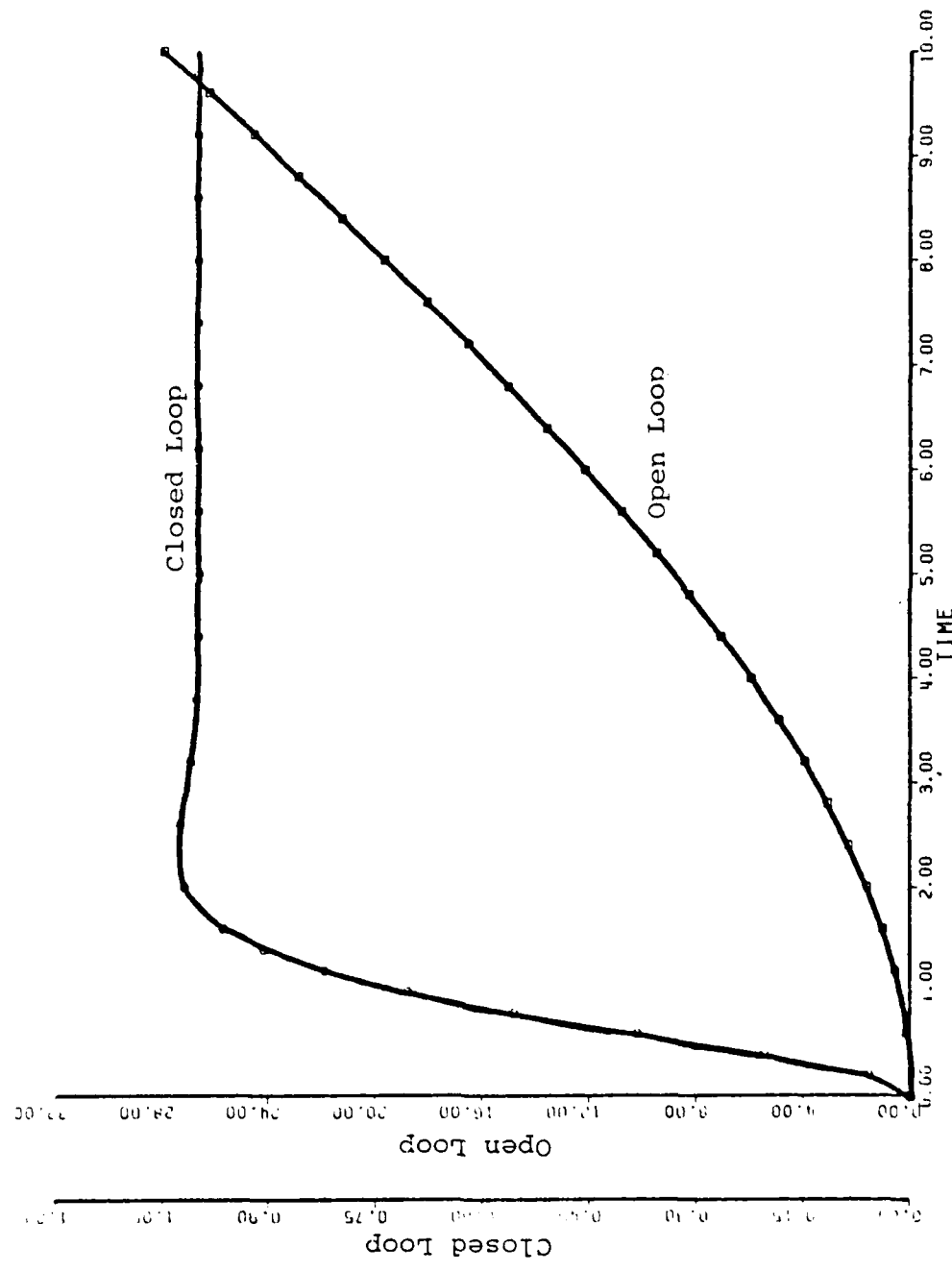


Figure 3-16 Simulation of SRFIMF position control for aircraft mode 5, table 3-3. The open loop plant has real poles at -0.2 and 0.

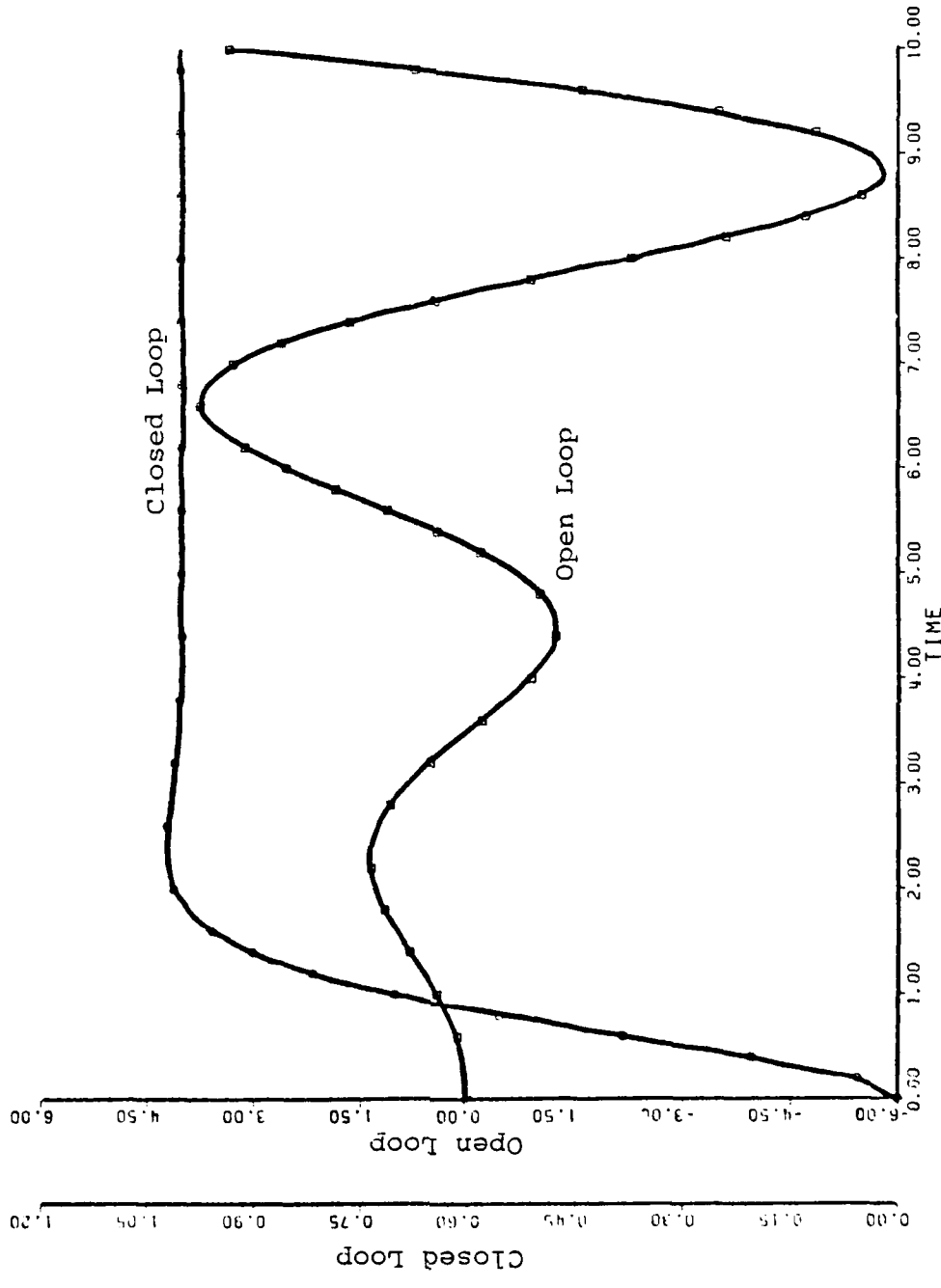


Figure 3-17 Simulation of SRFIMF position control for aircraft mode 6, table 3-3. The open loop plant has a natural frequency of 1.47 rad/sec and damping ratio of -204.

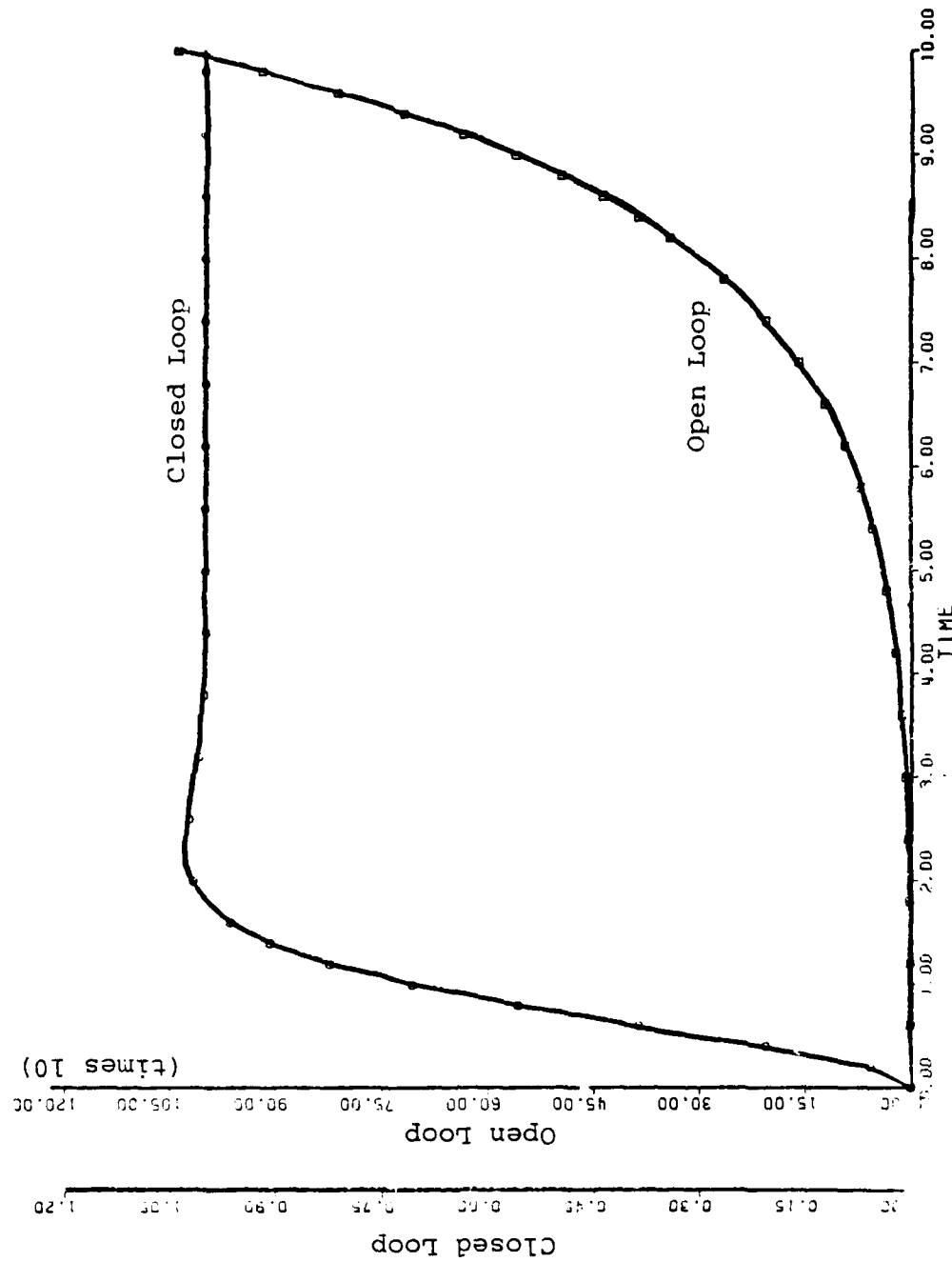


Figure 3-18 Simulation of SRPIMF position control for aircraft mode 7, table 3-3. The open loop plant has real poles at 0.30 and 0.

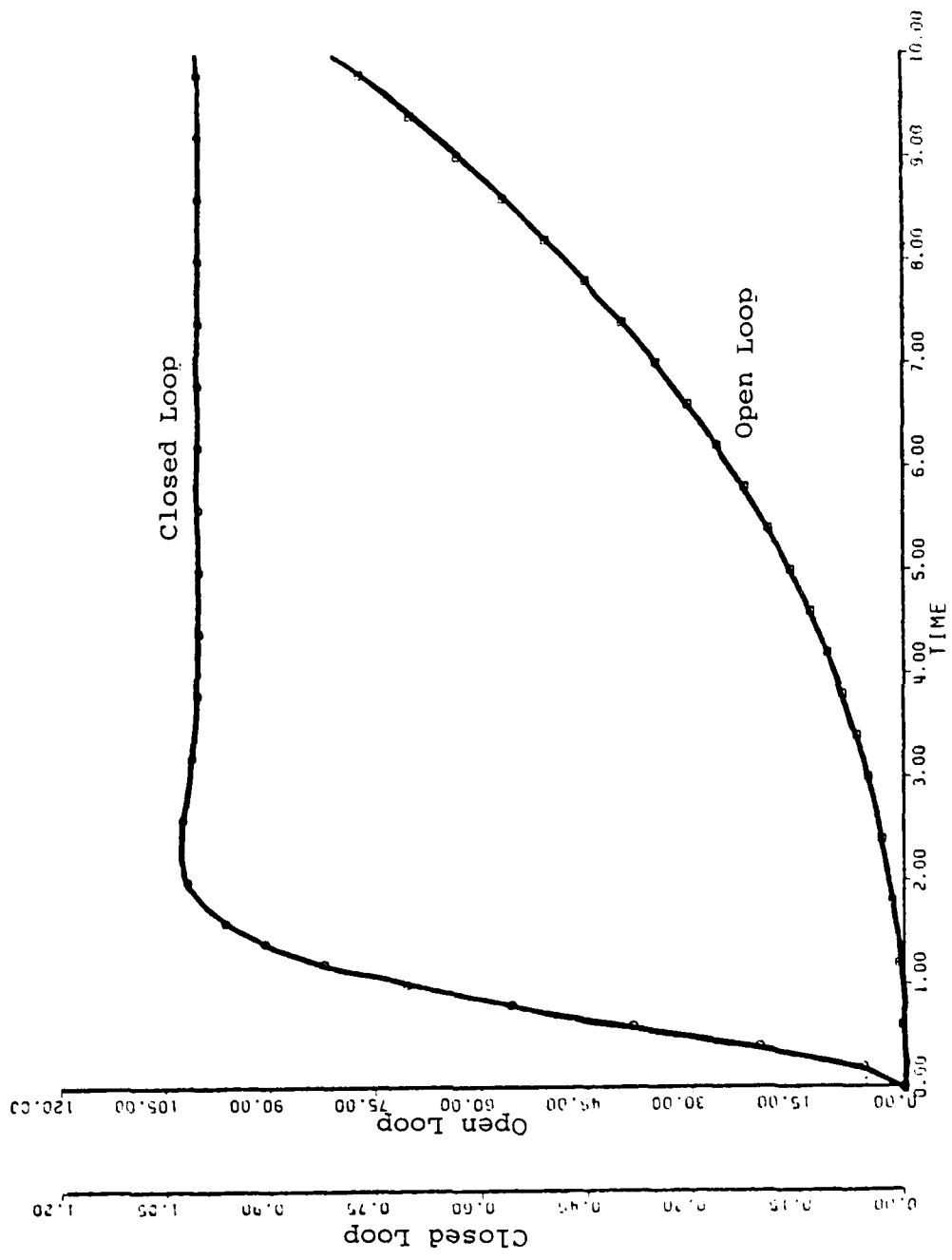


Figure 3-19 Simulation of SRFIMF position control for aircraft mode 8, table 3-3. The open loop plant has a natural frequency of 0.17 rad/sec and damping ratio of 0.590.

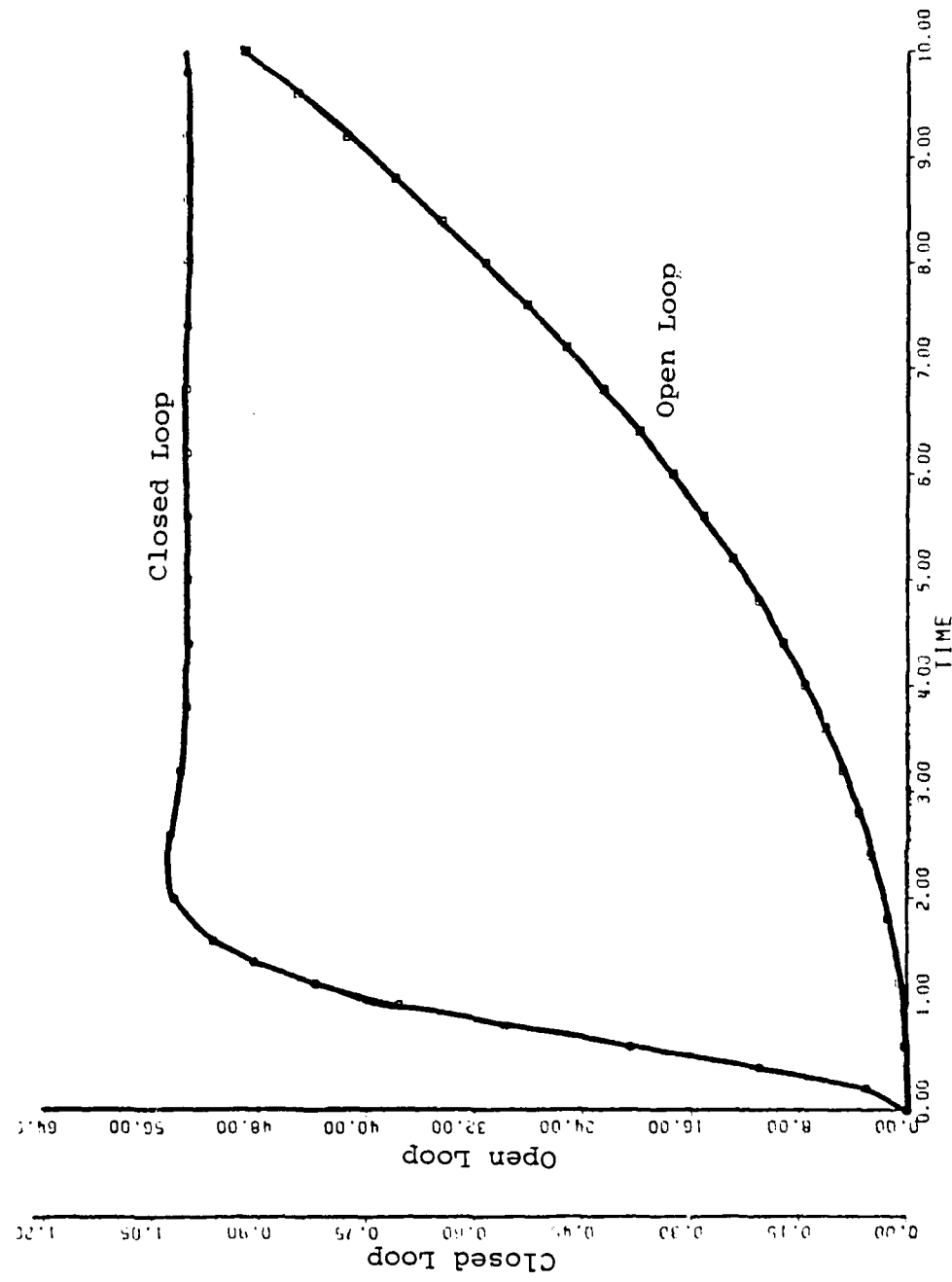


Figure 3-20 Simulation of SRFIMF position control of aircraft mode 9, table 3-3. The open loop plant has two poles at the origin.

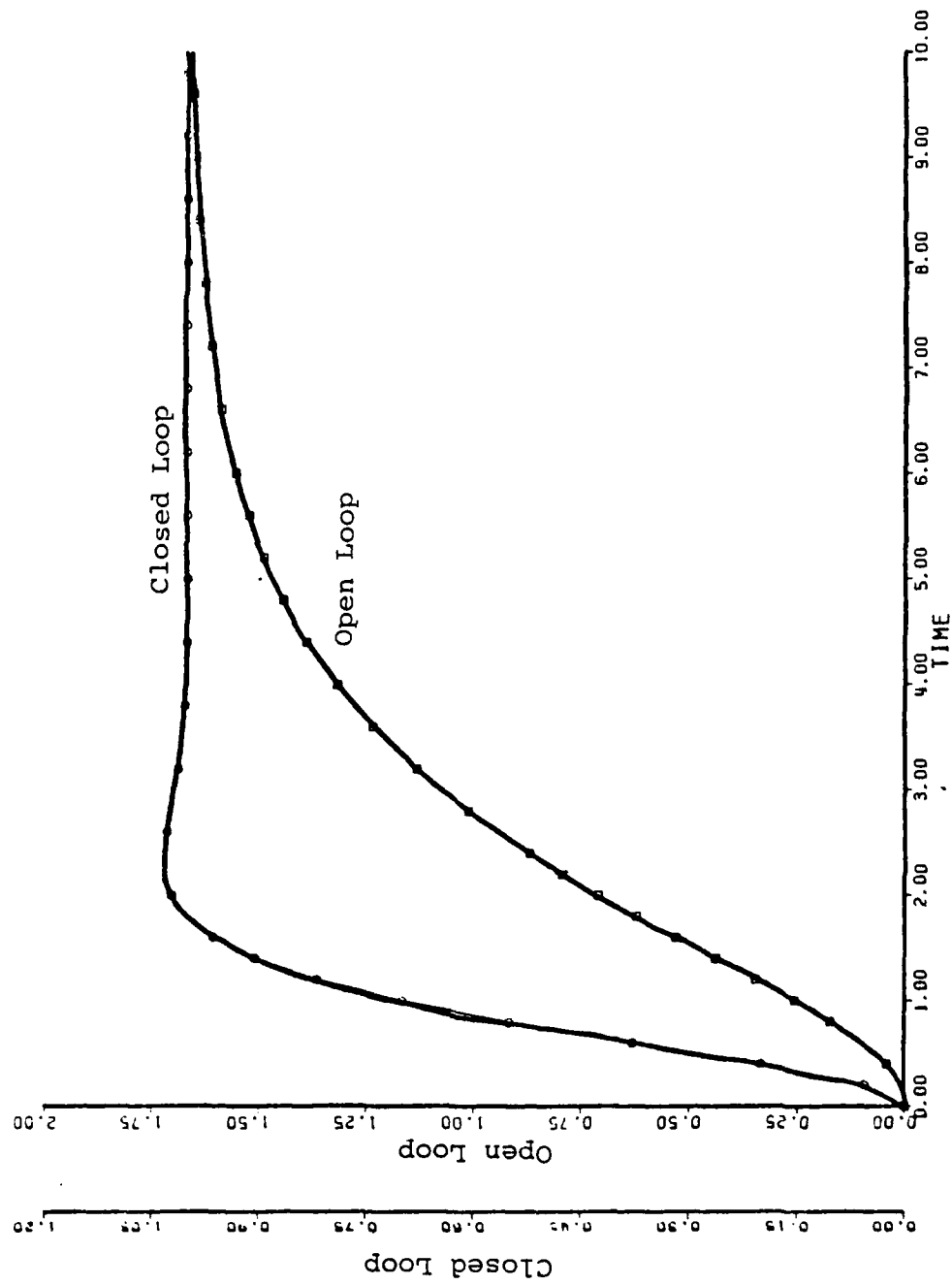


Figure 3-21 Simulation of SRFIMF position control of aircraft mode 10, table 3-3. The open loop plant has real poles at -1.0 and -0.6.

IV. SENSOR NOISE ANALYSIS

A. SRFIMF STOCHASTIC MODEL

The SRFIMF controller relies upon measurements to produce model following. We shall now examine the effect of measurement uncertainty on the operation of the closed loop system. In order to accomplish this we will consider a position controller with a representative second order plant given by

$$G(s) = \frac{CPG}{s^2 + bs + c} \quad 4-1$$

The position controller will be augmented with sensor noise sources and the observability and controllability of the closed loop system with these noise sources will be analyzed. Errors in the state variables will be determined by covariance analysis using the Lyapunov equation.

The measured quantities that are considered to be contaminated by sensor noise are the attitude position, attitude rate and attitude acceleration measurements. Two types of sensors will be considered. One is of high accuracy and typical of good quality inertial navigation system measurements. The second is of lower accuracy and might be considered typical of strapdown sensors. Sensor errors are assumed to be of two types, bias and high frequency. Bias errors are usually small relative to measured quantities and they are of constant value. Bias errors have little effect on the dynamic behavior of the control system and will not be considered in this study.

High frequency errors can be modeled in various ways. It is assumed that the sensor noise sources can be modeled by exponentially correlated noise. Exponentially correlated noise is obtained by passing Gaussian white noise through a first order shaping filter. A first order filter is represented by the differential equation

$$\dot{\xi} = -1/T_r \xi + W_t(t) \quad 4-2$$

where $W_t(t)$ is a scalar white, zero mean, Gaussian noise of constant strength, μ . μ is chosen so that the steady state value produced by the filter is the square of the sensor error standard deviation, σ^2 . Following Maybeck [9], the required value of μ as the input to the filter is given by

$$\mu = 2\sigma^2/T_r \quad 4-3$$

where T_r is the correlation time of the exponentially correlated noise. Figure 4-1 is a schematic representation of a typical shaping filter, in Laplace transform notation. $\xi(s)$ is resulting exponentially correlated noise.

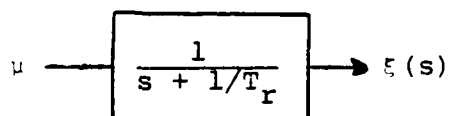


Figure 4-1 Exponentially correlated noise shaping filter

The standard deviation, σ , of the sensor error is a function of the sensors. The values of σ and T_r were obtained from a study by Analytical Mechanics Association (AMA), reference [10], in which an aircraft using a SRFIMF controller was studied. Table 4-1 is a list of the standard deviation estimates which were obtained from the AMA study. Also based upon the AMA study, we assume a value of T_r to be 10 seconds for both sensor models.

	<u>Strapdown</u>	<u>Inertial</u>
Attitude position, σ_p	1°	$0.1^\circ/$
Attitude rate, σ_v	$0.5^\circ/\text{sec}$	$0.5^\circ/\text{sec}$
Attitude acceleration, σ_a	$1^\circ/\text{sec}^2$	$0.1^\circ/\text{s}^2$

($T_r = 10$ seconds in all cases)

Table 4-1 Sensor error model parameters

The position controller shown in figure 2-4 is augmented with the sensor error sources and the resulting system is shown in figure 4-2.

To analyze the closed loop controller, we first obtain the state space representation of the plant given by equation 4-1. Taking position and velocity as the state variable of the plant we write

$$\text{Position} = X_1 \quad 4-4a$$

$$\text{Velocity} = \dot{X}_1 = X_2 \quad 4-4b$$

$$\text{Acceleration} = \dot{X}_2 = -cx_1 - bx_2 + CPGX_3 \quad 4-4c$$

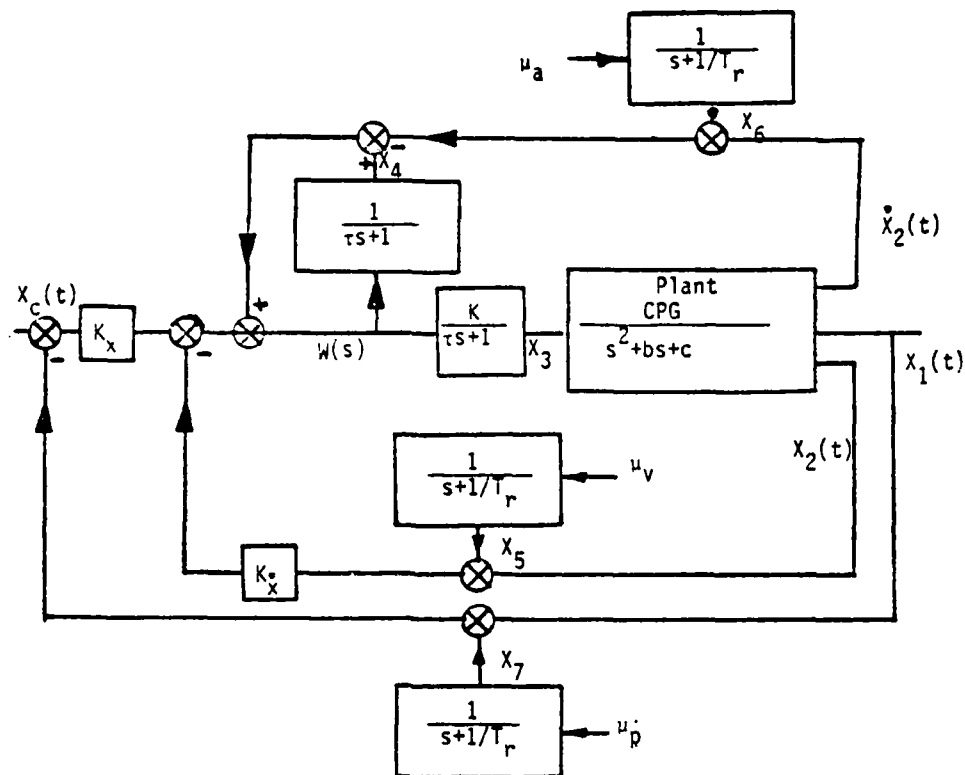


Figure 4-2 High frequency error model,
position controller

The additional state variables required for analysis of the controller as shown in figure 4-2 are

x_3 = output of the actuator which is also input to the plant

x_4 = output of the actuator compensator

x_5 = state variable representing the error in the velocity measurement

x_6 = state variable representing the error in acceleration measurement

x_7 = state variable representing the error in position measurement

From the figure we can write the control law $W(s)$, with

$x_c = 0$ as

$$\begin{aligned} W(t) &= -K_x(x_1 + x_7) - K_{\dot{x}}(x_2 + x_5) - (-cx_1 - bx_2 + CPGx_3 + x_6) + x_4 \\ &= (-K_x + c)x_1 + (-K_{\dot{x}} + b)x_2 - CPGx_3 + x_4 - K_{\dot{x}}x_5 - \\ &\quad x_6 - K_x x_7 \end{aligned} \quad 4-5$$

The remaining first order differential equations, obtained from figure 4-1, are given as

$$\dot{x}_3 = -1/\tau x_3 + K/\tau W(t) \quad 4-6a$$

$$\dot{x}_4 = -1/\tau x_4 + 1/\tau W(t) \quad 4-6b$$

$$\dot{x}_5 = -1/T_r x_5 + 2\sigma_v^2/T_r \quad 4-6c$$

$$\dot{x}_6 = -1/T_r x_6 + 2\sigma_a^2/T_r \quad 4-6d$$

$$\dot{x}_7 = -1/T_r x_7 + 2\sigma_p^2/T_r \quad 4-6e$$

Combining equation 4-4, 4-5 and 4-6 and expressing the system in matrix form*, we have the closed loop system whose inputs are the random sensor noise quantities given by

$$X = [A] X + [B][Q] \quad 4-7$$

$$Y = [C] X$$

where σ_p , σ_v , and σ_a are the standard deviation of the position measurement error of the velocity measurement error and of acceleration measurement error respectively and $[Q]$ is the matrix of input white noise powers given by

$$Q_{ii} = \mu_i = 2\sigma_i^2/T_r$$

*Matrices A, B, Q and C are shown on following page.

$$A = \begin{bmatrix} 0 & 1 & 0 & 0 & 0 & 0 \\ 0 & 0 & 1 & 0 & 0 & 0 \\ (c - K_x) \frac{K}{\tau} & (b - K_x) \frac{K}{\tau} & -(CPG \cdot K + 1) / \tau & \frac{K}{\tau} & -\frac{K \cdot K_x}{\tau} & -\frac{K \cdot K_x}{\tau} \\ (c - K_x) / \tau & (b - K_x) / \tau & -CPG / \tau & 0 & -\frac{K_x}{\tau} & -\frac{K_x}{\tau} \\ 0 & 0 & 0 & 0 & -1/\text{Tr} & 0 \\ 0 & 0 & 0 & 0 & 0 & -1/\text{Tr} \\ 0 & 0 & 0 & 0 & 0 & 0 \end{bmatrix}$$

$$B = \begin{bmatrix} 0 & 0 & 0 \\ 0 & 0 & 0 \\ 0 & 0 & 0 \\ 0 & 0 & 0 \\ 1 & 0 & 0 \\ 0 & 1 & 0 \\ 0 & 0 & 1 \end{bmatrix}$$

$$Q = \begin{bmatrix} 2\sigma_v/\text{Tr} & 0 & 0 \\ 0 & 2\sigma_a/\text{Tr} & 0 \\ 0 & 0 & 2\sigma_p/\text{Tr} \end{bmatrix}$$

$$C = \begin{bmatrix} -c & 0 & 0 & 0 & 0 & 1 \\ 0 & -b & 0 & 0 & 1 & 0 \\ -c & -b & CPG & 0 & 0 & 1 \\ 0 & 0 & 0 & 1 & 0 & 0 \end{bmatrix}$$

Having the matrix representation of the closed loop controller being driven by the sensor noise inputs, we can analyze the effect of the sensor error by considering the controllability and observability of the system with respect to the noise inputs and outputs of position, velocity and acceleration.

The linear control system computer programs, developed by Melsa and Jones [7], were first used with the result that the system is both observable and controllable. In order to gain a better understanding of the controllability and observability of the system, a second approach, following a method suggested by Bryson [11], was used. In the later method we decouple the system of equations by diagonalizing the system given by equation 4-7. This produces a system of equations in modal coordinates. The diagonalization procedure requires that we calculate the eigenvalues and eigenvectors of the A matrix. The transformation matrix, T, from the original coordinates to the new coordinates, is obtained by normalizing, in a complex sense, the matrix of eigenvectors. The matrix quantities corresponding to the modal coordinates are denoted with a superscript, *. The system, in modal coordinates is expressed as

$$X^* = A^*X^* + B^*Q \quad 4-8a$$

$$Y = C^*X^* \quad 4-8b$$

and the transformation is as follows

$$X^* = T^{-1}X \quad 4-9a$$

$$A^* = T^{-1}AT \quad 4-9b$$

$$B^* = T^{-1}B \quad 4-9c$$

$$C^* = CT \quad 4-9d$$

We will now apply the above coordinate transformation to examine the observability and controllability of the system when the plant is a specific second order system.

For this example we chose one of the representative VSTOL second order plants given by mode number 6 of table 3-2. The transfer function for this plant is given by

$$G(s) = \frac{1}{s^2 + .6s + 2.16}$$

4-10

We will assume the following additional parameters

$$\tau = .1 \text{ sec}, K_x = 4, K_{\dot{x}} = 3, K = 5, T_r = 10 \text{ sec}$$

with these choices the gain parameter KRL is

$$KRL = K CPG/\tau = 50$$

Because the system is linear with respect to the noise inputs we can solve the problem in general assuming a unit value for the individual noise standard deviations, or

$$\sigma_p = \sigma_v = \sigma_a = 1$$

where σ_p , σ_v and σ_a is the standard deviation of the position, velocity and acceleration measurement error. The original system and the resulting diagonalized system was determined by a fortran computer code called MODAL, listed in Appendix A.

The results are given

$$X = AX + BQ$$

$$X^* = A^*X^* + B^*Q$$

$$Y = CX$$

$$Y = C^*X^*$$

Matrices A, B, C, A*, B* and C* are shown on the following pages.

$$A = \begin{bmatrix} 0.0 & 1.0 & 0.0 & 0.0 & 0.0 \\ -2.16 & -0.6 & 1.0 & 0.0 & 0.0 \\ -92.0 & -120.0 & -60.0 & -150.0 & -50.0 \\ -18.4 & -24.0 & -10.0 & 0.0 & -30.0 \\ 0.0 & 0.0 & 0.0 & 0.0 & -0.1 \\ 0.0 & 0.0 & 0.0 & 0.0 & 0.0 \\ 0.0 & 0.0 & 0.0 & 0.0 & -0.1 \\ 0.0 & 0.0 & 0.0 & 0.0 & 0.0 \end{bmatrix}$$

$$B = \begin{bmatrix} 0.0 & 0.0 & 0.0 \\ 0.0 & 0.0 & 0.0 \\ 0.0 & 0.0 & 0.0 \\ 0.0 & 0.0 & 0.0 \\ 1.0 & 0.0 & 0.0 \\ 0.0 & 1.0 & 0.0 \\ 0.0 & 0.0 & 1.0 \end{bmatrix}$$

$$C = \begin{bmatrix} 1.0 & 0.0 & 0.0 & 0.0 & 1.0 \\ 0.0 & 1.0 & 0.0 & 1.0 & 0.0 \\ -2.16 & -0.6 & 1.0 & 0.0 & 1.0 \end{bmatrix}$$

$$A^* = \begin{bmatrix} -1.56 & 1.34 & 0.0 & -0.0 & 0.0 \\ -1.34 & -1.56 & -0.0 & 0.0 & -0.0 \\ -1.56 & -0.0 & -47.48 & 0.0 & 0.0 \\ -0.0 & 0.0 & -0.0 & -10.0 & 0.0 \\ -0.0 & 0.0 & 0.0 & 0.0 & -0.1 \\ 0.0 & 0.0 & 0.0 & 0.0 & 0.0 \\ 0.0 & 0.0 & 0.0 & 0.0 & -0.1 \\ 0.0 & 0.0 & 0.0 & 0.0 & 0.0 \end{bmatrix}$$

$$B^* = \begin{bmatrix} Q_v & Q_a & Q_p \\ 15.48 & 5.16 & 20.64 \\ 17.91 & 5.97 & 23.88 \\ -3.41 & -1.14 & -4.54 \\ 0.0 & 0.0 & 0.0 \\ 2.17 & 0.0 & 0.0 \\ 0.0 & 1.19 & 0.0 \\ 0.0 & 0.0 & 2.75 \end{bmatrix}$$

$$C^* = \begin{bmatrix} X_v^* & X_a^* & X_p^* \\ 0.05 & 0.0 & -0.0 \\ 0.08 & 0.07 & 0.02 \\ 0.03 & -0.22 & -0.99 \end{bmatrix}$$

It is instructive to observe the A matrix of the system. In the upper right corner, rows and columns 1 and 2 represent the plant. Row 3 is derived from the controller terms, $K \cdot W(t)/\tau$. These terms dominate the matrix.

The diagonal elements of A^* are the eigenvalues of the original system. All of the eigenvalues are negative, indicating that the system is stable. The system has one coupled oscillatory mode, -1.56, 1.34 in the upper right corner of A^* . This mode corresponds to the model and will be referred to as the model mode throughout the remainder of this study. The eigenvalue -47.48, row 3 column 3 of A^* , is the mode which represents the output of the controller. We refer to this as the controller mode. It physically represents the real pole whose location corresponds to the value of KRL as discussed in the root locus analysis of section III-C. Similarly the eigenvalue -10.00, row 4 column 4 of A^* , is the compensator mode. The other three eigenvalues correspond to the noise filter time constant, $-1/T_r$. From the transformed system, the controllability and observability of each of the previously mentioned modes with respect to the noise input can be determined.

In the B^* matrix the Q_v above the first column indicates that column 1 is the input vector corresponding to velocity error measurement input. The other columns are annotated similarly. The first two rows of the B^* matrix indicate that the model and controller modes are affected by all three

measurement errors and that acceleration measurement error is least significant. The zeroes in row 4 of the B^* matrix indicate that the compensator mode is unaffected by measurement noise. This indicates that the compensator does not contribute to the uncertainty of the system.

The C^* matrix has been annotated in a way similar to B^* so the X_v^* , X_a^* , and X_p^* correspond to the velocity, acceleration, and position error modes respectively. From the C^* matrix it is seen that the observation of position, corresponding to the first row of the matrix, is affected by all three measurement errors but that velocity and acceleration are only slightly affected. We conclude from the C^* matrix that measurement errors will affect the position, which is the quantity being controlled, but that the dynamic behavior, velocity and acceleration are only slightly affected. This result is perhaps due to the low frequency error model which results from the choice of T_r equal to 10 seconds.

From the modal analysis it is concluded that sensor errors can affect the model and controller mode of the closed loop system and that the errors can be observed in the measurement of the position. The exact relationship between the output quantities of position, velocity and acceleration will be determined in the next section where the variances of state variable X_1 , X_2 , and X_3 will be found by solving the Lyapunov equation for the system.

B. COVARIANCE ANALYSIS

The object of the covariance analysis is to determine the standard deviations of the error in the states x_1 , x_2 , and x_3 of the system developed in the previous section. The standard deviation of x_1 and x_2 are of interest because they represent position and velocity tracking accuracy. x_3 is of interest because it is the input to the plant. A large deviation in x_3 due to measurement error would mean unnecessarily high amounts of control energy lost because of measurement errors. The state variable representation of the system developed in section 4-1, where the inputs to the system are noise sources representing position, velocity and acceleration measurement error, will again be used.

The problem of determining the covariance of the states of a system in the presence of disturbances is typically encountered in the design of optimal estimators, the Kalman filter. In the estimator problem the system is expressed in the following way

$$\dot{X} = AX + BU + GW_t(t) \quad 4-11$$

where A is the matrix representation of the plant, B the control input matrix, $W_t(t)$ white noise disturbance to the plant states with

$$E[W_t(t)] = 0, \quad E[W_t(t), W_t^T(t)] = \mu$$

and G the input matrix of the disturbances. In estimation problems one assumes that measurements of the system are made

which can be expressed in terms of the states of the system by the relationship

$$\underline{Z}_N = H\underline{X} + V_N$$

Here N quantities are measured with an expected error of V_N .

In the developement of the SRFIMF controller, sensor noise was defined as a state of the system and the A matrix was augmented to include these states. The covariance analysis assumes quiescent operation of the controller, therefore, the only input to the system is white noise of strength, μ , given by equation 4-3. The white noise acts only to disturb the sensor error states. The governing equation for the covariance of the states is given by the Lyapunov differential equation

$$P = AP + PA^T + GQG^T \quad 4-12$$

where P is the matrix of the state variable covariances defined as

$$P_{ij} = \sigma_i \sigma_j$$

and Q is as before, the matrix of white noise input whose power is μ . We have chosen to rename the matrix G of equation 4-11 to B because the white noise sources are considered to be the inputs to the system.

Again a unit value of standard deviations was assumed and, because the system is linear with respect to the noise inputs, we can apply later the set of sensors. We will consider the

same plant as used in section 4-1. The transfer function for the plant is given by

$$\frac{G(s)}{U(s)} = \frac{CPG}{s^2 + .6s + 2.16}$$

4-13

At time equal to zero no uncertainties exist in the system, therefore the initial condition on P is zero.

A computer program, Vary, listed in Appendix A, was developed to solve the Lyapunov equation. The program uses an International Mathematical and Statistical Library (IMSL) subroutine called DVERK. This subroutine solves a system of first order differential equations using a Runge-Kutta Algorithm. The resulting covariance matrix, P, is printed by the program as a function of time, at a number of discrete times. The diagonal elements of the P matrix are interpreted as the square of the standard deviation or RMS value (σ_{ii}^2) of each of the state variable uncertainties as a result of the noise input. The data obtained from the computation of the P matrix is plotted in figures 4-3 to 4-5 and tabulated in Appendix B, table B-1. The figures show the standard deviation (sigma) of the states X_1 , X_2 and X_3 as functions of time from zero to ten seconds. When necessary, the steady state value is shown by a "+" on the figure.

Figures 4-3 to 4-5 can be interpreted in the following way. Each individual curve represents the contribution to the total state variable error as a result of one measurement

source. For example, in figure 4-3 we see that a unit value of standard deviation error in position measurement results in a standard deviation error in X_1 of approximately 0.8° at six seconds, and a steady state error of 0.98° . The total expected value of the uncertainty in X_1 is the sum of the errors resulting from position, velocity and acceleration measurements as given by

$$\sigma_i = \sigma_{ip} + \sigma_{iv} + \sigma_{ia}$$

4-14

Where the notation σ_{ij} refers to the i th state variable and j refers to a noise source. Thus, σ_{ip} refers to the standard deviation of X_1 as a result of position measurement error.

Table 4-2 summarizes the steady state values of the components of the state variable errors.

	X_1	X_2	X_3
Position measurement error	.980	.360	2.13
Velocity measurement error	.735	.270	1.60
Acceleration measurement error	.245	.089	0.53

Table 4-2 Steady state errors as a result of measurement errors

The actual measurements are made either by inertial navigation sensors or by strapdown sensors whose standard deviations are given by table 4-1. We can now apply the results obtained from the covariance analysis to obtain an estimate of the state variable errors for actual measurement

cases. For example, the steady state standard deviation of the error in X_1 when the measurements are made by an inertial system is given as

$$\sigma_1 = q_p \sigma_{1p} + q_v \sigma_{1v} + q_a \sigma_{1a} \quad 4-15$$

where q_p , q_v and q_a are the standard deviations of the inertial sensor measurements given by table 4-1 as

$$\begin{aligned} q_p &= 0.1^\circ \\ q_v &= 0.5^\circ/\text{sec} \\ q_a &= 0.1^\circ/\text{sec}^2 \end{aligned}$$

and σ_{1p} , σ_{1v} and σ_{1a} are given in table 4-2. The resulting expected error in X_1 in steady state is found from equation 4-15 to be 0.49° . In a similar way, the steady state errors in X_1 , X_2 and X_3 for both inertial measurements and strapdown measurements can be evaluated. The results are shown in table 4-3.

	$\frac{\sigma_1}{X_1}$	$\frac{\sigma_2}{X_2}$	$\frac{\sigma_3}{X_3}$
Inertial sensors	0.49°	$0.18^\circ/\text{sec}$	$1.07^\circ/\text{sec}^2$
Strapdown sensors	1.6°	$0.58^\circ/\text{sec}$	$3.46^\circ/\text{sec}^2$

Table 4-3 Steady state tracking errors produced by strapdown and inertial navigation sensors

The result of the covariance analysis indicates that the expected uncertainty in X_1 and X_2 as a result of measurement errors are not significant. For example, in the case of strapdown sensors, the expected error in position, X_1 , is 1.6°

while measurement errors had standard deviation values of 1° , $0.5^\circ/\text{sec}$ and $1^\circ/\text{sec}^2$.

To interpret the significance of the expected value of the error in X_3 , the value of X_3 will be determined when a 1° input is applied to the controller. Refer to figure 4-2 and, for this example, disregard the effect of the control actuator at the input to the plant. Assuming that initially the controller is in steady operation with feedbacks equal to zero, at the instant the 1° input is applied the value of X_3 is determined to be

$$X_3 = X_C \cdot K_X \cdot K = 20$$

4-16

Comparing the value of the standard deviation in X_3 to the value of X_3 when a 1° unit step input is applied to the controller, we conclude that the value of the standard deviation error in X_3 is only 17.3 percent of the value of X_3 when a 1° input is applied to the system.

From both the modal analysis and the variance analysis it can be concluded that high quality acceleration measurements are not necessary and that errors in the measurement of position and velocity are not amplified. The errors in the states are most affected by position measurement error. This result might have been expected because the controller is attempting to track to the commanded position and errors in the position measurement should dominate the uncertainty in the other states. Figures 4-3 thru 4-5 show that the uncertainty in the states reaches a

SIGMA XI VS. TIME

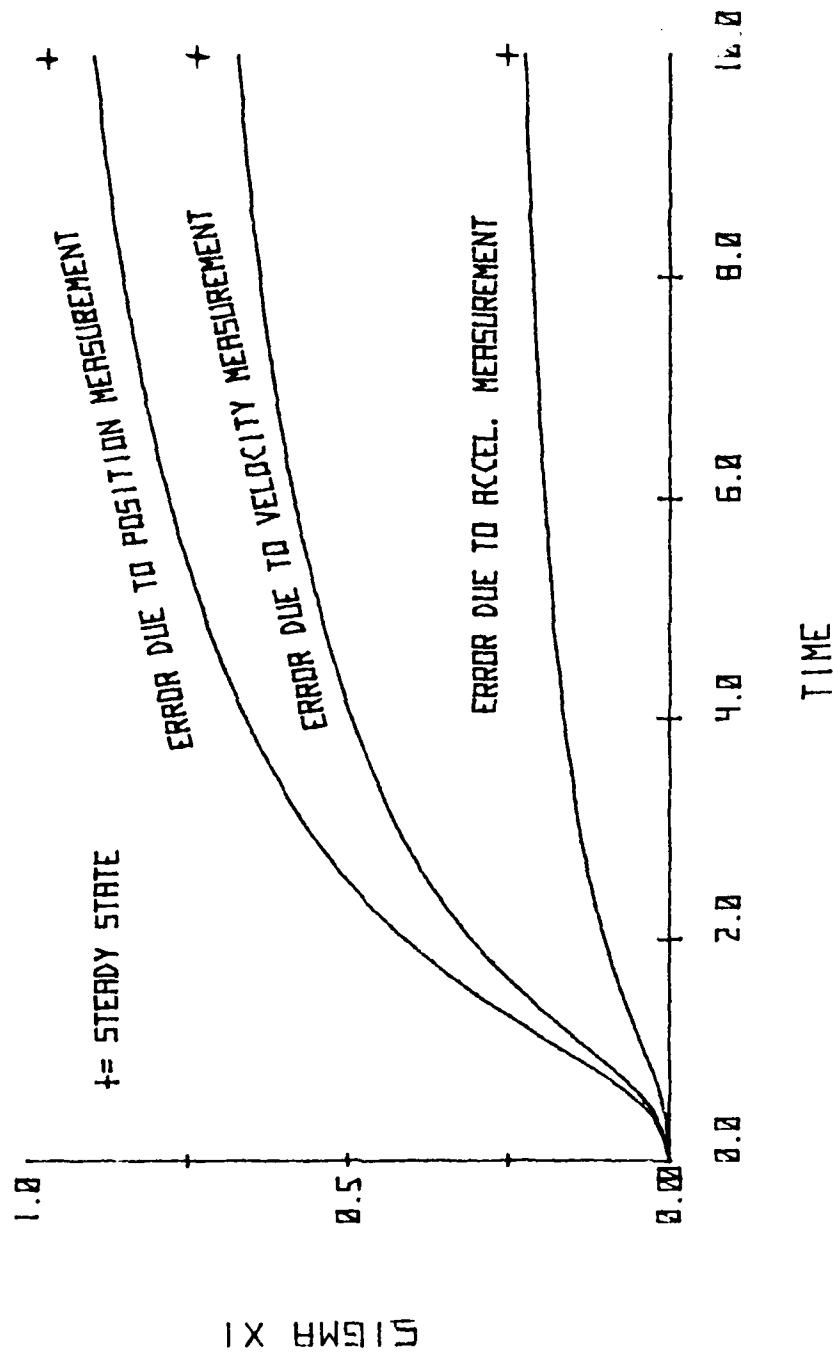


Figure 4-3 Tracking errors in Σ_{XI} as a result of measurement error in position, velocity and acceleration.

SIGMA X2 VS. TIME

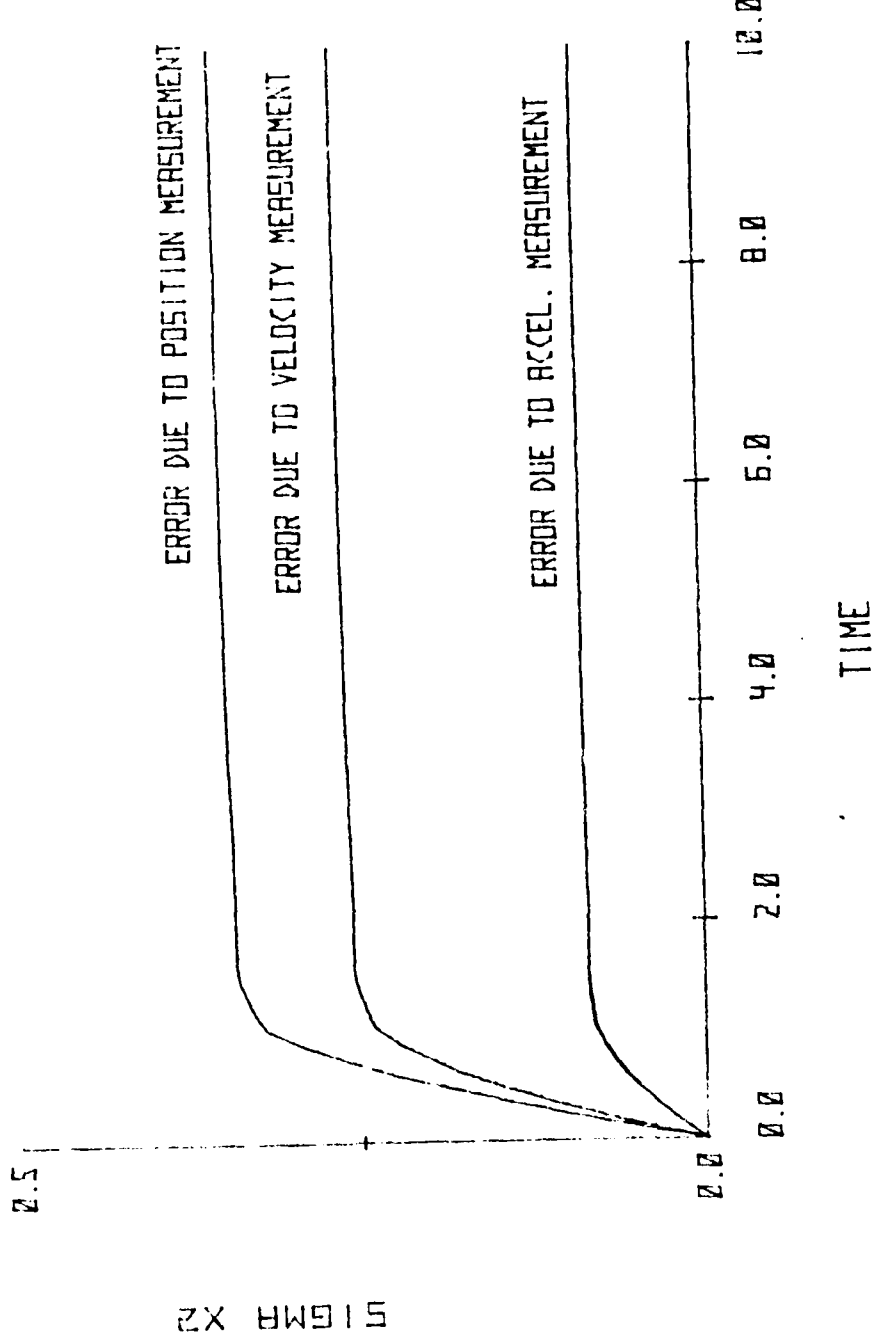


Figure 4-4 Tracking errors in X_2 as a result of measurement error position, velocity and acceleration.

SIGMA X3 VS. TIME

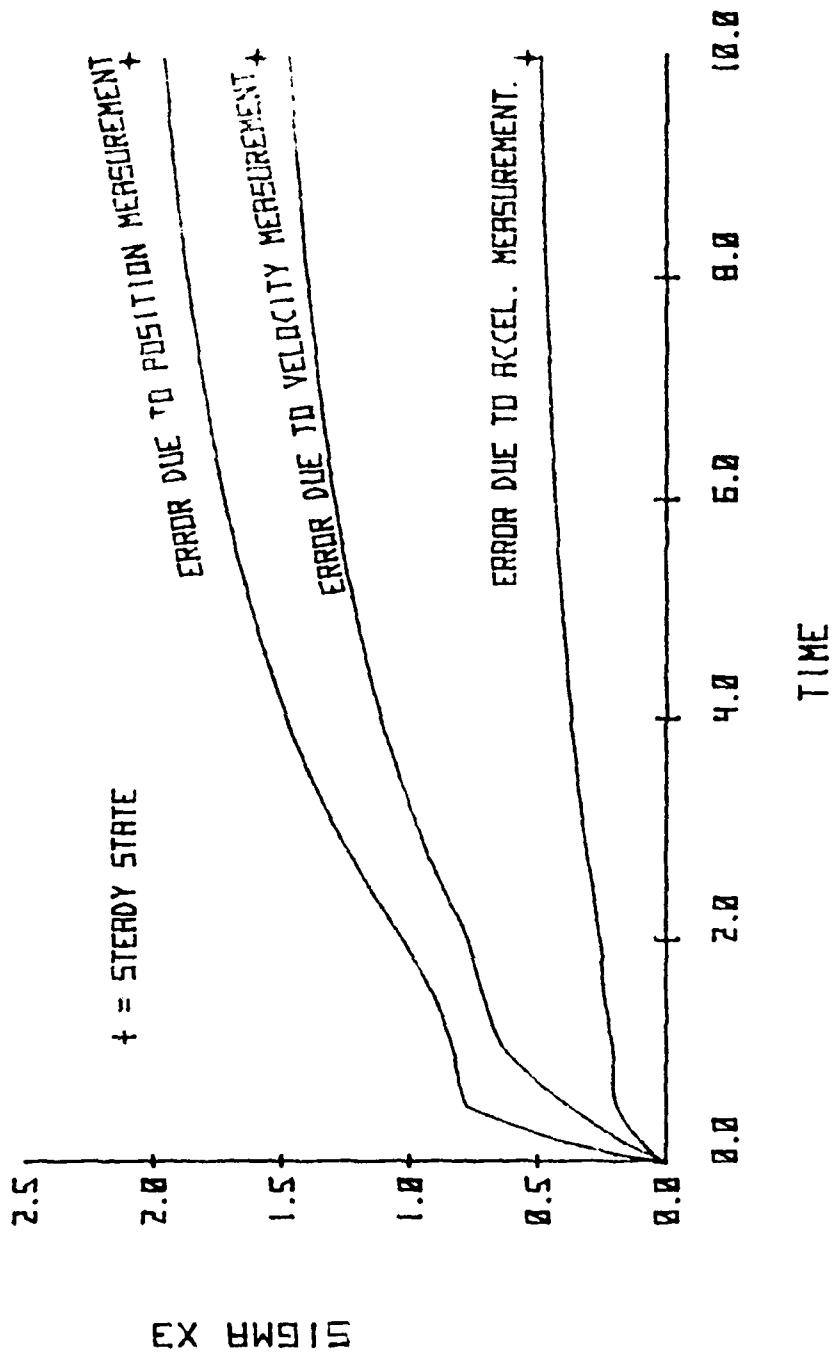


Figure 4-5 Tracking errors in X_3 as a result of measurement error in position, velocity and acceleration.

near steady state value in a short time, particularly in the case of x_2 . The rise time of the errors, seen in the figures, should not be interpreted as a lag in the response, since the figures represent the expected error in each of the states.

C. ALTERNATE MEASUREMENT SCHEMES

Two possible methods of reducing the number of measurements required by the SRFIMF controller will be considered. The first case is to measure acceleration and integrate to obtain velocity and position. In the second scheme, position and velocity will be measured and acceleration will be estimated from knowledge of the plant. The second case will be used to obtain an estimate of the added uncertainty caused by the acceleration measurement. Figure 4-6 is a schematic representation of the first case. As before the state representation of the system is obtained.

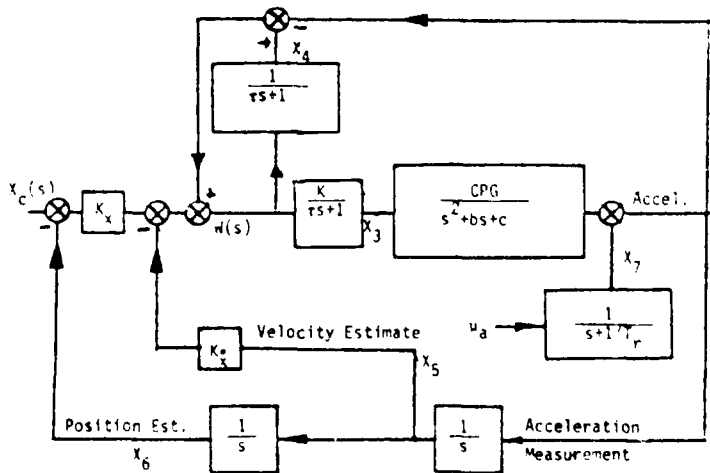


Figure 4-6 First alternate measurement scheme. Measured acceleration and implied position and velocity.

The state variables are defined as

- x_1 = position
- x_2 = velocity
- x_3 = output of the control actuator
- x_4 = output of the compensator
- x_5 = velocity estimate
- x_6 = position estimate
- x_7 = acceleration error

The control input, from figure 4-5 is written as

$$W(s) = cX_1 + bX_2 - CPGX_3 + X_4 - K_x X_5 - X_7 \quad 4-16$$

Following a development analogous to that used in section 2-3 we obtain the state representation of the system to be

$$\dot{X} = AX + BQ$$

$$A = \begin{bmatrix} 0 & 0 & 0 & 0 & 0 & 0 & 0 \\ -c & -b & CPG & 0 & 0 & 0 & 0 \\ K \cdot c / \tau & b \cdot K / \tau & -(CPG \cdot K + 1) / \tau & K / \tau & -K \cdot K_x / \tau & -K \cdot K_x / \tau & -K / \tau \\ c / \tau & b / \tau & -CPG / \tau & 0 & -KX / \tau & -KX / \tau & -1 / \tau \\ -c & -b & CPG & 0 & 0 & 0 & 1 \\ 0 & 0 & 0 & 0 & 1 & 0 & 1 \\ 0 & 0 & 0 & 0 & 0 & 0 & -1 / T_r \end{bmatrix}$$

$$B = \left\{ \begin{array}{l} 0 \\ 0 \\ 0 \\ 0 \\ 0 \\ 0 \\ 1 \end{array} \right\}$$

$$Q = \left[\frac{2\sigma_a}{T_r} \right]$$

AD-A093 253

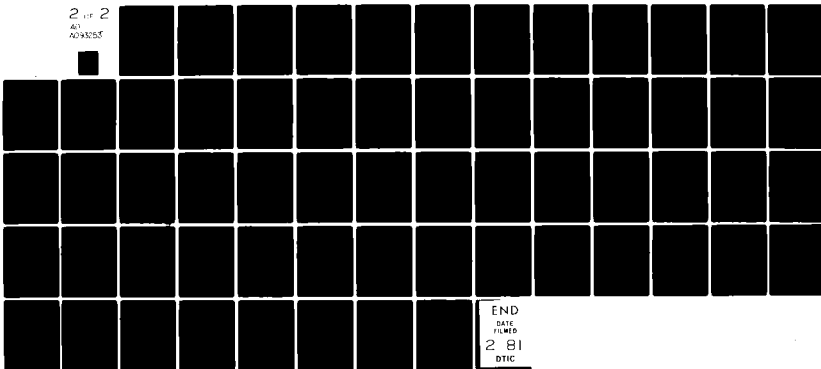
NAVAL POSTGRADUATE SCHOOL MONTEREY CA
A STUDY OF STATE FEEDBACK IMPLICIT MODEL FOLLOWING CONTROL FOR --ETC(U)
SEP 80 L E EPLEY

F/G 1/4

NL

UNCLASSIFIED

2 OF 2
AD-A093 253



END
DATE
FILED
2 81
DTIC

We apply the modal computer program to this system using the plant defined by equation 4-10 in order to determine the observability and controllability. The resulting system in modal coordinates is

$$\dot{X}^* = A^* X^* + B^* Q$$

$$A^* = \begin{bmatrix} -47.48 & 0.0 & 0.0 & 0.0 & 0.0 & 0.0 & 0.0 \\ 0.0 & -1.56 & 1.34 & 0.0 & 0.0 & 0.0 & 0.0 \\ 0.0 & -1.34 & -1.56 & 0.0 & 0.0 & 0.0 & 0.0 \\ 0.0 & 0.0 & 0.0 & 0.0 & 0.0 & 0.0 & 0.0 \\ 0.0 & 0.0 & 0.0 & 0.0 & 0.0 & 0.0 & 0.0 \\ 0.0 & 0.0 & 0.0 & 0.0 & 0.0 & -10.0 & 0.0 \\ 0.0 & 0.0 & 0.0 & 0.0 & 0.0 & 0.0 & -0.1 \end{bmatrix}$$

$$B^* = \begin{bmatrix} -1.07 \\ .17 \\ -.20 \\ -211.0 \\ 9989.68 \\ 0.0 \\ 237.0 \end{bmatrix}$$

$$C^* = \begin{bmatrix} 0.0 & -0.03 & -0.05 & 0.46 & 0.0 & -0.01 & -0.42 \\ 0.02 & 0.12 & 0.04 & 0.0 & 0.0 & 0.08 & 0.04 \\ -0.99 & -0.24 & 0.09 & 0.0 & 0.0 & -0.82 & 0.0 \end{bmatrix}^{x_a^*}$$

From the A^* matrix we can see that this system has two zero eigenvalues meaning that the modes of the system which correspond to the open loop integrators are neutrally stable. The modal control vector B^* indicates that the velocity and position estimate modes of this system are strongly affected by the noise input. In particular, mode five (row 5 of B^*) which represents the position estimate mode has a control coefficient from the noise source four orders of magnitude greater than the model mode (rows 2 and 3 of B^*). We expect that in this case acceleration sensor noise significantly affects the performance of the controller.

Applying the algorithm used in the previous section to this case we obtain the covariance estimate. Figure 4-7 is a plot of the standard deviation (sigma) of x_1 , x_2 and x_3 assuming

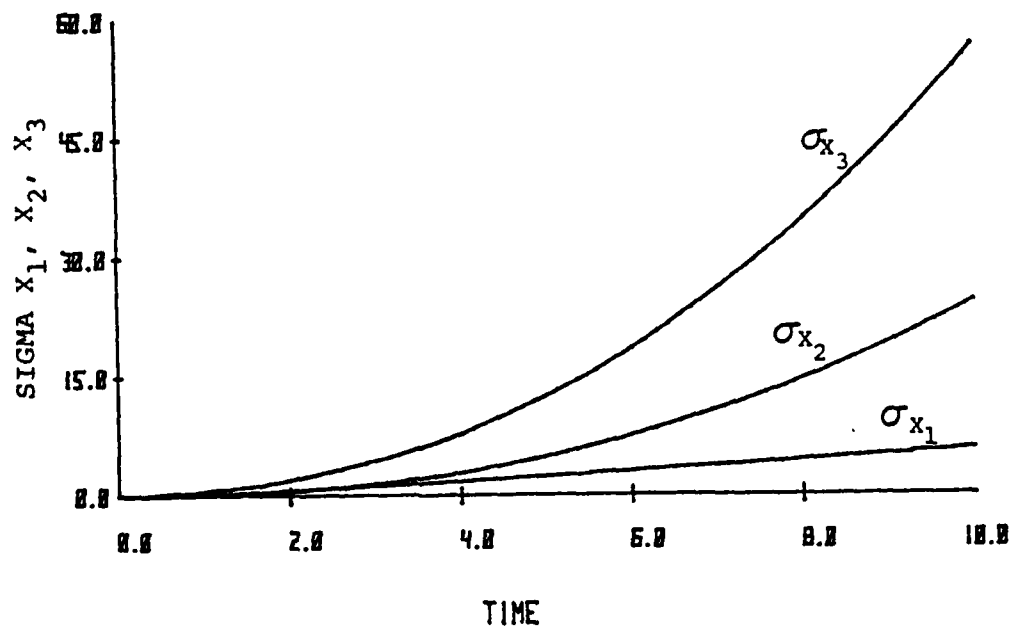


Figure 4-7 Error in x_1 , x_2 , and x_3 as a result of measurement errors in acceleration.

a unit standard deviation noise source as the acceleration measurement error. Data used to plot figure 4-7 is also tabulated in Appendix B, table B-2. It is seen from the figure that acceleration measurement error causes unbounded errors in X_1 and X_3 . Unbounded errors in any of the states are unacceptable in the controller and unless we can improve the method of estimating the position and velocity, we will be required to measure these quantities. A Luenberger observer could be used to estimate position and velocity, however the design of the observer would require use of knowledge of the plant. We wish to avoid using detailed knowledge of the plant.

The second alternate measurement scheme is the case of measured position and velocity with acceleration estimated from the plant parameters b and c. The estimation is given by

$$\text{Acceleration} = -cX_1 - bX_2 + \text{CPG } X_3$$

4-17

This scheme is shown in figure 4-8.

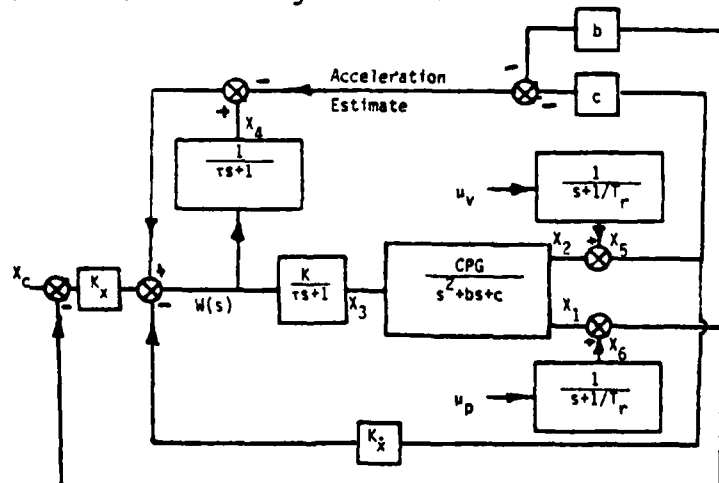


Figure 4-8 Second alternate measurement scheme, measured position and velocity. Estimated acceleration.

Following the same procedures as before we define the state variable as

x_1 = position
 x_2 = velocity
 x_3 = output of the control actuator
 x_4 = output of the compensator
 x_5 = position measurement error
 x_6 = velocity measurement error

From figure 4-8 we obtain the control law $W(t)$ as

$$W(t) = (-K_x + c)x_1 + (-K_{\dot{x}} + b)x_2 - CPG x_3 + x_4 \\ + (-K_x + c)x_5 + (-K_{\dot{x}} + b)x_6 \quad 4-18$$

Assuming the same second order plant given by equation 4-10 we obtain the modal transformation of the system.¹

$$\begin{aligned} X &= AX + BQ \\ Y &= CX \\ X^* &= A^*X^* + B^*Q \\ Y &= C^*X^* \end{aligned}$$

¹Matricies A , B , C , A^* , B^* and C^* are shown on the following pages.

$$A = \begin{bmatrix} 0.0 & 1.0 & 0.0 & 0.0 & 0.0 \\ -2.16 & -.6 & 1.0 & 0.0 & 0.0 \\ -92.0 & -120.0 & -60.0 & -50.0 & -92.0 \\ -18.0 & 24.0 & -10.0 & 0.0 & -18.0 \\ 0.0 & 0.0 & 0.0 & 0.0 & -24.0 \\ 0.0 & 0.0 & 0.0 & 0.0 & 0.0 \\ 0.0 & 0.0 & 0.0 & 0.0 & -.1 \end{bmatrix}$$

$$B = \begin{bmatrix} 0.0 & 0.0 \\ 0.0 & 0.0 \\ 0.0 & 0.0 \\ 0.0 & 0.0 \\ 1.0 & 0.0 \\ 0.0 & 1.0 \end{bmatrix}$$

$$C = \begin{bmatrix} 1.0 & 0.0 & 0.0 & 0.0 & 0.0 \\ 0.0 & 1.0 & 0.0 & 0.0 & 0.0 \\ -2.16 & -.6 & 1.0 & 0.0 & 0.0 \end{bmatrix}$$

$$A^* = \begin{bmatrix} -1.56 & 1.34 & 0.0 & 0.0 & 0.0 \\ -1.34 & -1.56 & 0.0 & 0.0 & 0.0 \\ 0.0 & 0.0 & -47.48 & 0.0 & 0.0 \\ 0.0 & 0.0 & 0.0 & -10.0 & 0.0 \\ 0.0 & 0.0 & 0.0 & 0.0 & -1 \\ 0.0 & 0.0 & 0.0 & 0.0 & 0.0 \end{bmatrix}$$

$A^* =$

$$B^* = \begin{bmatrix} Q_V & Q_P \\ 9.49 & 12.38 \\ 10.99 & 14.33 \\ -2.09 & -2.73 \\ 0.0 & 0.0 \\ 1.55 & 0.0 \\ 0.0 & 1.83 \end{bmatrix}$$

$B^* =$

$$C^* = \begin{bmatrix} 0.05 & 0.0 & 0.0 & 0.01 & x_V^* \\ -0.08 & 0.07 & 0.02 & -0.08 & x_P^* \\ 0.03 & -0.22 & -0.99 & 0.82 & -0.35 \\ & & & & 0.04 \\ & & & & 0.0 \\ & & & & 0.0 \end{bmatrix}$$

$$x_V^*$$

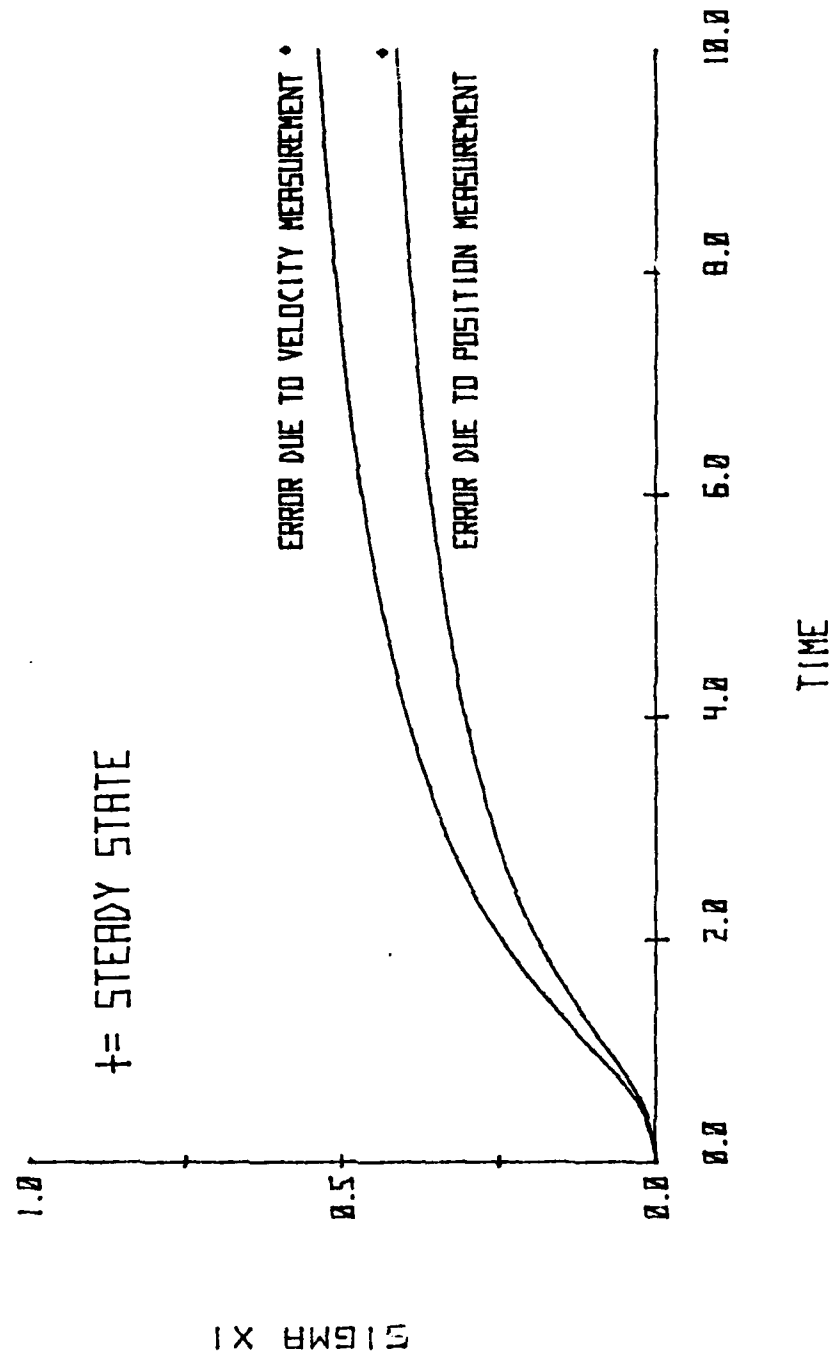
$$x_P^*$$

The results of the modal analysis are similar to those obtained when acceleration was a measured quantity rather than calculated as in this case. The model and controller modes are controllable from the noise sources. The position and velocity outputs (rows 1 and 2 of the C* matrix) contain sensor noise terms.

The covariance analysis results are shown in figures 4-9 to 4-11 and listed in Appendix B, table B-3. Here it is seen that the standard deviation of X_1 , X_2 and X_3 is slightly less than in the case when acceleration was measured. This is because the quantity taken to be acceleration does not contain the additional error of actual acceleration measurement. In this case the system requires only measurements of position and velocity.

The second alternate measurement scheme can be used to compare a state rate feedback control scheme to a state variable feedback controller, from the viewpoint of increased uncertainty in the state variable resulting from the additional measurement of acceleration. To make the comparison, assume that the measurements are made by strapdown type sensors whose measurement errors are given in table 4-1. Table 4-4 lists the total uncertainty of X_1 , X_2 and X_3 for both measurement schemes. It can be seen from table 4-4 that the overall uncertainty of X_1 , X_2 and X_3 is increased when acceleration is measured, as compared to the second alternate measurement scheme when acceleration is obtained without measurement. In a practical

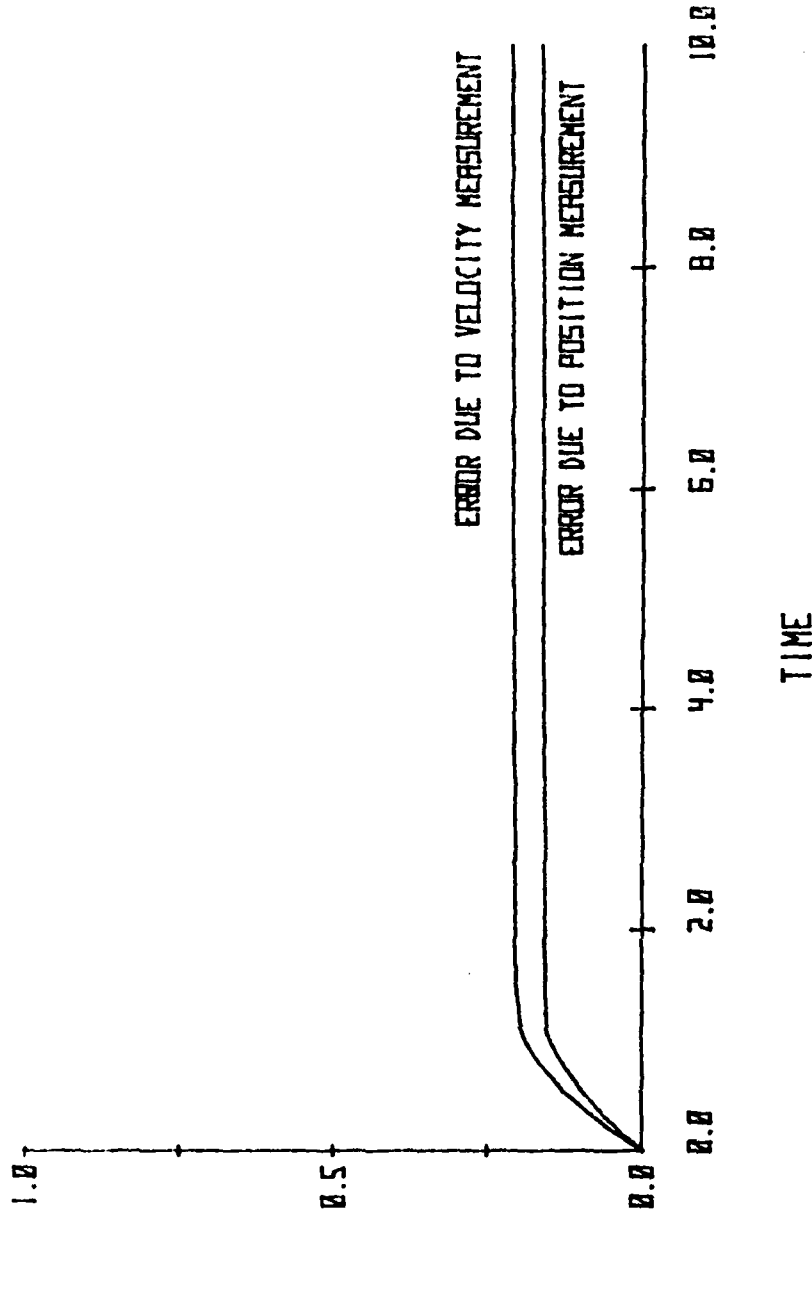
SIGMA XI VS. TIME



IX 22915

Figure 4-9 Tracking errors of x_1 as a result of measurement errors in position and velocity.

SIGMA X2 VS. TIME



2 X 10⁻¹⁵

104

Figure 4-10 Tracking errors in X_2 as a result of measurement errors in position and velocity.

SIGMA X₃ VS. TIME

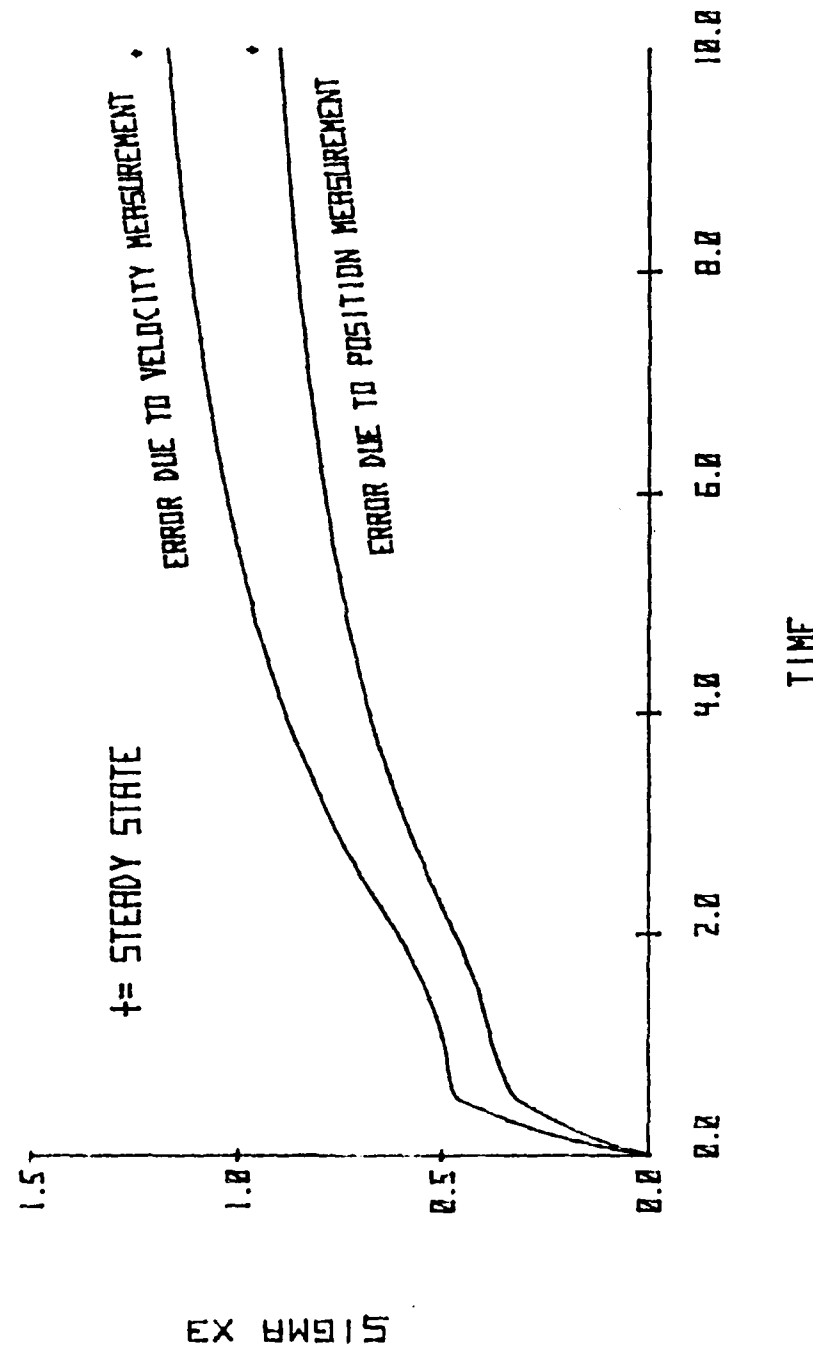


Figure 4-11 Tracking errors in X_3 as a result of measurement errors in position and velocity.

	$\frac{x_1}{}$	$\frac{x_2}{}/s$	$\frac{x_3}{}/s^2$
Second Alternate Measurement Scheme, Calculated Acceleration	0.75	0.267	
Measured Acceleration	1.6	0.58	3.46
Percent increase of expected error	113%	117%	116%

Table 4-4 Steady state error in x_1 , x_2 and x_3 for measurements made by strapdown sensors.

system, uncertainty would exist in the knowledge of constants b and c and it could be expected that this would result in additional uncertainty in the value of the state variables. It might be possible that the uncertainty in the knowledge of the plant could negate the advantage gained by estimating acceleration as in the second alternate measurement scheme.

In conclusion, it has been shown that sensor noise does not adversely affect the SRFIMF position controller. It was also shown that acceleration measurement alone is not sufficient for acceptable operation of the controller. The analysis technique used in this section will next be applied to the analysis of a SRFIMF controller when the plant is assumed to be the longitudinal axis of the Harrier aircraft.

V. APPLICATION OF THE SRFIMF CONCEPT TO THE HARRIER AIRCRAFT

A. PITCH ATTITUDE CONTROL

The preceding discussion dealt with the SRFIMF controller with the plant assumed to be a general second order system. In this section, the closed loop system will be modeled using the transfer function of a VSTOL aircraft. For this purpose the AV-8A Harrier, a jet-lift type VTOL aircraft, was chosen. The stability derivatives and transfer functions were obtained from reference [12]. The SRFIMF controller concept will be applied to the pitch attitude control of the aircraft and the analysis will be similar to that done earlier when the plant was assumed to be that of a second order system. As before, we will examine the root locus, time response and the effect of measurement errors. The effect of gust inputs to the plant will also be considered.

The transfer function between the pilot's stick and the pitch attitude of the Harrier, at 60 kts, 100 ft/sec, as given by reference [12] is

$$\frac{\theta(s)}{\delta_e(s)} = \frac{0.25 (s^2 + .246s + .00756)}{s^4 + .4896s^3 - .4495s^2 + .06736s + .00747} \quad 5-1a$$

$$= \frac{0.25 (s + .21)(s + .036)}{(s + 1)(s + .073)(s^2 - .1864s + .1024)} \quad 5-1b$$

$\theta(s)$ is given in radians and $\delta_e(s)$ in inches of stick displacement. The above transfer function does not include the effect of the control actuator which we include, as before, in the model of the controller.

The denominator factors of equation 5-1b indicate that at 60 kts the Harrier has an unstable oscillatory mode with a natural frequency, of 0.32 and damping ratio of -0.91, and that the constant plant gain, CPG, is 0.25. The plant, given by equation 5-1, is used to compute the root locus for the system by applying equation 3-21, developed for the controller in section III and rewritten here for convenience

$$1 + \frac{KRL(s^2 + K_x s + K_x)}{s} G'(s) = 0 \quad 3-21$$

where $G'(s)$ is the open loop plant given by

$$G'(s) = \frac{G(s)}{CPG}$$

For the root locus evaluation, KRL was varied from 1 to 100. The value of the actuator time constant, τ , was chosen to be 0.1 sec and K_x and $K_{\dot{x}}$ were 3 and 4 respectively.

The root locus of the oscillatory pole is given in figure 5-1. The trajectory of this pole is similar to those given in section III where the plant was assumed to be a second order system. As before, the closed loop system oscillatory poles are near those of the model (-1.5, 1.32) at KRL values of about 25 and greater. Because of the scale of the figure,

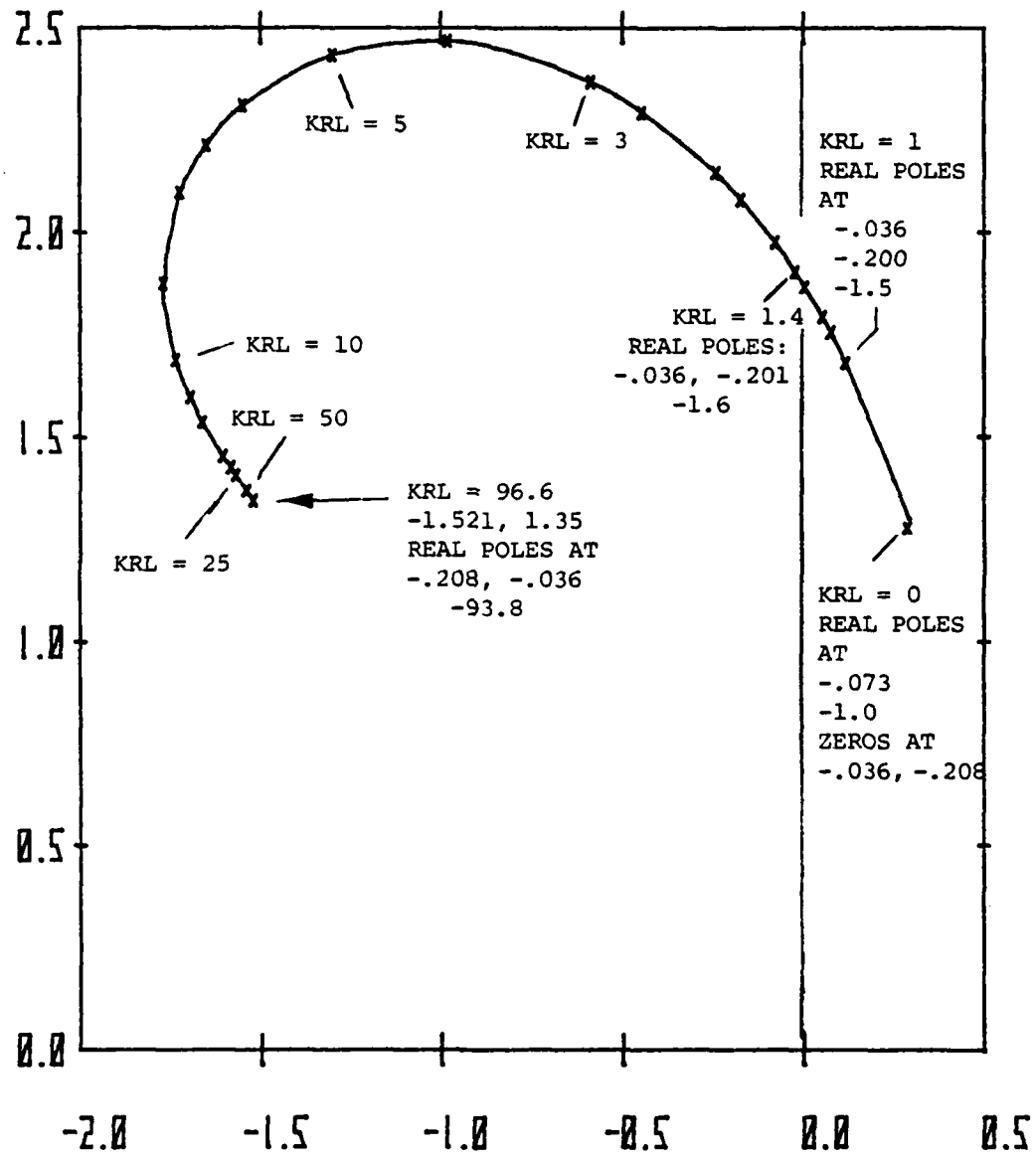


Figure 5-1 Root locus of the oscillatory poles of the longitudinal axis of the Harrier using SRFIMF position control. Note that the open loop zeros are nearly canceled at KRL = 1.0.

the real poles are not plotted, however their values are listed on the figure for various values of KRL. At the final value of KRL (96.6), the system's real poles were located at -93.82, -.2079 and -.036. The pole at -93.28 corresponds to the controller mode and its location is nearly equal to the value of KRL. This result was discussed in section three. The two other poles located at -.036 and -.2079 cancel the open loop zeroes of the plant located at -.036 and -.21 as seen in the open loop transfer function, equation 5-1b. Zero cancellation by a pole could be very detrimental to the response if the open loop zeroes are located in the right half of the complex plane, because it would be unreasonable to expect perfect pole-zero cancellation. This is a problem typically encountered in model following techniques when the plant has zeroes in the right half plane.

From the root locus, figure 5-1, it can be seen that the dynamic behavior of the SRFIMF controller is unchanged by the introduction of a more complicated plant. We shall now consider the time response of the closed loop system.

The controller and plant system was simulated using the CSMP program discussed in section III. The source code is listed in Appendix A. Simulation of the Harrier transfer function is illustrated using a signal flow graph shown in figure 5-2. The outputs of position, velocity and acceleration are shown in the figure as part of the overall transfer function simulation. For the simulation, KRL was chosen to be 50, τ was

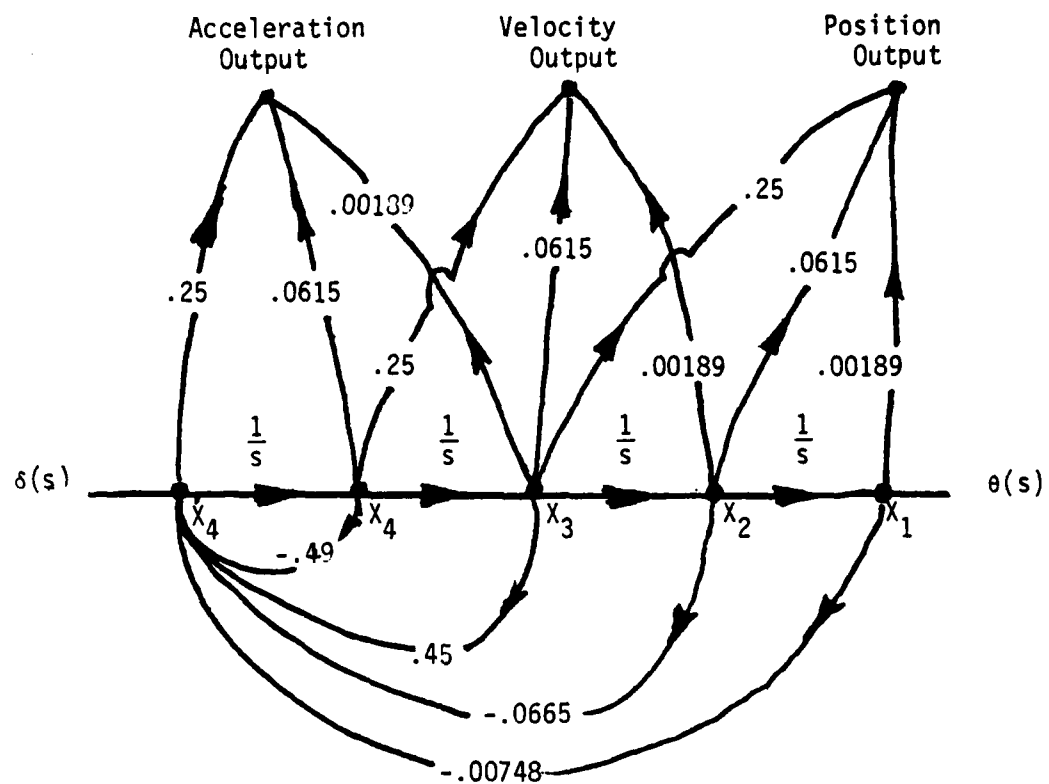


Figure 5-2 Harrier longitudinal signal flow graph transfer function simulation.

0.1 sec, K_x and K_x were 3 and 4. Plots of the time histories of the closed and open loop position, $\theta(t)$, as a result of the simulation, are given in figure 5-3. The figure indicates that the closed loop dynamic response is nearly identical to that of the model as shown in figure 3-5.

To evaluate the effect of the sensor noise, the state space representation of the system is required. Four states represent the plant. Defining X_1 and position and X_2 as velocity we write the transfer function for the Harrier, given

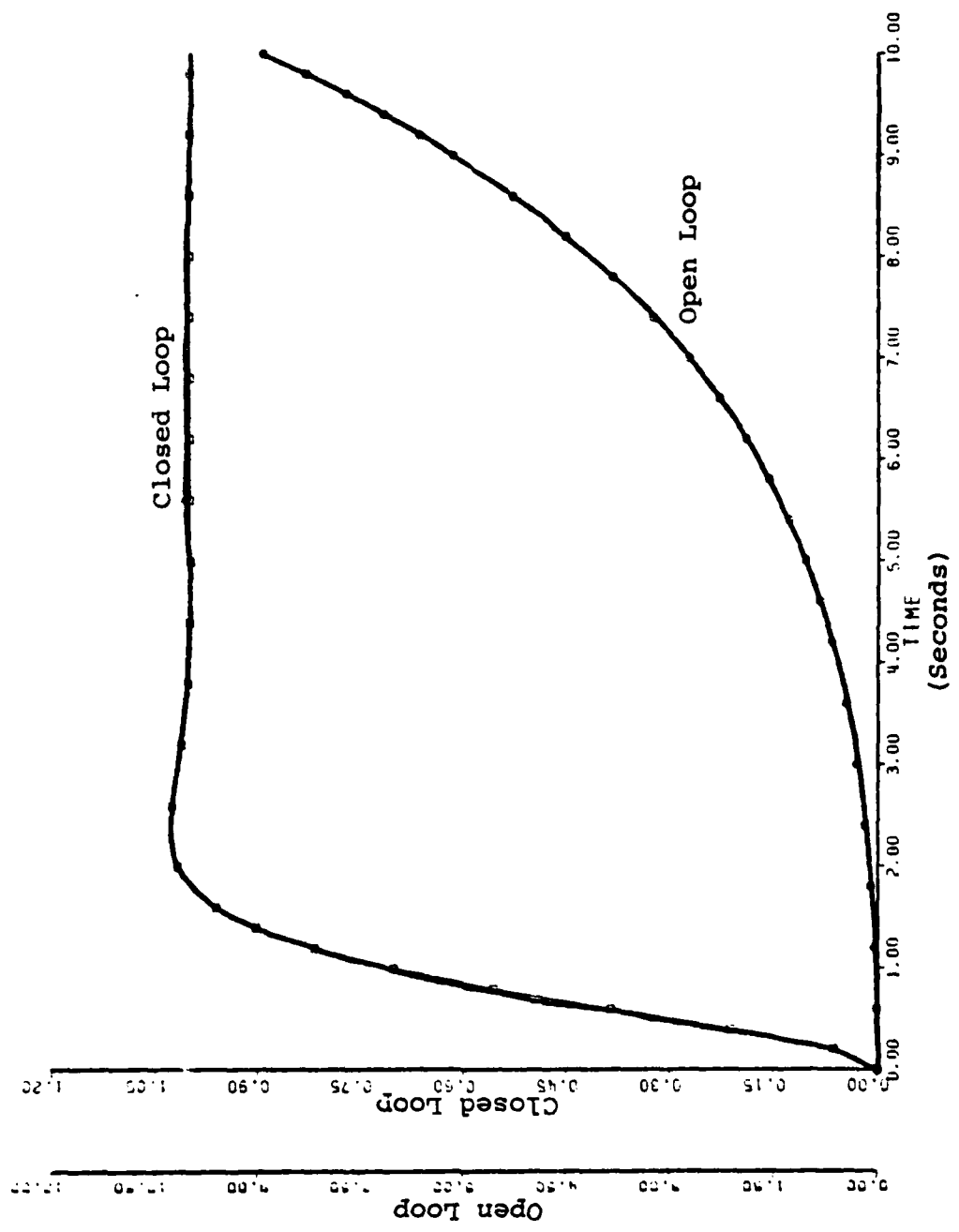


Figure 5-3 Simulation of the unit step response of the pitch attitude of the AV-8A Harrier with SRFIMF control.

in equation 5-1 in matrix notation as

$$\left\{ \begin{array}{l} \dot{x}_1 \\ \dot{x}_2 \\ \dot{x}_3 \\ \dot{x}_4 \end{array} \right\} = \begin{bmatrix} 0 & 1 & 0 & 0 \\ 0 & 0 & 1 & 0 \\ 0 & 0 & 0 & 1 \\ -.00747 & -.06736 & .4495 & -.4896 \end{bmatrix} \left\{ \begin{array}{l} x_1 \\ x_2 \\ x_3 \\ x_4 \end{array} \right\} + \left\{ \begin{array}{l} 0 \\ .25 \\ -.061 \\ .1443 \end{array} \right\} \delta_e$$

5-2

The control vector of equation 5-2 is determined by the numerator of equation 5-1 so that the states x_1 and x_2 are position and velocity. The algorithm for determining the required control vector is given by Ogata, reference [13].

The remaining state variables are defined in the following way

x_5 = output of the control actuator, input to the plant

x_6 = output of the compensator

x_7 = state variable representing velocity sensor error

x_8 = state variable representing acceleration sensor error

x_9 = state variable representing position sensor error

Figure 5-4 is the schematic representation of the system and from the figure the control law is obtained as

$$W(t) = -K_x x_1 - K_{\dot{x}} x_2 - x_3 - CPG x_5 + x_6 - K_x x_7 - x_8 - K_x x_9$$

5-3

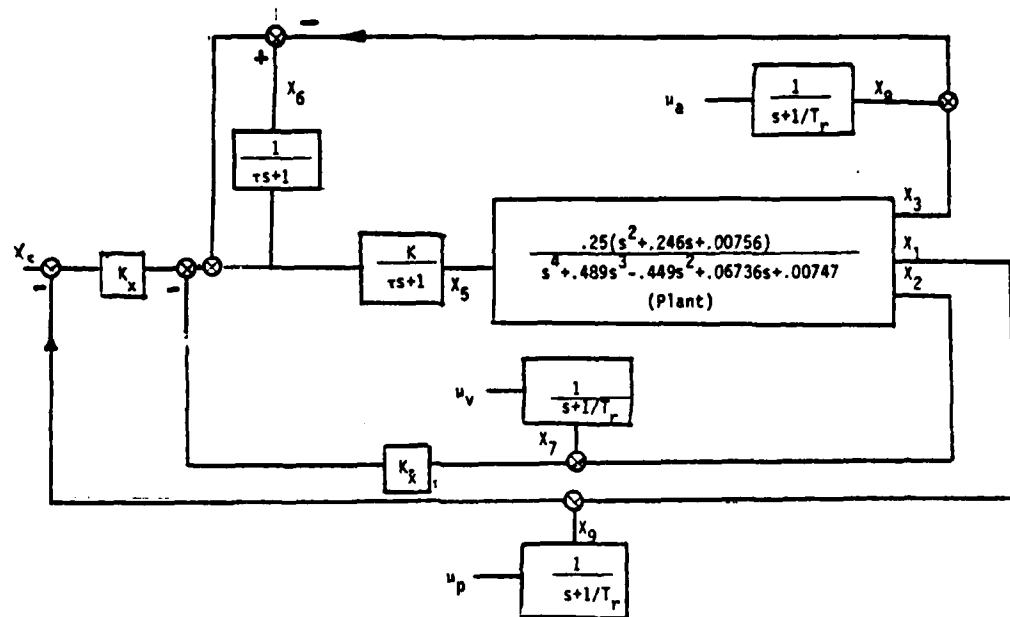


Figure 5-4 Schematic representation of the AV-8A Harrier pitch axis with the SRFIMF controller. Including sensor noise.

Combining and expressing the system in matrix form, the closed loop system is given by

$$\dot{X} = AX + BQ$$

5-4

$$A = \begin{bmatrix} 0 & 1 & 0 & 0 & 0 & 0 & 0 & 0 & 0 \\ 0 & 0 & 1 & 0 & .25 & 0 & 0 & 0 & 0 \\ 0 & 0 & 0 & 1 & -.06115 & 0 & 0 & 0 & 0 \\ .00748 & -.0675 & .45 & -.4906 & .1443 & 0 & 0 & 0 & 0 \\ -KK_x/\tau & -KK_x'/\tau & -K/\tau & 0 & -(.25K+1)/\tau & K/\tau & -KK_x'/\tau & -K/\tau & -KK_x/\tau \\ -K_x'/\tau & -K_x''/\tau & -1/\tau & 0 & -.25/\tau & 0 & -K_x'/\tau & -1/\tau & -K_x''/\tau \\ 0 & 0 & 0 & 0 & 0 & 0 & -1/T_r & 0 & 0 \\ 0 & 0 & 0 & 0 & 0 & 0 & 0 & -1/T_r & 0 \\ 0 & 0 & 0 & 0 & 0 & 0 & 0 & 0 & -1/T_r \end{bmatrix}$$

$$B = \begin{bmatrix} 0 & 0 & 0 \\ 0 & 0 & 0 \\ 0 & 0 & 0 \\ 0 & 0 & 0 \\ 0 & 0 & 0 \\ 0 & 0 & 0 \\ 0 & 0 & 0 \\ 1 & 0 & 0 \\ 0 & 1 & 0 \\ 0 & 0 & 1 \end{bmatrix} \quad Q = \begin{bmatrix} 2\sigma_v^2/T_r & 0 & 0 \\ 0 & 2\sigma_a^2/T_r & 0 \\ 0 & 0 & 2\sigma_p^2/T_r \end{bmatrix}$$

Having the system, represented in state space, the technique used in the previous section can be applied. The general solution will be obtained for a unit value of sensor error standard deviation and later applied to the specific sensor suits assumed earlier. The constants required to obtain the numerical solution are: $K = 20$; $\tau = 0.1$; $K_x = 4$; $K_{\dot{x}} = 3$; $KRL = K \cdot CPG/\tau = 50$. The resulting system is

$$\dot{X} = AX + BQ \quad 5-5$$

$$Y = CX$$

$$\dot{X}^* = A^*X^* + B^*Q \quad 5-6$$

$$Y = C^*X^*$$

(Matrices A, B, C, A*, B* and C* are shown on the following pages.)

The result of the modal transformation is that the noise sources have about the same controllability and observability as in the

$$A = \begin{bmatrix} 0.0 & 1.0 & 0.0 & 0.0 & 0.0 & 0.0 & 0.0 \\ 0.0 & 0.0 & 1.0 & 0.0 & 0.25 & 0.0 & 0.0 \\ 0.0 & 0.0 & 0.0 & 1.0 & -0.06 & 0.0 & 0.0 \\ -0.01 & -0.07 & 0.45 & -0.49 & 0.14 & 0.0 & 0.0 \\ -800.0 & -800.0 & -200.0 & 0.0 & -60.0 & 200.0 & -600.0 \\ -40.0 & -30.0 & -10.0 & 0.0 & -2.5 & 0.0 & -30.0 \\ 0.0 & 0.0 & 0.0 & 0.0 & 0.0 & 0.0 & -0.1 \\ 0.0 & 0.0 & 0.0 & 0.0 & 0.0 & 0.0 & 0.0 \\ 0.0 & 0.0 & 0.0 & 0.0 & 0.0 & 0.0 & -0.1 \\ 0.0 & 0.0 & 0.0 & 0.0 & 0.0 & 0.0 & 0.0 \end{bmatrix}$$

$$B = \begin{bmatrix} 0.0 & 0.0 & 0.0 \\ 0.0 & 0.0 & 0.0 \\ 0.0 & 0.0 & 0.0 \\ 0.0 & 0.0 & 0.0 \\ 0.0 & 0.0 & 0.0 \\ 0.0 & 0.0 & 0.0 \end{bmatrix}$$

B =

$$C = \begin{bmatrix} 1.0 & 0.0 & 0.0 & 0.0 & 0.0 & 0.0 & 1.0 \\ 0.0 & 1.0 & 0.0 & 0.0 & 0.0 & 1.0 & 0.0 \\ 0.0 & 0.0 & 1.0 & 0.0 & 0.0 & 0.0 & 1.0 \end{bmatrix}$$

$$A^* = \begin{bmatrix} -47.17 & 0.0 & 0.01 & 0.0 & 0.0 & 0.0 & 0.0 \\ 0.0 & -1.54 & 1.37 & 0.0 & 0.0 & 0.0 & 0.0 \\ 0.0 & -1.37 & -1.54 & 0.0 & 0.0 & 0.0 & 0.0 \\ 0.0 & 0.0 & 0.0 & -0.21 & 0.0 & 0.0 & 0.0 \\ 0.0 & 0.0 & 0.0 & 0.0 & -0.03 & 0.0 & 0.0 \\ 0.0 & 0.0 & 0.0 & 0.0 & 0.0 & -10.0 & 0.0 \\ 0.0 & 0.0 & 0.0 & 0.0 & 0.0 & 0.0 & 0.0 \\ 0.0 & 0.0 & 0.0 & 0.0 & 0.0 & 0.0 & -0.1 \\ 0.0 & 0.0 & 0.0 & 0.0 & 0.0 & 0.0 & -0.1 \\ 0.0 & 0.0 & 0.0 & 0.0 & 0.0 & 0.0 & 0.0 \end{bmatrix}$$

$$B^* = \begin{bmatrix} Q_V & Q_a & Q_p \\ -13.55 & -4.52 & -18.07 \\ 10.18 & 3.39 & 13.57 \\ -7.15 & -2.38 & -9.53 \\ 5.41 & 1.80 & 7.21 \\ 1.25 & 0.42 & 1.67 \\ 0.0 & 0.0 & 0.0 \\ 2.26 & 0.0 & 0.0 \\ 0.0 & 1.21 & 0.0 \\ 0.0 & 0.0 & 2.88 \end{bmatrix}$$

$$C^* = \begin{bmatrix} 0.0 & 0.01 & -0.1 & 0.0 & 0.0 & 0.0 & 0.0 \\ 0.01 & 0.11 & 0.16 & 0.0 & 0.0 & -0.03 & 0.48 \\ 0.0 & -0.01 & -0.1 & -0.24 & 0.24 & 0.01 & 0.19 \\ & & & & & & 0.95 \\ & & & & & & 0.20 \end{bmatrix}$$

$$\begin{bmatrix} x_v^* & x_a^* & x_p^* \end{bmatrix}$$

earlier cases. It can be seen from the A* matrix that the closed loop system has two additional eigenvalues. These correspond to the shifted poles of the system. Variance analysis was done in the same way as in the earlier examples and the results are shown plotted in figures 5-5 through 5-8 and tabulated in Appendix B, table B-4. Table 5-1 lists the steady state values of the expected error in states X_1 , X_2 and X_5 .

	X_1	X_2	X_5
Position measurement error	0.98	0.36	3.85
Velocity measurement error	0.73	0.27	2.90
Acceleration measurement error	0.25	0.089	0.96

Table 5-1 Steady state values of σ_1 , σ_2 and σ_5 as a result of position, velocity and acceleration measurement error.

Comparison of table 5-1 with table 4-2 indicates that the values of the standard deviation of the X_1 and X_2 errors are identical in both cases even though the two plants are very different. The standard deviation of the plan input error (X_5 here, X_3 in section IV) is slightly different in the two cases. This should be expected because of the difference in the value of control gain K, required to yield a value of KRL equal to 50 and the large difference between the two plants. From the variance analysis, we obtain an estimate of the expected errors in X_1 , X_2 and X_5 which result from the sensor suit assumed in section IV. These values are listed in table 5-2.

SIGMA XI VS. TIME

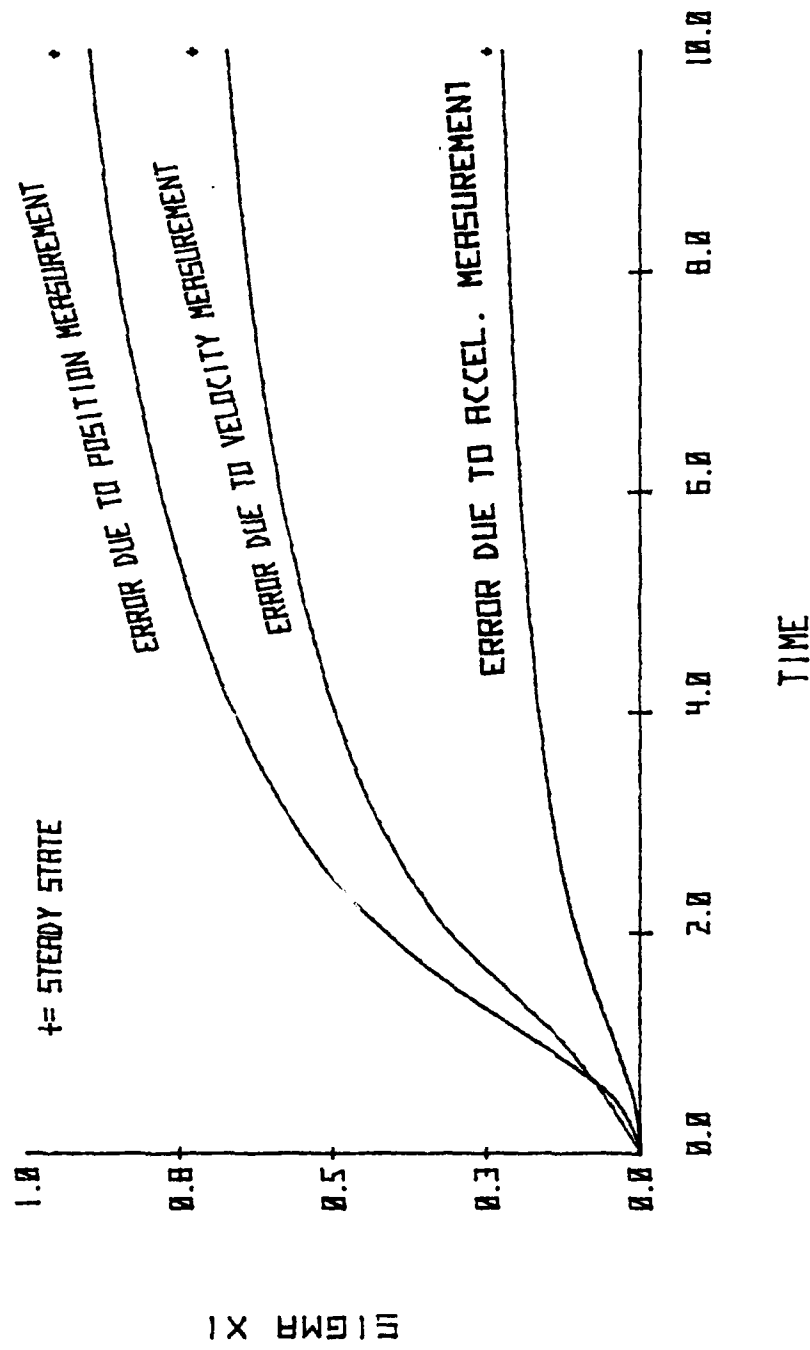


Figure 5-5 Tracking error in X_1 as a result of measurement error in position, velocity and acceleration for the Harrier longitudinal axis position control.

SIGMA X2 VS. TIME

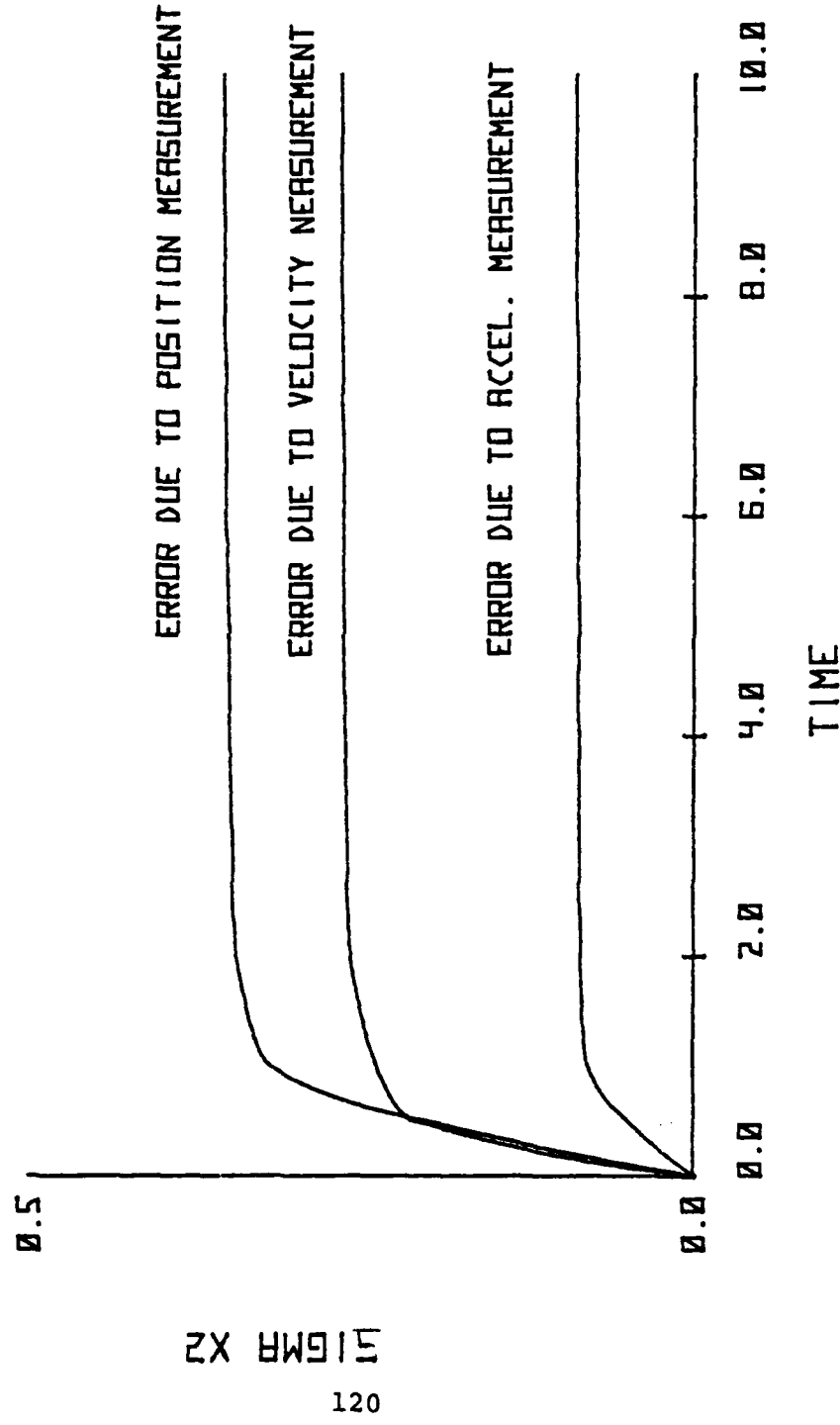


Figure 5-6 Tracking error in X_2 as a result of measurement error in position, velocity and acceleration for the Harrier longitudinal axis position control.

SIGMA X₅ VS. TIME

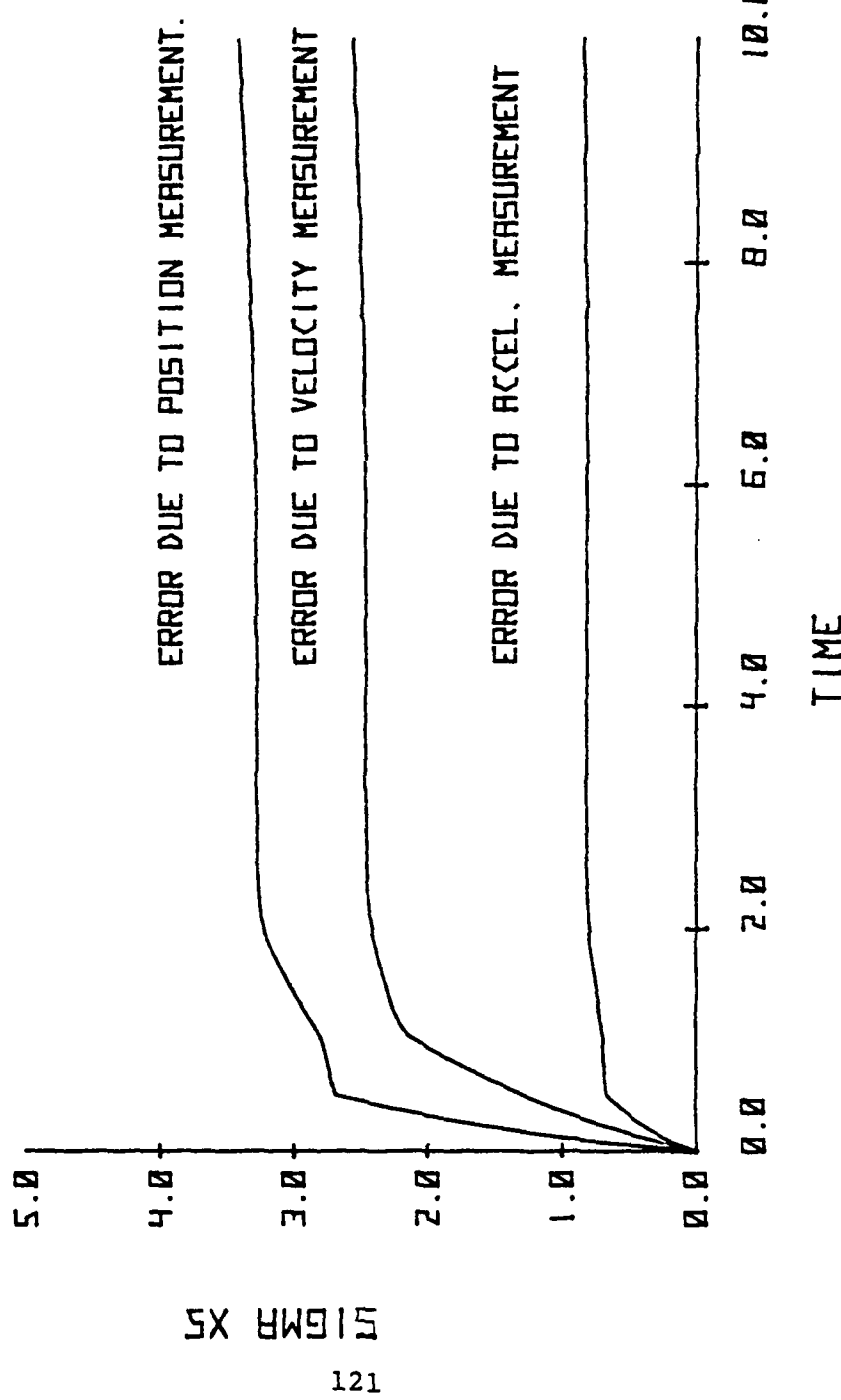


Figure 5-7 Tracking error in X_5 as a result of measurement error in position, velocity and acceleration for the Harrier longitudinal axis position control.

	X_1	X_2	X_5
Inertial sensors	0.49	0.18/sec	$1.93/\text{sec}^2$
Strapdown sensors	1.575	0.584/sec	$6.26/\text{sec}^2$

Table 5-2 Standard deviation of steady state tracking errors in X_1 , X_2 and X_5 as a result of sensor noise in the Harrier aircraft.

The Significance of the total tracking error in X_5 is determined by comparing the standard deviation of the error to the value of X_5 when a 1° input is applied to the system. In quiescent operation, a 1° step input results in an instantaneous value of X_5 of

$$X_5 = .0175\text{rad} \cdot 1^\circ K_x \quad K = 1.4 \text{ rad/sec}^2 \\ = 80^\circ/\text{sec}^2$$

The value of X_5 given in table 5-2 for strapdown sensors whose expected error is in the order of 1° is not large compared to a 1° input. We conclude that sensor measurement errors do not adversely affect the performance of the SRFIMF Harrier pitch controller.

B. PITCH ATTITUDE GUST RESPONSE

The pitch attitude response of the Harrier from a gust input will be considered by applying the same type of analysis used earlier. For this purpose assume that the gust acts as an additional, uncontrolled input to the system. The symbol δ_g is used to denote this input. The gust input will be

modeled as an exponentially correlated noise source in the same way that the sensor noise was modeled. The schematic representation of an external exponentially correlated noise source was shown in figure 4-1. In this case the output of the noise source, $\xi(s)$, is the gust input to the system and $w_t(s)$ is the white noise input of strength μ_g as given by equation 4-12. The standard deviation and correlation time for the gust can be determined by examining the Dryden wind model used in simulation by NASA. At altitudes of 500 ft. and above the Dryden model assumes that the RMS value of atmospheric turbulence, σ_g , is given as

$$\sigma_g = 0.2 V_{\text{wind}}$$

The correlation time, T_g , is determined by a characteristic length, L_w , divided by the vehicle speed, V , or

$$T_g = L_w/V$$

The Dryden model gives the characteristic length of the turbulence as

$$150 \text{ ft.} + h = L_w$$

where h is the altitude. Choosing 500 ft. as the flight altitude, a flight speed of 60 kts and 15 kts as the value of the wind, the standard deviation and correlation time is

$$\sigma_g = 5 \text{ ft/sec}, T_g = 6.5 \text{ sec}$$

The gust input is represented schematically by figure 5-8.

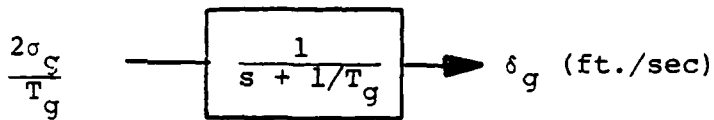


Figure 5-8 Gust shaping filter.

The transfer function between the gust and position, velocity and acceleration of the vehicle can be determined from the stability derivatives given by reference [14]. For This example we chose pitch attitude position control as was done in the previous example therefore the denominator of the gust transfer function is the same as the denominator of equation 5-1. The numerator is given by McRuer [14] for a vertical gust as

$$\frac{U_o N_g^w}{s} = (M_q - M_\alpha) s^2 + (M_\alpha - Z_w) (M_q - M_\alpha) s + X_u (M_\alpha + Z_w M_q) - X_w (V \cdot M_u + Z_u M_q) \quad 5-5$$

The stability derivatives for the Harrier at 60 kts are (6)

$$M_q = -2.6$$

$$M_\alpha = V \cdot M_w = .54$$

$$Z_w = -.190$$

$$Z_u = -.036$$

$$X_u = -0.43$$

$$X_w = -0.27$$

$$M_u = .022$$

From equation 5-5 and 5-1, we obtain the transfer function for the pitch attitude from a gust input

$$\frac{\theta(s)}{\delta_g(s)} = \frac{-0.0026s [s^2 + 2.31s + .073]}{s^4 + .4896s^3 - .4495s^2 + .0636s + .00747} \quad 5-6$$

The transfer function from the pilot's stick to the pitch angle is given by equation 5-1 where the input to the plant is δ_e . Expressing the plant, with multiple inputs of stick and gust load, in matrix notation with states X_1 and X_2 defined as position and velocity we have

$$\left\{ \begin{array}{c} \dot{x}_1 \\ \dot{x}_2 \\ \dot{x}_3 \\ \dot{x}_4 \end{array} \right\} = \begin{bmatrix} 0 & 1 & 0 & 0 \\ 0 & 0 & 1 & 0 \\ 0 & 0 & 0 & 1 \\ -.00747 & -.06736 &+.4495 &-.4896 \end{bmatrix} \left\{ \begin{array}{c} x_1 \\ x_2 \\ x_3 \\ x_4 \end{array} \right\} + \begin{bmatrix} 0 & -.0026 \\ .25 & -.00473 \\ -.061 & .00306 \\ .1443 & .00345 \end{bmatrix} [\delta_e \delta_g]$$

The B matrix has been determined as before so that states X_1 and X_2 represent position and velocity.

Having the plant transfer function defined by 5-7 we can develope the equation to represent the closed loop controller. The additional state variables required are defined

X_5 = output of the control actuator, input to plant

X_6 = output of the compensator

X_7 = gust input to the plant, $\delta_g(s)$, figure 5-5.

The schematic of the closed loop system is shown in figure 5-9.

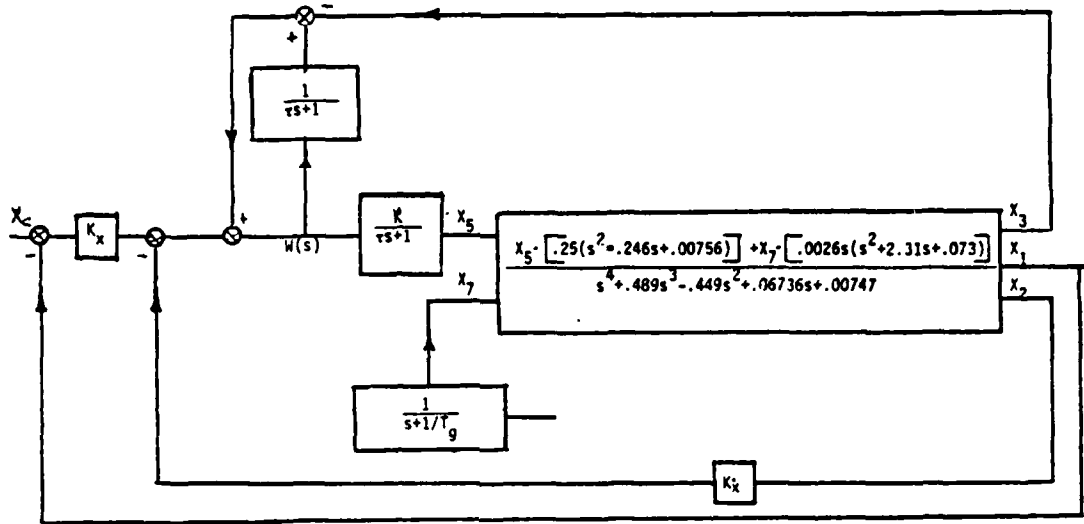


Figure 5-9 Schematic representation of the AV-8A Pitch control using a SRFIMF controller with wind gust input.

With $X_C = 0$, the control law $W(t)$ is

$$W(t) = -K_x X_1 - K_x X_2 - X_3 - .25X_5 + X_6 + (K_x \cdot .0026 + .00473)X_7$$

Rearranging in a manner similar to earlier work, we write the closed loop equation in matrix notation as

$$\dot{X} = AX + BQ$$

5-8

$$A = \begin{bmatrix} 0 & 1 & 0 & 0 & 0 & 0 & -.0026 \\ 0 & 0 & 1 & 0 & .25 & 0 & -.00473 \\ 0 & 0 & 0 & 1 & -.061 & 0 & .00306 \\ -.00748 & -.0675 & .45 & -.49 & .1443 & 0 & .00346 \\ -K_x/\tau & -KK_x/\tau & -K/\tau & 0 & -(.25 \cdot K + 1)/\tau & K/\tau & (K_x \cdot .0026 + .00473)K/\tau \\ -K_x/\tau & -KK_x/\tau & -1/\tau & 0 & -.25/\tau & -K_x/\tau & (K_x \cdot .0026 + .00473)/\tau \\ 0 & 0 & 0 & 0 & 0 & 0 & -1/T_g \end{bmatrix}$$

$$B = \begin{pmatrix} 0 \\ 0 \\ 0 \\ 0 \\ 0 \\ 0 \\ 0 \\ 1 \end{pmatrix} \quad Q = \begin{bmatrix} 2\sigma_g/T_g \end{bmatrix}$$

The covariance of the states were calculated for the system described above as was done in previous examples. The results of the covariance analysis was that the RMS values of X_1 and X_2 are very small and quickly reach the steady state values of

$$\sigma_p = \sigma_{X_1} = .0017 \quad \sigma_v = \sigma_{X_2} = .0134$$

In the case of the gust we are interested in the pitch acceleration of the vehicle as a result of the gust input. Acceleration is given as \dot{X}_2 and from equation 5-8 is

$$\text{Acceleration} = X_3 + .25X_5 - .00473X_7 \quad 5-9$$

Recalling that the elements of the covariance matrix, P, are the squares of the standard deviations of the state variables, we write from equation 5-9 that

$$\sigma_{\text{accel}} = P_{33}^{1/2} + .25P_{55}^{1/2} - .00473P_{77}^{1/2}$$

The standard deviation in pitch acceleration as a result of a gust input was plotted along with the gust input and the RMS value of X_5 as a function of time in figure 5-7. The results are also listed in Appendix B table B-5. The gust is shown for comparison of response time.

It is seen from the figure that the rise time in the RMS value of the vehicle acceleration is much slower than the gust itself. This result can be interpreted as a smoothing of the gust by the aircraft. This is primarily due to the slow response of the aircraft to the gust. The controller has a relatively fast reaction time and can maintain the output X_1 with only very small errors as a result of a gust input.

The analysis of the SRFIMF controller applied to the Harrier has indicated that the qualities of the controller found by analysis when the plant is assumed to be a second order system apply equally well when the plant is an actual VSTOL aircraft. We have also seen that the controller does not produce undesirable dynamic response when the vehicle is subjected to gust inputs and that the dynamic response of the aircraft and controller is due to the response of the aircraft alone to the gust.

HARRIER GUST RESPONSE

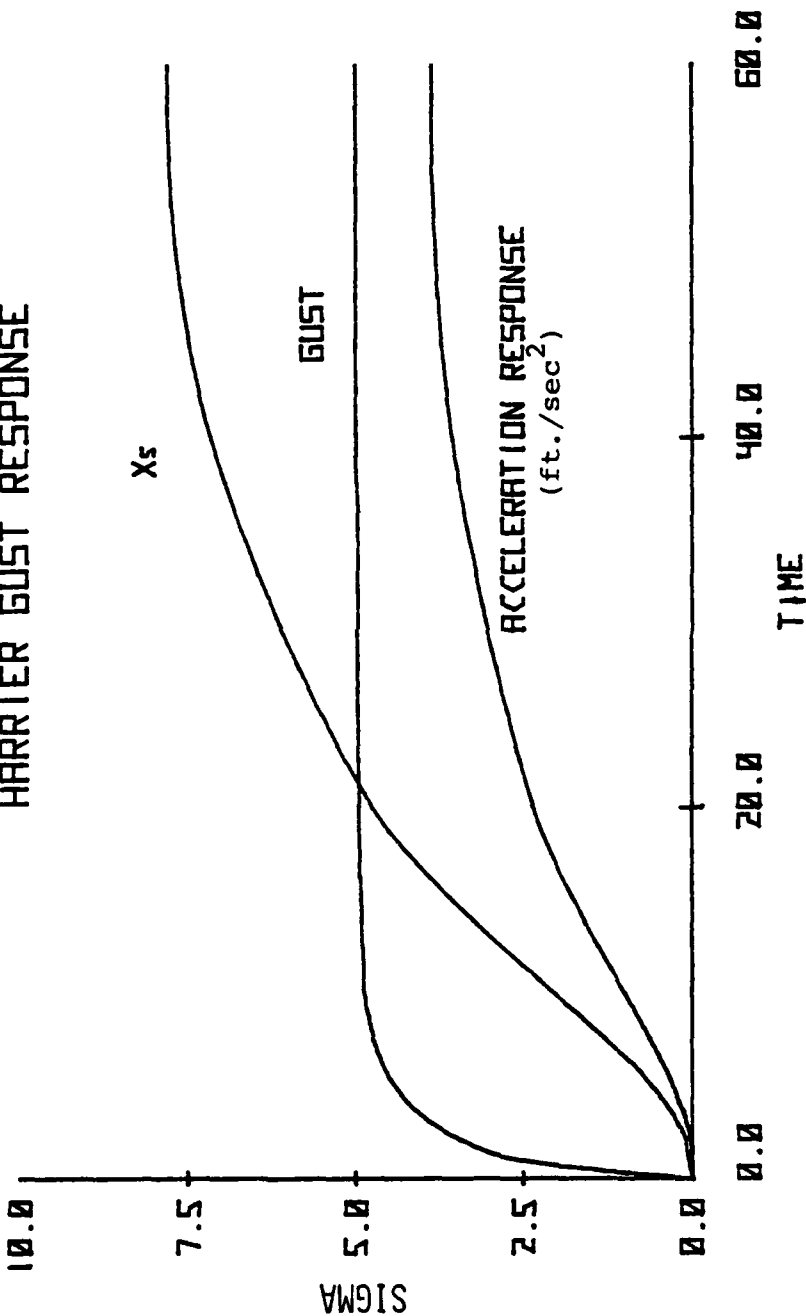


Figure 5-10 Standard deviation of vehicle pitch acceleration and plant input, X_5 , as a result of a gust.

VI. CONCLUSIONS

The use of State Rate Feedback Implicit Model Following, for the attitude control of VSTOL aircraft, has been studied. The SRFIMF control scheme is simple, easy to implement and can be expected to be reliable. It was shown that the dynamic response of the closed loop system is a second order response and that the natural frequency and damping are free choices of the designer. It was also shown that sensor noise does not adversely affect the operation of the system. Detailed conclusions of this study are:

1. Model following was shown in section III-D by simulations to be very good. Despite changing plant dynamics, representing a variety of flight conditions, the closed loop system had a response characteristic of that of the model and that the output of the closed loop system was driven to the value of the input.
2. The frequency response of the system is that of a low pass filter and that there was no phase shift between the output and the input at low frequencies.
3. Non-minimum phase system, pole-zero cancellation can lead to unstable performance.
4. High quality sensors are not required. It was shown by the covariance analysis in section IV-B that the error in position is approximately equal to the error in position

measurement plus 75 percent of the error in velocity measurement plus 25 percent of the error in acceleration measurement. The general result is that sensor errors do not adversely affect the performance of the system.

5. Estimation of position and velocity by integration of acceleration was shown to lead to unstable performance because of neutrally stable modes resulting from the integration. It was shown in section IV-C that acceleration sensor noise disturbs the neutrally stable modes with the result that the system diverges. It is then concluded that the quantities of position and velocity must be measured in order to have a stable system which does not require knowledge of the plant.

6. The system is capable of compensating for gust inputs. The analysis of section V-C showed that the error in position output was small as a result of the gust. Secondly, the response of the system to the gust is smoothed by the action of the uncontrolled plant.

APPENDIX A
COMPUTER LISTINGS

```
*****  
* *** SRFIMF SIMULATION SOURCE CODE ***  
*  
* CSMP SOURCE CODE USED TO SIMULATE THE RESPONSE OF  
* THE SRFIMF AND AN ARBITRARY SECOND ORDER PLANT.  
* THE FUNCTIONS INTGRL AND REALPL ARE CSMP FUNCTIONS  
* WHICH PREFORM INTEGRATION OR SIMULATE A FIRST ORDER  
* RESPONSE. THE ORDER OF THE STATEMENTS IS UNIMPORTANT IN  
* CSMP.  
*  
*****  
// EXEC CSMPXV  
//X.COMPRINT DD DUMMY  
//X.SYSPRINT DD DUMMY  
//X.SYSIN DD *  
AS=REALPL(0,TOU,WS)  
X=INTGRL(0,VX)  
VX=INTGRL(0,AX)  
AX1=REALPL(0,TOU,IS)  
AX=AX1*CPG-C*X-B*VX  
IS=WS*K  
WS=-KXD*VX+(XC-X)*KX+VS  
VS=AS-AX  
*  
* SIMULATION OF THE OPEN LOOP PLANT  
*  
XDD=CPG*AX2-C*XP-VXP*B  
AX2=REALPL(0.,TOU,XC)  
VXP=INTGRL(0,XDD)  
XP=INTGRL(0,VXP)  
XC=G*STEP(0)  
G=1.  
CPG=4.  
TOU=.1  
K=5.  
KXD=3.  
KX=4.  
B=.6  
C=2.16  
TIMER FINTIM=10,OUTDEL=.2  
OUTPUT X,XP  
OUTPUT TIME,XP  
PAGE XYPLOT  
END  
STOP
```

```

***** MAIN 1 *****

MAIN 1 IS THE CODE USED TO GENERATE THE A,B AND C MATRICES FOR
THE BASIC STOCHASTIC SRFIM. POSITION, VELOCITY AND ACCELERATION
ARE ASSUMED TO BE MEASURED AND THE PLANT IS A SECOND ORDER
SYSTEM. THE PROGRAM CALLS VARY TO DETERMINE THE SOLUTION TO
THE LYAPUNOV EQUATION AND MODAL FOR THE MODAL ANALYSIS.

***** DIMENSION B(8,4),TR(4),H(3,8)
REAL K,KX,KD
COMMON BP,CP,K,KX,KD,TOU,CVG,N,PD(64),Q(8,8),A(8,8)
WRITE(6,100)
FORMAT('20X*90(*'1*',//40X*'MODEL 1, POSITION, VELOCITY AND *',
1,ACCELERATION MEASURED',//20X,90(*1*),N=8
NCOUNT = 0
N=3
L=4
BP=.6
CP=.15
K=.5
KD=.3.
KX=.4.
TR(1)=10.
TR(2)=10.
TR(3)=10.
TR(4)=10.
SIGMA1=1.
TODU=.1
CVG=.1
SIGMA2=.1.
SIGMA3=.1.
COMPUTE A,B,C
DO 9 I=1,N
DO 9 J=1,N
9 A(I,J)=0.0
DO 5 I=1,L
DO 5 J=1,L
5 B(I,J)=0.0
A(1,2)=1.
A(2,1)=-CP

```

```

A(2,2)=-BP
A(2,3)=CPG
A(3,2)=((CP-KX)*K/TOU
A(3,3)=((BP-KXD)*K+1.)/TOU
A(3,4)=K/TOU
A(3,5)=-KXD*K/TOU
A(3,6)=-K*X/TOU
A(3,7)=-K*X/KX/TOU
A(3,8)=-A(3,7)
A(4,1)=A(3,1)/K
A(4,2)=A(3,2)/K
A(4,3)=-CPG/TOU
A(4,4)=-KXD/TOU
A(4,5)=-K*X/TOU
A(4,6)=-1.*TOU
A(4,7)=-K*X/TOU
A(4,8)=KX/TOU
A(5,5)=-1.*TR(1)
A(5,6)=-1.*TR(2)
A(5,7)=-1.*TR(3)
A(5,8)=-1.*TR(4)

C      B(5,1)=1.
      B(6,2)=1.
      B(7,3)=1.

C      DO 1 I=1,N
      DO 1 J=1,N
      H(1,1)=0.
      H(1,7)=1.
      H(2,2)=1.
      H(2,5)=1.
      H(3,1)=CP
      H(3,12)=-CPG
      H(3,3)=CPG
      H(3,6)=1.

C      DO 4 I=1,L
      DO 4 J=1,L
      Q(1,1)=0.0
      Q(1,1)=(2./TR(1))*SIGMA1**2
      Q(2,2)=(2./TR(2))*SIGMA2**2
      Q(3,3)=(2./TR(3))*SIGMA3**2
      Q(4,4)=(2./TR(4))*SIGMA4**2
      NPT=3
      T1=0.0

```

```

T2=60. CALL ECHO(A,B,Q,H,TR,N,M,L)
CALL VARY(B,L,N,P,T1,T2)
CALL MODAL(A,B,H,N,M,L)
STOP
END
****

C          MAIN 2
C
C          MAIN 2 IS THE CODE USED TO GENERATE THE A,B AND C
C          MATRICES FOR THE FIRST ALTERNATE MEASUREMENT SCHEME.
C          IN THIS CASE ACCELERATION IS MEASURED, POSITION
C          AND VELOCITY ARE ESTIMATED.
C*****
C***** DIMENSION B(8,4),H(3,8),TR(2)
REAL KX,KXD
COMMON BP,CP,<,KX,KXD,TOJ,CVG,N,PD(64),Q(8,8),A(8,8)
WRITE(6,100)
100  FORMAT(20X,90('**'),//,40X,'MODEL 2, MEASURED ACCELERATION',
      1,' IMPLIED POSITION AND VELOCITY, /, 20X, 90(*')) ,N=8
M=3
L=2
NCOUNT=0
C          INITIALIZE MATRICES TO ZERO
DO 1 I=1,N
  DO 1 J=1,N
    A(I,J)=0.0
    DO 2 I=1,N
      DO 2 J=1,L
        B(I,J)=0.0
        DO 3 I=1,L
          DO 3 J=1,L
            Q(I,J)=0.0
            DO 4 I=1,M
              DO 4 J=1,N
                H(I,J)=0.0
1       4
C          CALCULATE THE A,B,C MATRICES
A(1,2)=1.0
A(2,1)=-CP
A(2,2)=-BP
A(2,3)=CP

```

```

MOD01480
MOD01490
MOD01500
MOD01510
MOD01520
MOD01530
MOD01540
MOD01550
MOD01560
MOD01570
MOD01580
MOD01590
MOD01600
MOD01610
MOD01620
MOD01630
MOD01640
MOD01650
MOD01660
MOD01670
MOD01680
MOD01690
MOD01700
MOD01710
MOD01720
MOD01730
MOD01740
MOD01750
MOD01760
MOD01770
MOD01780
MOD01790
MOD01800
MOD01810
MOD01820
MOD01830
MOD01840
MOD01850
MOD01860
MOD01870
MOD01880
MOD01890
MOD01900
MOD01910
MOD01920
MOD01930
MOD01940
MOD01950

A(3,1)=CP*K/TOU
A(3,2)=BP*K/TJJ
A(3,3)=-(CPG*K+1.)/TOU
A(3,4)=-K*/TOU
A(3,5)=-K*X0/TOU
A(3,6)=-K*/TOU
A(3,7)=K*X0/TOU
A(3,8)=CP/TOU
A(4,1)=BP/TOU
A(4,2)=BP/TJJ
A(4,3)=-CPG/TJJ
A(4,4)=-K*X0/TOU
A(4,5)=-K*X/TOU
A(4,6)=-K*X/TOU
A(4,7)=-1./TOU
A(4,8)=KX/TOU
A(5,1)=-CP
A(5,2)=-BP
A(5,3)=CPG
A(5,4)=1.
A(5,5)=1.
A(5,6)=1.
A(5,7)=1.
A(6,7)=-1./TR(1)
A(8,7)=-1./TR(2)
A(8,8)=-1./TR(2)

C
B(7,1)=1.
B(8,2)=0.
H(1,1)=1.
H(2,2)=1.
H(3,1)=-CP
H(3,2)=-BP
H(3,3)=CPG
SIGMA1=1.
SIGMA2=1.
H(3,7)=1.

C
Q(1,1)=(2./TR(1))*SIGMA1**2
Q(2,2)=(2./TR(2))*SIGMA2**2
NPT=1
T1=0.0
T2=.5
CALL ECHO(A,B,Q,H,TR,N,M,L)
CALL VARY(B,L,NPT,T1,T2)
CALL MODAL(A,B,H,N,M,L)
1151 STOP
END
C***** C MAIN 3 IS THE CODE USED TO GENERATE THE A,B AND C MATRICES
C

```

```

C FOR THE SECOND ALTERNATE MEASUREMENT SCHEME. IN THIS
C CASE POSITION AND VELOCITY ARE MEASURED AND ACCELERATION IS
C ESTIMATED.
C ****
C***** DIMENSION B(7,3),TR(3),H(3,7)
C      REAL K,KX,KXD
C      COMMON BP,K,KX,KXD,TDU,CPG,N,PD(49),Q(7,7),A(7,7)
C      WRITE(6,100)
C      FORMAT(20X,'90(*,*','/','0X','MODEL 3 MEASURED POSITION AND VELOCI*'
C      1,'TV IMPLIED ACCELERATION ','/','0X,90(*,*))')
C      N=7
C      M=3
C      L=3
C      NCOUNTI=0
C      WRITE(6,502)
C      FORMAT(1/'10X, ' ERROR DUE TO POSITION MEASUREMENT',//)
C      502
C      SIGMA1=1.
C      SIGMA2=1.
C      SIGMA3=1.
C
C      COMPUTE A,B,C,Q
C      INITIALIZE ALL MATRICES
C
C      DO 1 I=1,N
C      DO 1 J=1,N
C      A(I,J)=0.0
C      DO 2 I=1,N
C      DO 2 J=1,L
C      B(I,J)=0.0
C      DO 3 I=1,L
C      DO 3 J=1,L
C      C(I,J)=0.0
C      DO 4 I=1,N
C      DO 4 J=1,M
C      H(I,J)=0.0
C
C      1
C      2
C      3
C      4
C
C      A(1,2)=1.0
C      A(2,1)=-BP
C      A(2,2)=-CP
C      A(2,3)=CP
C      A(3,1)=K*(CP-KX)/TOU
C      A(3,2)=K*(BP-KXD)/TOU
C      A(3,3)=-K*CPG+1./TOU
C      A(3,4)=K/TOU
C      A(3,5)=A(3,1)
C      A(3,6)=A(3,2)

```

```

A(3,7)=K*KX/TD
A(4,1)=(CP-KX)/TOU
A(4,2)=(BP-KXD)/TOU
A(4,3)=-CPG/TD
A(4,5)=A(4,1)
A(4,6)=A(4,2)
A(4,7)=KX/TOU
A(5,5)=-1./TR(1)
A(5,6)=-1./TR(2)
A(5,7)=-1./TR(3)
B(5,1)=1.
B(5,2)=0.
B(5,3)=0.
H(1,1)=1.
H(2,2)=1.
H(3,1)=-CP
H(3,2)=-BP
H(3,3)=CPG
C
Q(1,1)=(2./TR(1))*SIGMA1**2
Q(2,2)=(2./TR(2))*SIGMA2**2
Q(3,3)=(2./TR(3))*SIGMA3**2
NPT=40
T1=0.
T2=20.
CALL ECHO(A,B,Q,H,TR,N,M,L)
CALL VARY(B,L,N,P,T1,T2)
CALL MODAL(I,A,B,H,N,M,L)
STOP
END
C***** HARRIER 1 IS THE CODE USED TO GENERATE THE A,B AND C MATRICES
C FOR THE COVARIANCE CALCULATIONS OF THE SRFIM CONTROLLER
C AND THE LONGITUDINAL MODE OF THE HARRIER.
C***** DIMENSION B(9,3),H(3,9),TR(3)
REAL K,KX,KXD
COMMON BP,CP,K,KX,KXD,TOU,CPG,N,PD(81),Q(9,9),A(9,9)
WRITE(6,100)
100 FORMAT('/*20X,90(*'1'/*40X,'HARRIER MODEL ','1',
1. ALL QUANTITIES MEASURED',//,20X,90(*.*),/,/
N=9
L=3
M=3
K=20.

```

KX=4.
KXD=3.

TOU=.1.
SIGMA1=1.
SIGMA2=1.
SIGMA3=1.
TR(1)=10.
TR(2)=10.
TR(3)=10.

C C C CALCULATE THE A MATRIX

```
DO 1 I=1,N  
DO 1 J=1,N  
A(1,J)=0.  
A(1,2)=1.  
A(2,3)=1.  
A(2,5)=2.5  
A(3,4)=1.  
A(3,5)=-0.6115  
A(4,1)=-0.0748  
A(4,2)=-0.675  
A(4,3)=0.45  
A(4,4)=-4.906  
A(4,5)=0.14428  
A(5,1)=-K*KX/TOU  
A(5,2)=-K*KXD/TOU  
A(5,3)=-K/TOU  
A(5,5)=-(25*K+1.)/TOU  
A(5,6)=K/TOU  
A(5,7)=-K*KXD/TOU  
A(5,8)=-K/TOU  
A(5,9)=-K*X/TOU  
A(6,1)=-KXD/TOU  
A(6,2)=-KX/TOU  
A(6,3)=-1./TOJ  
A(6,5)=-0.25/TOU  
A(6,7)=-KXD/TOU  
A(6,8)=-1./TOJ  
A(6,9)=-KX/TOU  
A(7,7)=-1./TR(1)  
A(8,8)=-1./TR(2)  
A(9,9)=-1./TR(3)
```

C C C 1

B MATRIX

```
DO 2 I=1,N  
DO 2 J=1,L
```

```

2      B(I,J)=0.0
      B(7,1)=1.
      B(8,2)=1.
      B(9,3)=1.
CONTINUE
C      Q MATRIX
C      DO 3   I=1,M
      DO 3   J=1,N
      Q(1,1)=0.0*TR(1)*SIGMA1**2
      Q(1,2)=(2./TR(2))*SIGMA2**2
      Q(2,3)=(2./TR(3))*SIGMA3**2
      C      MATRIX
      DO 4   I=1,M
      DO 4   J=1,N
      H(1,J)=0.0
      H(1,9)=1.0
      H(2,2)=1.0
      H(2,7)=1.0
      H(3,3)=1.0
      H(3,8)=1.0
      NPT=40
      T1=0
      T2=20
      CALL ECHO(A,B,Q,H,TR,N,M,L)
      CALL MODAL(A,B,H,N,M,L)
      CALL VARY(B,L,NPT,T1,T2)
      STOP
      END
*****
C***** HARRIER G
C***** HARRIER G IS THE CODE USED TO GENERATE THE A,B AND C
C***** MATRICES FOR THE COVARIANCE CALCULATION OF THE HARRIER
C***** LONGITUDINAL AXIS SRFIMF CONTROL WITH A GUST INPUT.
C***** DIMENSION B(10,4),H(3,10),TR(4)
C***** REAL K,KX,KXD
C***** COMMON BP'CP,K,KX,KXD,TOU,CPG,N,PD(1000),Q(10,10),A(10,10)
C***** WRITE(6,100) FORMAT(//,20X,90('*'),//,40X,'HARRIER MODEL ',M0003870
100

```

1. ALL QUANTITIES MEASURED*, //,20X,90(''**'),//)

N=10

L=4

M=3

KX=20.

KXD=3.

TOU=.1.

SIGMA1=1.

SIGMA2=1.

SIGMA3=1.

SIGMA4=1.

TR(1)=10.

TR(2)=10.

TR(3)=10.

TR(4)=6.5

CALCULATE THE A MATRIX

```
DO 1 I=1,N
DO 1 J=1,N
A(1,1)=0.0
A(1,2)=1.
A(1,10)=-.0026
A(2,3)=1.
A(2,5)=.25
A(2,10)=-.00473
A(3,4)=1.
A(3,5)=-.06115
A(3,10)=.00306
A(4,1)=-.00748
A(4,2)=-.0675
A(4,3)=.45
A(4,4)=-.4906
A(4,5)=.14428
A(4,10)=.00346
A(5,1)=-K*KX/TOU
A(5,2)=-K*KXD/TOU
A(5,3)=-K/TOU
A(5,4)=-(25*K+1.)/TOU
A(5,5)=K/TOU
A(5,6)=-K*KXD/TOU
A(5,7)=-K/TOU
A(5,8)=-K*KX/TOU
A(5,9)=-K*KXD/TOU
A(5,10)=(KXD*.0026+.00473)*K/TOU
A(6,1)=-KX/TOU
A(6,2)=-KXD/TOU
A(6,3)=-1./TOU
```

CCC 1

```

A(6,5)=-25/TRU
A(6,7)=-KX0/TRU
A(6,8)=-1./TRU
A(6,9)=-KX/TRU
A(6,10)=A(5,10)/K
A(7,7)=-1./TR(1)
A(8,8)=-1./TR(2)
A(9,9)=-1./TR(3)
A(10,10)=-1./TR(4)

```

B MATRIX

```

DO 2 I=1,N
DO 2 J=1,L
B(1,J)=0.0
B(7,1)=1.
B(8,2)=1.
B(9,3)=1.
B(10,4)=1.

```

Q MATRIX

```

DO 3 I=1,L
DO 3 J=1,L
Q(1,J)=0.0
Q(1,1)=(2./TR(1))*SIGMA1**2
Q(2,2)=(2./TR(2))*SIGMA2**2
Q(3,3)=(2./TR(3))*SIGMA3**2
Q(4,4)=(2./TR(4))*SIGMA4**2

```

C MATRIX

```

DO 4 I=1,N
DO 4 J=1,N
H(I,J)=0.0
H(1,1)=1.0
H(2,2)=1.0
H(3,3)=1.0
NPT=60
T1=0.
T2=60
CALL ECHO(A,B,C,H,TR,N,M,L)
CALL MODAL(A,B,H,N,M,L)
CALL VARY(B,L,NPT,T1,T2)
STOP
END

```

CCC 2 CCC 3 CCC 4

```

***** SUBROUTINE MODAL (A,B,H,N,M,L)
***** THIS SUBROUTINE IS USED TO TRANSFORM A SYSTEM OF THE FORM
***** XDOT=AX+BU
***** Y=CX
***** TO MODAL COORDINATES.
***** SUBROUTINE MODAL (A,B,H,N,M,L)
***** DIMENSION A(N,N) B(N,L) H(M,N) ,AC(10,10),C(10,10),D(10,10)
***** I G(4,10) T(10,10) COMPLEX Z(10,10),W(10),WK(99),ENORM,VNORM
***** REAL K,KX,KXD
***** DO 1 I=1,N
***** DO 1 J=1,N
***** AC(I,J)=A(I,J)
***** WRITE(6,210)
***** 210 FORMAT(120X,70('**',/20X,'**',/20X,'**',/20X,'**',/))
***** MODAL ANALYSIS
***** 1A=N
***** 1Z=N
***** 1JOB=1
***** CALL EIGRF(A,N,N,1JOB,W,Z,IZ,WK,IER)
***** WRITE OUT THE EIGENVALUES
***** 201 WRITE(6,201)
***** 201 FORMAT(110X,'THE EIGENVALUES ARE',//)
***** 101 WRITE(6,101){W(I)}{I=1,N}
***** 101 FORMAT(1X,16F6.2,/)
***** C WRITE THE EIGENVECTORS-
***** C WRITE(6,202)
***** 202 FORMAT(110X,'THE EIGENVECTORS ARE',//)
***** 202 WRITE(6,101){{Z(I,J)}{J=1,N}}{I=1,N}
***** C EIGENVECTOR NORMALIZATION
***** C J=1
***** C CONTINUE

```

```

FNorm=00
IF(IAIMAG(W(J)).NE.0) GO TO 4
C EIGENVECTOR IS REAL
DO 2 I=1,N
FNORM=FNORM+REAL(Z(I,J))**2
DO 3 I=1,N
T(I,J)=REAL(Z(I,J))/SQRT(FNORM)
GO TO 7
C COMPLEX NORMALIZATION
DO 5 I=1,N
TAT=REAL(Z(I,J))**2
IF(TAT.LE.FNORM) GO TO 5
IMAX=I
FNORM=TAT
CONTINUE
5 C THE ITH ROW WILL BE NORMALIZED TO 1.0
XN1=REAL(Z(IMAX,J))
XN2=AIMAG(Z(IMAX,J))
ENORM=CMPLX(XN1/(XN1+XN2**2),-XN2/(XN1+XN2**2))
DO 6 I=1,N
VNORM=Z(I,J)*ENORM
T(I,J)=REAL(VNORM)
T(I,J+1)=AIMAG(VNORM)
J=J+1
6 IF(J.LE.N) GO TO 10
C WRITE THE NORMALIZED MATRIX
WRITE(5,203)
FORMAT(5,100) ((T(I,J),J=1,N),I=1,N)
203 C INVERT T
IDGT=0
CALL LINV2F(T,N,IA,ADGT,WK,IER)
WRITE(6,204)
FORMAT(5,100) ((THE NORMALIZED TRANSFER MATRIX IS*,//)
204 C TAKE T INV*A*T
      
```

```

C      CALL VMULFF(A,AC,N,N,N,IA,AC,N,IER)
C      CALL VMULFF(C,T,N,N,N,IA,IA,AC,N,IER)
C      WRITE(6,205)
C      FORMAT(//10X,'THE DIAGONAL MATRIX IS',//)
C      WRITE(6,100) {(AC(I,J),J=1,N),I=1,N}
C
C      CALCULATE THE CONTROL MATRIX
C
C      WRITE(6,206)
C      FORMAT(//10X,'THE CONTROL MATRIX IS',//)
C      CALL VMULFF(A,B,N,N,L,N,N,D,N,IER)
C      DO 30 I=1,N
C      WRITE(6,104) {(D(I,J),J=1,L)
C      FORMAT(/,8(2X,F7.2,2X)) 104
C
C      CALCULATE Y=CF
C
C      WRITE(6,207)
C      FORMAT(//10X,'THE MEASUREMENT VECTOR IS',//)
C      CALL VMULFF(H,T,N,M,IA,G,M,IER)
C      WRITE(6,100) {(G(I,J),J=1,N),I=1,M)
C      FORMAT(/,10(2X,F7.2))
C      RETURN 100
C
C
C      **** SUBROUTINE VARY (B,L,NPT,T1,T2)
C
C      VARY IS USED TO CALCULATE THE COVARIANCE OF THE STATES OF
C      A SYSTEM. THE COVARIANCE IS FOUND BY SOLVING THE LYAPUNOV
C      DIFFERENTIAL EQUATION USING THE ISML SUBROUTINE DVERK.
C
C      **** SUBROUTINE VARY (B,L,NPT,T1,T2)
C      DIMENSION B(10,4),P(100),PDOT(100),D(10,10),W(100,10),
C      16(10,10),C(24)
C      EXTERNAL FCN
C      COMMON BP,CP,K,KX,TQD,CPG,N,PD(100),Q(10,10),A(10,10)
C      WRITE(6,200)
C      FORMAT(//20X,'90(*,*),//,40X,'VARIANCE ANALYSIS',/
C
C      START CLACULATIONS

```

C
TST=.00005
NSQ=N*N
NW=NSQ
TIME=T1
TOL=.001
XNP=NP
STEP=(T2-T1)/XNP
DO 1 I=1,N
DO 1 J=1,N
G(1,J)=0.0
DO 1 K=1,L
G(1,J)=G(1,J)+B(I,J)*Q(K,J)
G=B*QA

DO 2 I=1,N
DO 2 J=1,N
Q(I,J)=0.0
DO 2 K=1,L
Q(I,J)=Q(I,J)+G(I,K)*B(J,K)
Q=B*QT
NOW SET INITIAL VALUES OF P
DO 3 I=1,N
DO 3 J=1,N
G(I,J)=0.0
G IS THE MATRIX OF THE P VECTOR SET TO 0.0
SET UP TO CALL DVERK
DO 4 I=1,24
C(I)=0.
4 WRITE(6,700),TIME
FORMAT(/,10X,A1,TIME=,F5.2,/)
CALL DVERK(NSQ,FCN,TIME,P,TIMEE,TOL,IND,C,NW,W,IER)
TIMEE=TIME+STEP
IND=1
CALL DVERK(NSQ,FCN,TIME,P,TIMEE,TOL,IND,C,NW,W,IER)
WRITE(6,750),IND
FORMAT(10X,A1,IND=,I3,,AFTER CALL TO DVERK)
CALL DVERK(NSQ,FCN,TIME,P,TIMEE,TOL,IND,C,NW,W,IER)
700 FORMAT(10X,A1,IND=,I3,,AFTER CALL TO DVERK)
CALL DVERK(NSQ,FCN,TIME,P,TIMEE,TOL,IND,C,NW,W,IER)
WRITE(6,800),TIME
WRITE(6,800),TIME
FORMAT(//,20X,A1,THE P MATRIX IS',/)

15000

20000000

```

      WRITE(6,100) ((G(I,J), J=1,N), I=1,N)
      X5=SQRT((G(5,5))
      CALL VTM(N,NSQ,D,PD)
      WRITE(6,901)
      FORMAT(//,10X,'P DOT IS',/N), I=1,N)
      WRITE(6,100) ((D(I,J), J=1,N), I=1,N)
      SUM=0.0
      DO 5 I=1,NSQ
      SUM=SUM+ABS(PD(I))
      WRITE(6,802) SUM
      FORMAT(10X,'THE SUM OF THE P DOT TERMS IS ',E15.5)
      IF(SUM.LE.1.0E-50) GO TO 50
      IF(TIME.E.GE.T2) GO TO 51
      GO TO 20
      WRITE(6,710)
      FORMAT(//,10X,'THE LAST P IS A STEADY STATE',//)
      RETURN
      50
      CALL VTM(N,NSQ,G,PD)
      WRITE(6,720)
      FORMAT(//,10X,'END OF RUN, THE FINAL P00T IS',//)
      WRITE(6,100) ((G(I,J), J=1,N), I=1,N)
      FORMAT(102X,E10.4),/
      RETURN
      END

      CCCCCCCC
      802
      51
      720
      100
      1
      2
      CCCCCCCC
      147
      20
      21
      22
      23
      24
      25
      26
      27
      28
      29
      30
      31
      32
      33
      34
      35
      36
      37
      38
      39
      40
      41
      42
      43
      44
      45
      46
      47
      48
      49
      50
      51
      52
      53
      54
      55
      56
      57
      58
      59
      60
      61
      62
      63
      64
      65
      66
      67
      68
      69
      70
      71
      72
      73
      74
      75
      76
      77
      78
      79
      80
      81
      82
      83
      84
      85
      86
      87
      88
      89
      90
      91
      92
      93
      94
      95
      96
      97
      98
      99
      100
      101
      102
      103
      104
      105
      106
      107
      108
      109
      110
      111
      112
      113
      114
      115
      116
      117
      118
      119
      120
      121
      122
      123
      124
      125
      126
      127
      128
      129
      130
      131
      132
      133
      134
      135
      136
      137
      138
      139
      140
      141
      142
      143
      144
      145
      146
      147
      148
      149
      150
      151
      152
      153
      154
      155
      156
      157
      158
      159
      160
      161
      162
      163
      164
      165
      166
      167
      168
      169
      170
      171
      172
      173
      174
      175
      176
      177
      178
      179
      180
      181
      182
      183
      184
      185
      186
      187
      188
      189
      190
      191
      192
      193
      194
      195
      196
      197
      198
      199
      200
      201
      202
      203
      204
      205
      206
      207
      208
      209
      210
      211
      212
      213
      214
      215
      216
      217
      218
      219
      220
      221
      222
      223
      224
      225
      226
      227
      228
      229
      230
      231
      232
      233
      234
      235
      236
      237
      238
      239
      240
      241
      242
      243
      244
      245
      246
      247
      248
      249
      250
      251
      252
      253
      254
      255
      256
      257
      258
      259
      260
      261
      262
      263
      264
      265
      266
      267
      268
      269
      270
      271
      272
      273
      274
      275
      276
      277
      278
      279
      280
      281
      282
      283
      284
      285
      286
      287
      288
      289
      290
      291
      292
      293
      294
      295
      296
      297
      298
      299
      300
      301
      302
      303
      304
      305
      306
      307
      308
      309
      310
      311
      312
      313
      314
      315
      316
      317
      318
      319
      320
      321
      322
      323
      324
      325
      326
      327
      328
      329
      330
      331
      332
      333
      334
      335
      336
      337
      338
      339
      340
      341
      342
      343
      344
      345
      346
      347
      348
      349
      350
      351
      352
      353
      354
      355
      356
      357
      358
      359
      360
      361
      362
      363
      364
      365
      366
      367
      368
      369
      370
      371
      372
      373
      374
      375
      376
      377
      378
      379
      380
      381
      382
      383
      384
      385
      386
      387
      388
      389
      390
      391
      392
      393
      394
      395
      396
      397
      398
      399
      400
      401
      402
      403
      404
      405
      406
      407
      408
      409
      410
      411
      412
      413
      414
      415
      416
      417
      418
      419
      420
      421
      422
      423
      424
      425
      426
      427
      428
      429
      430
      431
      432
      433
      434
      435
      436
      437
      438
      439
      440
      441
      442
      443
      444
      445
      446
      447
      448
      449
      450
      451
      452
      453
      454
      455
      456
      457
      458
      459
      460
      461
      462
      463
      464
      465
      466
      467
      468
      469
      470
      471
      472
      473
      474
      475
      476
      477
      478
      479
      480
      481
      482
      483
      484
      485
      486
      487
      488
      489
      490
      491
      492
      493
      494
      495
      496
      497
      498
      499
      500
      501
      502
      503
      504
      505
      506
      507
      508
      509
      510
      511
      512
      513
      514
      515
      516
      517
      518
      519
      520
      521
      522
      523
      524
      525
      526
      527
      528
      529
      530
      531
      532
      533
      534
      535
      536
      537
      538
      539
      540
      541
      542
      543
      544
      545
      546
      547
      548
      549
      550
      551
      552
      553
      554
      555
      556
      557
      558
      559
      560
      561
      562
      563
      564
      565
      566
      567
      568
      569
      570
      571
      572
      573
      574
      575
      576
      577
      578
      579
      580
      581
      582
      583
      584
      585
      586
      587
      588
      589
      590
      591
      592
      593
      594
      595
      596
      597
      598
      599
      600
      601
      602
      603
      604
      605
      606
      607
      608
      609
      610
      611
      612
      613
      614
      615
      616
      617
      618
      619
      620
      621
      622
      623
      624
      625
      626
      627
      628
      629
      630
      631
      632
      633
      634
      635
      636
      637
      638
      639
      640
      641
      642
      643
      644
      645
      646
      647
      648
      649
      650
      651
      652
      653
      654
      655
      656
      657
      658
      659
      660
      661
      662
      663
      664
      665
      666
      667
      668
      669
      670
      671
      672
      673
      674
      675
      676
      677
      678
      679
      680
      681
      682
      683
      684
      685
      686
      687
      688
      689
      690
      691
      692
      693
      694
      695
      696
      697
      698
      699
      700
      701
      702
      703
      704
      705
      706
      707
      708
      709
      710
      711
      712
      713
      714
      715
      716
      717
      718
      719
      720
      721
      722
      723
      724
      725
      726
      727
      728
      729
      730
      731
      732
      733
      734
      735
      736
      737
      738
      739
      740
      741
      742
      743
      744
      745
      746
      747
      748
      749
      750
      751
      752
      753
      754
      755
      756
      757
      758
      759
      760
      761
      762
      763
      764
      765
      766
      767
      768
      769
      770
      771
      772
      773
      774
      775
      776
      777
      778
      779
      770
      771
      772
      773
      774
      775
      776
      777
      778
      779
      780
      781
      782
      783
      784
      785
      786
      787
      788
      789
      780
      781
      782
      783
      784
      785
      786
      787
      788
      789
      790
      791
      792
      793
      794
      795
      796
      797
      798
      799
      790
      791
      792
      793
      794
      795
      796
      797
      798
      799
      800
      801
      802
      803
      804
      805
      806
      807
      808
      809
      800
      801
      802
      803
      804
      805
      806
      807
      808
      809
      810
      811
      812
      813
      814
      815
      816
      817
      818
      819
      810
      811
      812
      813
      814
      815
      816
      817
      818
      819
      820
      821
      822
      823
      824
      825
      826
      827
      828
      829
      820
      821
      822
      823
      824
      825
      826
      827
      828
      829
      830
      831
      832
      833
      834
      835
      836
      837
      838
      839
      830
      831
      832
      833
      834
      835
      836
      837
      838
      839
      840
      841
      842
      843
      844
      845
      846
      847
      848
      849
      840
      841
      842
      843
      844
      845
      846
      847
      848
      849
      850
      851
      852
      853
      854
      855
      856
      857
      858
      859
      850
      851
      852
      853
      854
      855
      856
      857
      858
      859
      860
      861
      862
      863
      864
      865
      866
      867
      868
      869
      860
      861
      862
      863
      864
      865
      866
      867
      868
      869
      870
      871
      872
      873
      874
      875
      876
      877
      878
      879
      870
      871
      872
      873
      874
      875
      876
      877
      878
      879
      880
      881
      882
      883
      884
      885
      886
      887
      888
      889
      880
      881
      882
      883
      884
      885
      886
      887
      888
      889
      890
      891
      892
      893
      894
      895
      896
      897
      898
      899
      890
      891
      892
      893
      894
      895
      896
      897
      898
      899
      900
      901
      902
      903
      904
      905
      906
      907
      908
      909
      900
      901
      902
      903
      904
      905
      906
      907
      908
      909
      910
      911
      912
      913
      914
      915
      916
      917
      918
      919
      920
      921
      922
      923
      924
      925
      926
      927
      928
      929
      920
      921
      922
      923
      924
      925
      926
      927
      928
      929
      930
      931
      932
      933
      934
      935
      936
      937
      938
      939
      930
      931
      932
      933
      934
      935
      936
      937
      938
      939
      940
      941
      942
      943
      944
      945
      946
      947
      948
      949
      940
      941
      942
      943
      944
      945
      946
      947
      948
      949
      950
      951
      952
      953
      954
      955
      956
      957
      958
      959
      950
      951
      952
      953
      954
      955
      956
      957
      958
      959
      960
      961
      962
      963
      964
      965
      966
      967
      968
      969
      960
      961
      962
      963
      964
      965
      966
      967
      968
      969
      970
      971
      972
      973
      974
      975
      976
      977
      978
      979
      970
      971
      972
      973
      974
      975
      976
      977
      978
      979
      980
      981
      982
      983
      984
      985
      986
      987
      988
      989
      980
      981
      982
      983
      984
      985
      986
      987
      988
      989
      990
      991
      992
      993
      994
      995
      996
      997
      998
      999
      990
      991
      992
      993
      994
      995
      996
      997
      998
      999
      1000
      1001
      1002
      1003
      1004
      1005
      1006
      1007
      1008
      1009
      1000
      1001
      1002
      1003
      1004
      1005
      1006
      1007
      1008
      1009
      1010
      1011
      1012
      1013
      1014
      1015
      1016
      1017
      1018
      1019
      1010
      1011
      1012
      1013
      1014
      1015
      1016
      1017
      1018
      1019
      1020
      1021
      1022
      1023
      1024
      1025
      1026
      1027
      1028
      1029
      1020
      1021
      1022
      1023
      1024
      1025
      1026
      1027
      1028
      1029
      1030
      1031
      1032
      1033
      1034
      1035
      1036
      1037
      1038
      1039
      1030
      1031
      1032
      1033
      1034
      1035
      1036
      1037
      1038
      1039
      1040
      1041
      1042
      1043
      1044
      1045
      1046
      1047
      1048
      1049
      1040
      1041
      1042
      1043
      1044
      1045
      1046
      1047
      1048
      1049
      1050
      1051
      1052
      1053
      1054
      1055
      1056
      1057
      1058
      1059
      1050
      1051
      1052
      1053
      1054
      1055
      1056
      1057
      1058
      1059
      1060
      1061
      1062
      1063
      1064
      1065
      1066
      1067
      1068
      1069
      1060
      1061
      1062
      1063
      1064
      1065
      1066
      1067
      1068
      1069
      1070
      1071
      1072
      1073
      1074
      1075
      1076
      1077
      1078
      1079
      1070
      1071
      1072
      1073
      1074
      1075
      1076
      1077
      1078
      1079
      1080
      1081
      1082
      1083
      1084
      1085
      1086
      1087
      1088
      1089
      1080
      1081
      1082
      1083
      1084
      1085
      1086
      1087
      1088
      1089
      1090
      1091
      1092
      1093
      1094
      1095
      1096
      1097
      1098
      1099
      1090
      1091
      1092
      1093
      1094
      1095
      1096
      1097
      1098
      1099
      1100
      1101
      1102
      1103
      1104
      1105
      1106
      1107
      1108
      1109
      1100
      1101
      1102
      1103
      1104
      1105
      1106
      1107
      1108
      1109
      1110
      1111
      1112
      1113
      1114
      1115
      1116
      1117
      1118
      1119
      1110
      1111
      1112
      1113
      1114
      1115
      1116
      1117
      1118
      1119
      1120
      1121
      1122
      1123
      1124
      1125
      1126
      1127
      1128
      1129
      1120
      1121
      1122
      1123
      1124
      1125
      1126
      1127
      1128
      1129
      1130
      1131
      1132
      1133
      1134
      1135
      1136
      1137
      1138
      1139
      1130
      1131
      1132
      1133
      1134
      1135
      1136
      1137
      1138
      1139
      1140
      1141
      1142
      1143
      1144
      1145
      1146
      1147
      1148
      1149
      1140
      1141
      1142
      1143
      1144
      1145
      1146
      1147
      1148
      1149
      1150
      1151
      1152
      1153
      1154
      1155
      1156
      1157
      1158
      1159
      1150
      1151
      1152
      1153
      1154
      1155
      1156
      1157
      1158
      1159
      1160
      1161
      1162
      1163
      1164
      1165
      1166
      1167
      1168
      1169
      1160
      1161
      1162
      1163
      1164
      1165
      1166
      1167
      1168
      1169
      1170
      1171
      1172
      1173
      1174
      1175
      1176
      1177
      1178
      1179
      1170
      1171
      1172
      1173
      1174
      1175
      1176
      1177
      1178
      1179
      1180
      1181
      1182
      1183
      1184
      1185
      1186
      1187
      1188
      1189
      1180
      1181
      1182
      1183
      1184
      1185
      1186
      1187
      1188
      1189
      1190
      1191
      1192
      1193
      1194
      1195
      1196
      1197
      1198
      1199
      1190
      1191
      1192
      1193
      1194
      1195
      1196
      1197
      1198
      1199
      1200
      1201
      1202
      1203
      1204
      1205
      1206
      1207
      1208
      1209
      1200
      1201
      1202
      1203
      1204
      1205
      1206
      1207
      1208
      1209
      1210
      1211
      1212
      1213
      1214
      1215
      1216
      1217
      1218
      1219
      1210
      1211
      1212
      1213
      1214
      1215
      1216
      1217
      1218
      1219
      1220
      1221
      1222
      1223
      1224
      1225
      1226
      1227
      1228
      1229
      1220
      1221
      1222
      1223
      1224
      1225
      1226
      1227
      1228
      1229
      1230
      1231
      1232
      1233
      1234
      1235
      1236
      1237
      1238
      1239
      1230
      1231
      1232
      1233
      1234
      1235
      1236
      1237
      1238
      1239
      1240
      1241
      1242
      1243
      1244
      1245
      1246
      1247
      1248
      1249
      1240
      1241
      1242
      1243
      1244
      1245
      1246
      1247
      1248
      1249
      1250
      1251
      1252
      1253
      1254
      1255
      1256
      1257
      1258
      1259
      1250
      1251
      1252
      1253
      1254
      1255
      1256
      1257
      1258
      1259
      1260
      1261
      1262
      1263
      1264
      1265
      1266
      1267
      1268
      1269
      1260
      1261
      1262
      1263
      1264
      1265
      1266
      1267
      1268
      1269
      1270
      
```

```
DIMENSION A(N,N), B(NSQ)
K=1
DO 1 I=1,N
DO 1 J=1,N
B(K)=A(I,J)
K=K+1
DEBUG SUBCHK
RETURN
END

C      SUBROUTINE VTM (N,NSQ,A,B)
DIMENSION A(N,N),B(NSQ)
K=1
DO 1 I=1,N
DO 1 J=1,N
A(I,J)=B(K)
K=K+1
DEBUG SUBCHK
RETURN
END
```

1

1

```

*****
*
*      ** HARRIER LONGITUDINAL SRFIMF CONTROL SIMULATION **
*
*****
// EXEC CSMPXV
// X.COMPRINT DD DUMMY
// X.SYSPRINT DD DUMMY
// X.SYSIN DD *
*
*      SIMULATION OF OPEN LOOP PLANT
*
X1P=INTGRL(0.0,X2P)
X2P=INTGRL(0.0,X3P)
X3P=INTGRL(0.0,X4P)
X4P=INTGRL(0.0,X4PDOT)
X4PDOT=.25*XC-.49*X4P+.45*X3P-.0665*X2P-.00748*X1P
ACCEL_P=-.00189*X1P-.016625*X2P+.1144*X3P-.061*X4P+.25*XC
POSIT_P=.00189*X1P+.0615*X2P+.25*X3P
VEL_P=.00189*X2P+.0615*X3P+.25*X4P
*
*
*      CLOSED LOOP SYSTEM SIMULATION
*
X1=INTGRL(0.0,X2)
X2=INTGRL(0.0,X3)
X3=INTGRL(0.0,X4)
X4=INTGRL(0.0,X4DOT)
X4DOT=X5-.49*X4+.45*X3-.0665*X2-.00748*X1
ACCEL=-.00189*X1-.016625*X2+.1144*X3-.061*X4+.25*X5
POSIT=.00189*X1+.0615*X2+.25*X3
VEL=.00189*X2+.0615*X3+.25*X4
X5=REALPL(0.0,TOU,IS)
XC=STEP(0.0)
WS=-KXD*VX+KX*(XC-X)+VS
IS=K*WS
VS=AS-AX
AS=REALPL(0.0,TOJ,WS)
AX=ACCEL
VX=VEL
X=POSIT
K=100.
KX=4.
KXD=3.
TOU=.1
TIMER FINTIM=10,OUTDEL=.2
OUTPUT POSIT,POSIT_P
OUTPUT TIME,POSIT,PGSITP
PAGE XYPILOT
END
STOP

```

APPENDIX B

TABULATED DATA

Time (sec)	σ_{1p}	σ_{1v}	σ_{1a}	σ_{2p}	σ_{2v}	σ_{2a}	σ_{3p}	σ_{3v}	σ_{3a}
0	0	0	0	0	0	0	0	0	0
.5	.045	.033	.011	.191	.149	.050	.764	.573	.191
1.0	.164	.123	.074	.315	.236	.079	.825	.619	.206
2.0	.410	.307	.102	.342	.256	.085	1.022	.767	.256
3.0	.564	.423	.141	.344	.258	.086	1.283	.962	.321
4.0	.660	.495	.165	.347	.260	.087	1.475	1.106	.369
5.0	.728	.546	.182	.348	.261	.087	1.613	1.210	.403
6.0	.780	.585	.195	.349	.262	.087	1.717	1.288	.429
7.0	.819	.615	.205	.350	.262	.087	1.797	1.348	.449
8.0	.851	.638	.213	.351	.263	.088	1.861	1.395	.465
9.0	.875	.657	.219	.351	.263	.088	1.911	1.433	.478
10.0	.895	.671	.224	.352	.264	.088	1.950	1.464	.488
20.0	.968	.726	.242	.354	.265	.088	2.100	1.576	.525
40.0	.979	.734	.245	.354	.265	.089	2.123	1.592	.531
60.0	.979	.734	.245	.354	.266	.089	2.123	1.592	.531
S.S.	.979	.734	.245	.354	.266	.089	2.123	1.592	.531

Table B-1 Tabulated Data
for figures 4-4 through 4-6.

Time (sec)	σ_{1a}	σ_{2a}	σ_{3a}
0	0	0	0
2.0	.530	.675	2.005
4.0	2.858	1.781	7.745
6.0	8.070	3.060	18.515
8.0	14.649	4.412	34.742
10.0	24.399	5.791	56.569

The rate of change in P , \dot{P} after 10 seconds was

	$\sigma_{\dot{P}1}$	$\sigma_{\dot{P}2}$	$\sigma_{\dot{P}3}$
10.0	16.422	2.826	37.350

Table B-2
Tabulated data for figure 4-7.

Time (sec)	σ_{1p}	σ_{1v}	σ_{2p}	σ_{2v}	σ_{3p}
0	0	0	0	0	0
.5	.020	.026	.091	.119	.351
1.0	.076	.099	.149	.189	.379
2.0	.189	.246	.157	.205	.470
3.0	.259	.338	.158	.206	.590
4.0	.304	.396	.160	.208	.679
5.0	.335	.437	.160	.209	.740
6.0	.359	.468	.160	.209	.790
7.0	.377	.492	.161	.210	.827
8.0	.391	.510	.161	.210	.856
9.0	.403	.525	.162	.211	.879
10.0	.412	.537	.162	.211	.898
20.0	.445	.581	.163	.212	.966
S.S	.450	.590	.163	.212	.970
					1.300

Table B-3 Tabulated data for figures 4-9 through 4-11.

Time (sec)	σ_{1p}	σ_{1v}	σ_{1a}	σ_{2p}	σ_{2v}	σ_{2a}	σ_{5p}	σ_{5v}	σ_{5a}
0	0	0	0	0	0	0	0	0	0
.5	.440	.081	.011	.201	.210	.050	2.672	2.010	.668
1.0	.166	.125	.042	.319	.239	.080	2.807	2.106	.702
2.0	.413	.310	.103	.345	.259	.086	3.237	2.428	.809
3.0	.566	.425	.142	.348	.261	.087	3.286	2.465	.822
4.0	.662	.496	.165	.350	.263	.088	3.288	2.466	.822
5.0	.730	.547	.182	.351	.264	.088	3.291	2.468	.822
6.0	.781	.586	.195	.353	.264	.088	3.300	2.475	.825
7.0	.820	.615	.205	.353	.265	.088	3.320	2.490	.830
8.0	.852	.639	.213	.354	.266	.089	3.345	2.511	.837
9.0	.876	.657	.219	.355	.266	.089	3.384	2.538	.846
10.0	.896	.672	.224	.355	.266	.089	3.425	2.570	.856
20.0	.969	.727	.242	.357	.268	.089	3.821	2.866	.955
S.S.	.980	.734	.245	.360	.270	.089	3.900	2.900	.970

Table B-4 Tabulated data for figures 5-4 through 5-6.

Time (sec)	σ_{1g}	σ_{2g}	σ_{5g}	σ_{acc_g}	σ_g
0	0	0	0	0	0
1.0	.0013	.006	.076	.013	2.573
2.0	.0014	.009	.110	.040	3.390
3.0	.0014	.011	.227	.102	3.882
4.0	.0015	.011	.402	.191	4.207
5.0	.0015	.012	.622	.301	4.431
6.0	.0015	.012	.874	.427	4.588
7.0	.0016	.013	1.150	.564	4.701
8.0	.0016	.013	1.442	.701	4.782
9.0	.0016	.013	1.743	.860	4.840
10.0	.0016	.013	2.050	1.013	4.884
20.0	.0016	.013	4.750	2.360	4.959
40.0	.0016	.013	7.169	3.567	5.00
60.0	.0017	.013	7.783	3.874	5.00
S.S.	.0017	.013	7.800	4.00	4.00

Table B-5 Tabulated data for figure 5-7.

LIST OF REFERENCES

1. Merrick, V.K. and Gerdes, R.M., "Design and Piloted Simulation of a VTOL Flight Control System," Journal of Guidance and Control, v. 1 no. 3, May - June 1978.
2. NASA Technical Report 1040, Study of the Application of an Implicit Model Following Flight Controller to Lift Fan VTOL Aircraft, by V.K. Merrick, November 1977.
3. NASA Contractor Report 1519, Mathematical Model for Lift/Cruise for V/STOL Aircraft Simulator Programming Data, by M. P. Bland and B. Fajfar, 6 December 1976.
4. Tyler, J. S., Jr., "The Characteristics of Model Following Systems as Synthesized by Optimal Control," IEEE Trans. Automatic Control, v. 9 no. 4, p. 485-498, October 1964.
5. NASA Technical Note D-4663, On the Use of Algebraic Methods in the Analysis and Design of Model-Following Control Systems, by H. Erzberger, July 1968.
6. Nobel, B., Applied Linear Algebra, Prentice-Hall, 1969.
7. Melsa, J. L. and Jones, S. K., Computer Programs for Computational Assistance in the Study of Linear Control Theory, 2d ed., McGraw - Hill, 1973.
8. Speckhart, F. H. and Green, W. L., A Guide to Using CSMP - The Continuous System Modeling Program, Prentice - Hall, 1976.
9. Maybeck, P. S., Stochastic Models, Estimation, and Control, v. 1, Academic Press, 1979.
10. Analytical Mechanics Associates, Inc. Report No. 80-13, An Investigation of Automatic Guidance Concepts to Steer VTOL Aircraft to Small Aviation Facility Ships, Sorensen, J. A., Goka, T., Phatak, A., Schmidt, S. F., July 1980.
11. Bryson, A. E., "Kalman Filter Divergence and Aircraft Motion Estimators", Journal of Guidance and Control, v. 1 no. 1, January-February 1978.

12. Calspan Report AK-5876-F-1, A Study to Determine the Feasibility of Simulating the AV-8A Harrier With the X-22A Variable Stability Aircraft, J. V. Lebacqz and F. W. Aiken, July 1976.
13. Ogata, K., Modern Control Engineering, Prentice - Hall, 1970.
14. McRuer, D., Ashkenas, I., and Graham, D., Aircraft Dynamics and Automatic Control, Princeton University Press, 1973.

INITIAL DISTRIBUTION LIST

	No. Copies
1. Defense Technical Information Center Cameron Station Alexandria, Virginia 22314	2
2. Library, Code 0142 Naval Postgraduate School Monterey, California 93940	2
3. Department Chairman, Code 67 Department of Aeronautics Naval Postgraduate School Monterey, California 93940	1
4. Prof. D. J. Collins, Code 67fo Department of Aeronautics Naval Postgraduate School Monterey, California 93940	2
5. LT Lawrence E. Epley, USN HEANTISUBRON LIGHT THRITY-THREE NAS North Island San Diego, California 92135	1
6. Dr. Tsuyoshi Goka Analytical Mechanics Associates, Inc. Suite 210 2483 Old Middlefield Way Mountain View, California 94043	1
7. Prof. A. E. Fuhs, Code 67Fu Department of Aeronautics Naval Postgraduate School Monterey, California 93940	1
8. Mr. Vernon Merrick Mail Stop N211-2 NASA Ames Research Center NAS Moffett Field, California 94035	5

